DEPARTMENT OF CHEMISTRY, UNIVERSITY OF JYVÄSKYLÄ
RESEARCH REPORT No. 195

COMPUTATIONAL AND THEORETICAL STUDIES ON LATTICE THERMAL CONDUCTIVITY AND THERMAL PROPERTIES OF SILICON CLATHRATES

BY
VILLE HÄRKÖNEN

Academic Dissertation
for the Degree of
Doctor of Philosophy

To be presented, by permission of the Faculty of Mathematics and Natural Sciences of the University of Jyväskylä, for public examination in Auditorium KEM-4 of the University of Jyväskylä on October 21, 2016 at 12 noon

Jyväskylä, Finland
ISBN 978-951-39-6764-2
ISSN 0357-346X

Preface

The work presented in this thesis was conducted at the Department of Chemistry of the University of Jyväskylä during the years 2013-2016.

First of all, I thank my supervisors Asst. Prof. Antti Karttunen and Dr. Gerrit Groenhof for all the advices and guidance they have given me during these years. Especially, I thank Prof. Robert van Leeuwen for giving me the opportunity to work with him as a part of my studies and for all of his guidance. I would also like to thank the pre-examiners Prof. Gyaneshwar Srivastava and Dr. Ari Harju for their valuable comments and Dr. Vesa Apaja for being helpful in problems related to our computational resources. I thank Dr. Janne Nevalaita, Mr. Niko Säkkinen, Mr. Markku Hyrkäs, Mr. Kalle Machal, Mr. Juha Hurmalainen and Mr. Lauri Kivijärvi for interesting discussions. I also thank Prof. Jan Lundell, Prof. Matti Haukka and Dr. Rose Matilainen.

I gratefully acknowledge funding from the Foundation for Research of Natural Resources in Finland and Department of Chemistry.

Lastly, I thank my family and friends. In particular, I thank my mom, dad, brother, sister and grandmother for all the support. A special thanks goes to my other half Jennika for all the support during these years.

Jyväskylä, September 2016

Ville Härkönen

Abstract

The lattice thermal conductivity is usually an intrinsic property in the study of thermoelectricity. In particular, relatively low lattice thermal conductivity is usually a desired feature when higher thermoelectric efficiency is pursued. The mechanisms which lower the lattice thermal conductivity are not known in sufficient detail and deeper understanding about the phenomena is needed and if such understanding is achieved it can be used to design more efficient thermoelectric materials. In this thesis, the lattice thermal conductivity and other thermal properties of several silicon clathrates, which are known to be promising candidates for the thermoelectric applications, are studied by theoretical and computational techniques. The studied clathrates were the silicon clathrate frameworks I, II, IV, V, VII, VIII (Si_{23}), H and the semiconducting (Zintl) clathrates $[Si_{19}P_4]Cl_4$ and $Na_4[Al_4Si_{19}]$. The relevance of seemingly unrelated phenomena such as the negative thermal expansion on the lattice thermal conductivity was studied.

The harmonic phonon dispersion relations of the studied structures were investigated. In particular, the number of the so-called phonon band gaps was found to be two in the case of the silicon clathrate framework V differing in this respect from the other structures studied. In general, it was found that all the other clathrates, except VII and $Na_4[Al_4Si_{19}]$, have rather similar phonon dispersion relations. Also, an anomalous negative thermal expansion temperature range was found for the silicon clathrate framework VII, which appears to be mostly due to stronger third-order interatomic force constants.

At 300 K, the lattice thermal conductivity of the clathrate $Na_4[Al_4Si_{19}]$ was found to be about ten times smaller than obtained for the clathrate $[Si_{19}P_4]Cl_4$ which possess the same space group symmetry than the former. It appears that the main reason for the preceding is in the second-order interatomic force constants of the clathrate $Na_4[Al_4Si_{19}]$, which change the phonon spectrum such that the phonon group velocities are lower and the anharmonicity of the lattice increases, which in turn leads to the reduction in the relaxation times of acoustic phonons. The results indicate, that the effect of harmonic quantities can be rather large on the anharmonicity of two similar crystals and may lead to one-order lower lattice thermal conductivities, even when there are no such large differences in the third-order interatomic force constants.

Expressions to calculate different elastic and thermal properties of crystal were derived by using the technique of many-body Green's functions and many-body perturbation theory. The expressions derived extend the existing results and allow a systematic study of elastic and thermal properties of crystals. For instance, the results obtained can be used to calculate the kth-order elastic constants such that the so-called phonon contribution is taken into account, a contribution which is usually neglected in the computational studies applied to real materials at the present.

Author's address Ville Härkönen
Department of Chemistry
University of Jyväskylä
Finland

Supervisor Asst. Prof. Antti Karttunen
Department of Chemistry
Aalto University
Finland

Supervisor Dr. Gerrit Groenhof
Department of Chemistry
Nanoscience Center
University of Jyväskylä
Finland

Reviewers Prof. Gyaneshwar Srivastava
School of Physics
University of Exeter
United Kingdom

Dr. Ari Harju
Department of Applied Physics
Aalto University
Finland

Opponent Prof. Esa Räsänen
Department of Physics
Tampere University of Technology
Finland

List of publications

The results presented in this thesis are based on the publications and manuscripts listed below and they are referred by the Roman numerals (I-IV).

I V. J. Härkönen and A. J. Karttunen, *Ab initio* lattice dynamical studies of silicon clathrate frameworks and their negative thermal expansion, *Phys. Rev. B* **89**, 024305 (2014).

II V. J. Härkönen and A. J. Karttunen, *Ab initio* studies on the lattice thermal conductivity of silicon clathrate frameworks II and VIII, *Phys. Rev. B* **93**, 024307 (2016).

III V. J. Härkönen and A. J. Karttunen, *Ab initio* computational study on the lattice thermal conductivity of Zintl clathrates $[Si_{19}P_4]Cl_4$ and $Na_4[Al_4Si_{19}]$, *Phys. Rev. B* **94**, 054310 (2016).

IV V. J. Härkönen, Elastic constants and thermodynamical quantities for crystal lattices from many-body perturbation theory, *arXiv*:1603.06376.

Author's contribution

The author has done most of the numerical calculations in Articles I, II and III. The author is the principal writer of Articles I, II and III. The author has written and derived the results of Article IV.

Contents

Abbreviations

BTE	Boltzmann transport equation
CTE	coefficient of thermal expansion
DFPT	density functional perturbation theory
DFT	density functional theory
d-Si	silicon diamond structure
GGA	generalized gradient approximation
IFC	interatomic force constant
LDA	local density approximation
LSDA	local spin density approximation
MFP	mean free path
NTE	negative thermal expansion
PR	participation ratio
QHA	quasi-harmonic approximation
QE	Quantum Espresso
RT	relaxation time
SMRT	single mode relaxation time

1 Introduction

Thermoelectric materials can be used to produce electricity from temperature differences. Since waste heat is available in several circumstances, such as in the production of electricity by steam turbines, there are numerous applications of thermoelectric materials, where the energy efficiency of the system can be improved. An obstacle in the more extensive use of the thermoelectric materials is, for instance, the lack of materials with sufficiently high thermoelectric efficiency. In some cases, toxic elements such as lead included in the thermoelectric material [1] can be a problem when more extensive practical applications are considered. One class of crystalline solids, which can have rather high thermoelectric efficiency, are the so-called semiconducting clathrates [1–7], also known as Zintl clathrates. The semiconducting clathrates are usually known as host-guest compounds in which the framework of silicon atoms, for example, is partially filled with some guest atoms. Some practically guest free examples of such structures are also known [8, 9]. In this work, the properties related to thermoelectricity, in particular the lattice thermal conductivity of silicon clathrates, were studied by computational means.

One challenge in the development of more efficient thermoelectric materials is that the mechanisms to increase the thermoelectric efficiency are not known in sufficient detail. One measure of the thermoelectric efficiency is the thermoelectric figure of merit defined as [10, 11]

$$ZT = \frac{\sigma S^2 T}{\kappa_l + \kappa_{el}}, \tag{1.1}$$

where T is the absolute temperature, σ is the electrical conductivity, S the Seebeck coefficient, κ_l is the lattice thermal conductivity and κ_{el} is the electric contribution on the thermal conductivity. In particular, the Seebeck coefficient can be defined as $S = -\Delta V/\Delta T$, where ΔV is the electric potential energy difference per unit charge (voltage) measured between the ends of a thermoelectric material and ΔT is the temperature difference between the ends. To increase ZT and thus the thermoelectric efficiency, one has to maximize $\sigma S^2 T$ and minimize $\kappa_l + \kappa_{el}$. This can be a rather difficult task, since these terms are not independent, that is, a change in some term may lead to an unexpected change in some other term. In this work, the mechanisms which minimize the lattice thermal conductivity were studied. Deeper understanding about these mechanisms may in part give clues on how to develop more efficient thermoelectric materials.

The description of thermoelectric phenomenon is a challenge since in calculating the

thermoelectric efficiency one has to solve the quantum mechanical many-body problem with an appropriate method. The many-body problem itself includes several branches of research of its own [12–14]. Furthermore, in order to calculate the lattice thermal conductivity values for instance, one has to calculate several non-trivial lattice dynamical quantities, such as the interatomic force constants (IFCs), usually up to third-order. The foundations of the dynamical theory of the crystal lattices applied in modern calculations have been known for over half a century [15]. The *ab initio* computational methods, on the other hand, have been developed in past decades to a point, that it is possible to calculate the second-order IFCs in a systematic manner for arbitrary crystal structures by applying the density functional theory (DFT) and density functional perturbation theory (DFPT) [16, 17]. The preceding can be established, for instance, by using an open source program package Quantum Espresso (QE) [18], as it is done in the present work. Also, a third and higher-order IFCs have been calculated for some special cases by using DFPT [19]. A systematic calculation of the third-order IFCs for arbitrary crystal structures at the present can be established by using the finite displacement method implemented, for example, in an open source program package ShengBTE [20–22].

There are several theoretical and computational difficulties in the calculation of the lattice thermal conductivity. The measurement of the lattice thermal conductivity is performed when the system is not in an equilibrium, which makes the description rather complicated. For instance, at the present, there is no rigorous way to define the temperature when a system considered is not in an equilibrium [23]. Usually, as in the present work, methods used assume the system to be in a steady state in which one assumes a local equilibrium to exist [24, 25]. For instance, the linear response method applied on the thermal conductivity is expected to be valid only if the preceding assumption is made [24]. In this work, the description of lattice thermal conductivity was established by using the iterative solution of the linearized Boltzmann transport equation (BTE) implemented in ShengBTE. Theoretical and computational issues related to the present method were also investigated. In order to apply the linearized BTE to the calculation of lattice thermal conductivity, several lattice dynamical quantities are usually needed. The necessary lattice dynamical quantities can be obtained with the methods mentioned in the previous paragraph.

Seemingly unrelated properties may have some significance on the lattice thermal conductivity and discussions on these different properties are usually conducted separately. For instance, the negative thermal expansion (NTE) [26, 27] and thermal expansion in general, have a connection to the lattice thermal conductivity and there are some experimental evidence for this statement [28, 29] (measurements made for polycrystalline samples). The connection of the lattice thermal conductivity and the coefficient of thermal expansion (CTE) is also mathematical in the sense that the same quantities can be used to calculate them. This becomes evident when the quasiharmonic approximation (QHA) is used to calculate the CTE [30] and the lattice thermal

conductivity is approximated at higher temperatures with an expression derived from the linearized BTE [25]. A material is called a NTE material when the CTE has negative values within a particular temperature range. That is, a NTE material contracts when it is heated, which is an opposite what is perhaps usually expected to happen. Usually, the effect of CTE is neglected in the *ab initio* lattice thermal conductivity calculations for realistic materials, but there is at least one exception, namely the calculations conducted in Ref. [31]. The effect of thermal expansion on the electronic structure may also have a rather significant effect on the electrical conductivity and eventually on the thermoelectric properties of crystals.

The CTE is partly an anharmonic effect and it is usually studied by using the QHA [26, 30, 32–39]. When the anharmonic effects are sufficiently strong, the QHA may not describe CTE and related quantities appropriately and more accurate methods are needed. One approach to obtain the elastic and thermal properties is the many-body perturbation theory [40–42]. In Article IV, a systematic listing of the lowest-order terms was established such that the resulting formulas can be used to calculate various elastic and thermodynamical properties beyond the QHA, including the CTE. The resulting equations were also represented in diagrams.

This thesis is organized as follows. Some central entities in the description of the lattice thermal conductivity and thermal properties of the crystals are the phonons. Thus, the dynamical theory of crystal lattices, from which the concept of phonon arises, is presented in some detail in Sec. 2.2. The lattice thermal conductivity is discussed in Sec. 2.3 and the many-body perturbation theory, used to derive the results of Article IV, is considered in Sec. 2.4. The computational aspects of the quantum many-body problem are considered in Sec. 2.5 and some principles of the methods used to calculate the IFCs are described. The studied silicon clathrate structures are described in the beginning of Chapter 2 and the results of this thesis are summarized in Chapter 3.

2 Theory and computational methods

2.1 Semiconducting clathrates

The structural characteristics of the semiconducting clathrates have been considered, for example, in Refs. [4–6, 43]. Schematic figures of the silicon clathrate frameworks are shown in Fig. 2.1. The silicon clathrate frameworks are allotropes of silicon. That is, all structures consist of only Si atoms as in the case of the silicon diamond structure (d-Si), but the arrangement of the atoms is different. The mathematical description of the positions of atoms within a crystal structure is considered in Sec. 2.2. In this work, seven different silicon clathrate frameworks (I, II, IV, V, VII, VIII, H, see for instance Ref. [5]) and two different Zintl clathrates ($[Si_{19}P_4]Cl_4$, $Na_4[Al_4Si_{19}]$), were studied. As an example, the crystallographic body-centered cubic unit cell of the clathrates $[Si_{19}P_4]Cl_4$ and $Na_4[Al_4Si_{19}]$ is depicted in Fig. 2.2. The silicon clatharate framework VIII (or Si_{23}, shown also in Fig. 2.1) can be obtained by replacing the framework heteroatoms (also called framework guest atoms) Al/P with silicon atoms and by removing the Na/Cl guest atoms from the structure. In general, the number of possible combinations of guest atoms and clathrate frameworks is rather large, which makes possible to pursue the properties desired by changing the constituent elements. Also C, Ge or Sn could be used in the place of Si, which gives further possibilities to modify the properties in a direction desired. However, to the author's knowledge, only Si, Ge and Sn clathrates are experimentally known. The problem is that it is relatively difficult to say to which direction the different properties of the material change when something in the structure is changed. One approach is to try different combinations and experimentally measure what happens. An alternative approach, for example, is to use theoretical and computational methods in order to gather information about the structures and perhaps gain some further understanding about the mechanisms, which lead to certain properties. If a sufficient regularity with respect to some property is found, perhaps some deductions can be made to facilitate the search of more efficient thermoelectric materials, for instance. The latter approach was used in the present work.

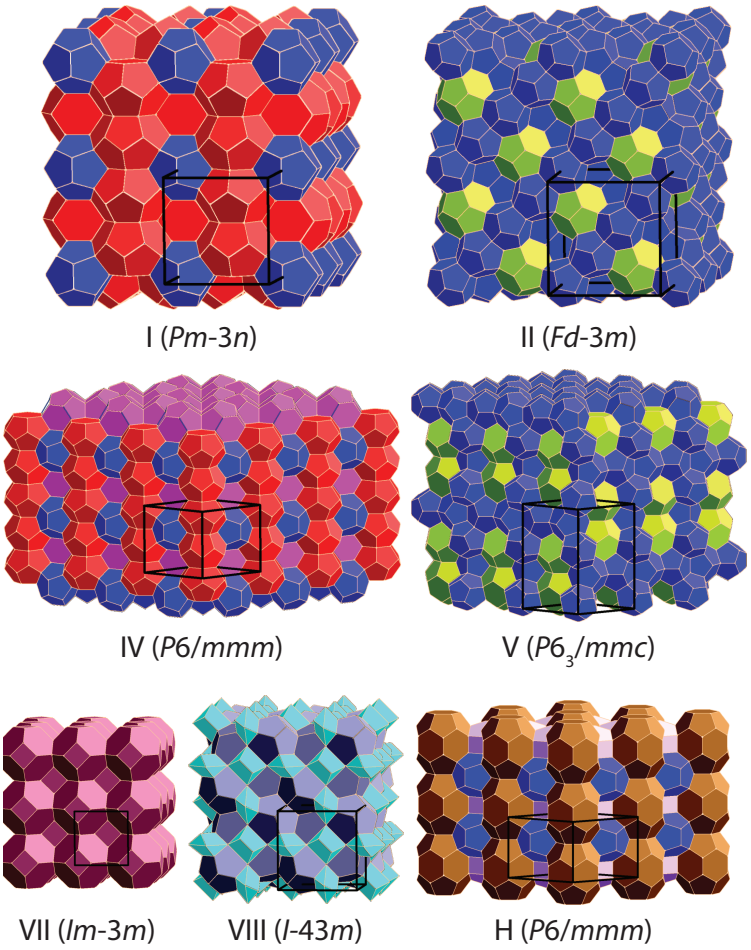

Figure 2.1: Schematic figures of the silicon clathrate frameworks. The vertices of the polyhedral cages present silicon atoms and crystallographic unit cell edges are drawn in black. Structural details and atomic positions of these structures can be found from Ref. [5] (optimized with different computational methods than used here). Copyright © 2014, American Physical Society.

2.2 Lattice dynamics

The description of lattice thermal conductivity and other quantities considered in this work can be made by using the theory of lattice dynamics [15, 42, 45, 46]. A crystal lattice can be considered a periodic array of atoms comprising the crystal. The rest positions of the atoms in a crystal lattice can be described by the vector $\mathbf{x}(l\kappa) \equiv \mathbf{x}(l) + \mathbf{x}(\kappa)$, $\kappa = 1, 2, \ldots, n$, where $\mathbf{x}(\kappa)$ is the position vector of atom κ within the unit cell and $\mathbf{x}(l)$ is the lattice translational vector given by

$$\mathbf{x}\left(l^{(1)}, l^{(2)}, l^{(3)}\right) \equiv \mathbf{x}(l) = l^{(1)}\mathbf{a}_1 + l^{(2)}\mathbf{a}_2 + l^{(3)}\mathbf{a}_3, \quad l^{(i)} \in \mathbb{Z}. \tag{2.1}$$

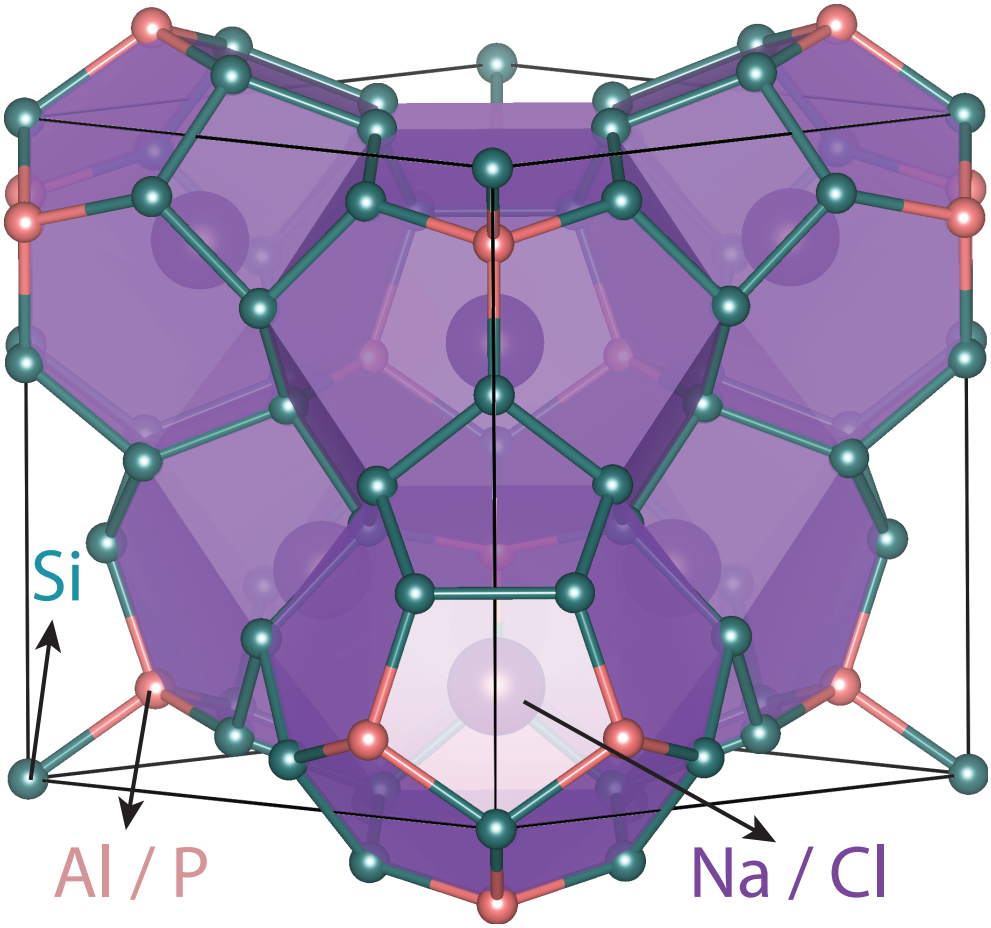

Figure 2.2: The crystallographic body-centered cubic unit cell of the semiconducting clathrates $[Si_{19}P_4]Cl_4$ and $Na_4[Al_4Si_{19}]$. The figure was prepared using the VESTA visualization program [44].

In Eq. (2.1), the vectors $\mathbf{a}_i$ are the primitive lattice translational vectors of the lattice. The rest positions, are also equilibrium positions if [15]: net forces for each atom vanish and in this configuration the stresses vanish. The atoms are expected to vibrate around the rest positions and these displacements are denoted as $\mathbf{u}(l\kappa)$ such that the instantaneous positions of the atoms can be written as $\mathbf{x}(l\kappa) + \mathbf{u}(l\kappa)$.

The lattice dynamical Hamiltonian H of the system is assumed to be a sum of kinetic T_n and potential energy terms Φ, that is $H = T_n + \Phi$. The kinetic energy is assumed to be

$$T_n = \frac{1}{2} \sum_{l,\kappa,\alpha} \frac{p_\alpha^2(l\kappa)}{M_\kappa}, \tag{2.2}$$

where $p_\alpha(l\kappa)$ is the αth Cartesian component of the momentum of the atom, M_κ the atomic mass of atom κ and the potential energy is assumed to be a function of

instantaneous positions of the atoms

$$\Phi = \Phi\left[\mathbf{x}\left(l_1\kappa_1\right) + \mathbf{u}\left(l_1\kappa_1\right), \ldots, \mathbf{x}\left(l_n\kappa_n\right) + \mathbf{u}\left(l_n\kappa_n\right)\right]. \tag{2.3}$$

The potential energy is expanded to a Taylor series in the displacements

$$\Phi = \sum_{n=0} \frac{1}{n!} \sum_{l_1,\kappa_1,\alpha_1} \cdots \sum_{l_n,\kappa_n,\alpha_n} \Phi_{\alpha_1\cdots\alpha_n}\left(l_1\kappa_1;\ldots;l_n\kappa_n\right) u_{\alpha_1}\left(l_1\kappa_1\right)\ldots u_{\alpha_n}\left(l_n\kappa_n\right), \tag{2.4}$$

where the so-called n*th*-order interatomic force constants (IFCs) are defined as

$$\Phi_{\alpha_1\cdots\alpha_n}\left(l_1\kappa_1;\ldots;l_n\kappa_n\right) \equiv \left.\frac{\partial^n\Phi}{\partial x'_{\alpha_1}\left(l_1\kappa_1\right)\cdots\partial x'_{\alpha_n}\left(l_n\kappa_n\right)}\right|_{\{x'(l_i\kappa_i)=x(l_i\kappa_i)\}}. \tag{2.5}$$

In the lattice dynamical context, the static potential energy contribution of the lattice in the expansion with $n = 0$ can usually be neglected and if the rest positions are equilibrium positions, the potential term with $n = 1$ vanishes. Since the lattice is assumed to be infinite, the quantities such as the potential energy of the lattice is infinite as well. To obtain finite and normalized values of physical quantities, the Born-von Karman boundary conditions are imposed [15]. Instead of an infinite crystal, macro crystals of finite size are considered and are assumed to be larger than the primitive unit cell of the lattice. It is assumed that, each macro crystal is composed of $L^3 = N$ primitive unit cells, L being arbitrary positive integer. The boundary conditions can be written as

$$\mathbf{u}\left(l\kappa\right) = \mathbf{u}\left(L + l\kappa\right), \quad \mathbf{x}\left(l\kappa\right) = \mathbf{x}\left(L + l\kappa\right), \tag{2.6}$$

which means that the displacements $\mathbf{u}\left(l\kappa\right)$ have equal values at the same site $l\kappa$ of every macro crystal. When the macro crystal is sufficiently large, the surface effects become relatively small as the number of surface atoms decreases rather rapidly with respect to the total number of atoms within the macro crystal. However, due to the periodic boundary conditions, the surface effects are absent. The convergence as a function of the macro crystal size can be tested by numerical calculations.

The next step could be the substitution of the Hamiltonian to the Hamiltonian equations of motion, but by doing so one obtains a coupled set of differential equations. There is an alternative approach in which the Hamiltonian is written as $H = H_0 + H_a$, with

$$H_0 = \frac{1}{2}\sum_{l,\kappa,\alpha} \frac{p_\alpha^2\left(l\kappa\right)}{M_\kappa} + \frac{1}{2!}\sum_{l,\kappa,\alpha}\sum_{l',\kappa',\beta} \Phi_{\alpha\beta}\left(l\kappa;l'\kappa'\right) u_\alpha\left(l\kappa\right) u_\beta\left(l'\kappa'\right), \tag{2.7}$$

$$H_a = \sum_{n\neq 0,2} \frac{1}{n!} \sum_{l_1,\kappa_1,\alpha_1} \cdots \sum_{l_n,\kappa_n,\alpha_n} \Phi_{\alpha_1\cdots\alpha_n}\left(l_1\kappa_1;\ldots;l_n\kappa_n\right) u_{\alpha_1}\left(l_1\kappa_1\right)\ldots u_{\alpha_n}\left(l_n\kappa_n\right), \tag{2.8}$$

Sometimes, H_0 and H_a are called the harmonic and anharmonic Hamiltonian, respectively. It turns out that by finding a set of suitable canonical transformations, one

can obtain the diagonal for the harmonic Hamiltonian H_0 and one obtains a set of decoupled equations of motion for $3n$ different modes of vibration.

For instance, the harmonic potential energy can be written as

$$\Phi_2 = \frac{1}{2} \sum_{l,\kappa,\alpha} \sum_{l',\kappa',\beta} D_{\alpha\beta}\left(l\kappa; l'\kappa'\right) w_\alpha\left(l\kappa\right) w_\beta\left(l'\kappa'\right), \tag{2.9}$$

where the mass reduced second-order IFCs and the mass reduced displacements are of the following form

$$D_{\alpha\beta}\left(l\kappa; l'\kappa'\right) = \frac{\Phi_{\alpha\beta}\left(l\kappa; l'\kappa'\right)}{\sqrt{M_\kappa M_{\kappa'}}}, \quad w_\alpha\left(l\kappa\right) = \sqrt{M_\kappa} u_\alpha\left(l\kappa\right). \tag{2.10}$$

One may obtain the diagonal form for the potential energy with the following transformations [15] (the justification of these steps is given below)

$$w_\alpha\left(l\kappa\right) = \frac{1}{N} \sum_{\mathbf{q}}^{N} w_\alpha\left(\kappa|\mathbf{q}\right) e^{i\mathbf{q}\cdot\mathbf{x}(l)}, \tag{2.11}$$

$$w_\alpha\left(\kappa|\mathbf{q}\right) = \sum_j e_\alpha\left(\kappa|\mathbf{q}j\right) Q_{\mathbf{q}j}, \tag{2.12}$$

and thus

$$w_\alpha\left(l\kappa\right) = \frac{1}{N} \sum_{\mathbf{q}j} e_\alpha\left(\kappa|\mathbf{q}j\right) e^{i\mathbf{q}\cdot\mathbf{x}(l)} Q_{\mathbf{q}j}. \tag{2.13}$$

In Eqs. (2.11)-(2.13), $\mathbf{q}$ is the wave vector times 2π, $j = 1, 2, \ldots, 3n$ is the mode index, $\mathbf{e}\left(\kappa|\mathbf{q}j\right)$ is the phonon eigenvector and $Q_{\mathbf{q}j}$ the (complex) normal coordinate. As in Refs. [42,46], the following notation $w_\alpha\left(\kappa|\mathbf{q}\right) = w_\alpha\left(\kappa; \mathbf{q}\right)$ is used. Further transformation to real normal coordinates is needed to obtain the real displacements (or waves) of the lattice [15, 46] from the displacements given by Eq. (2.13), but this is not established in the present work. In Eq. (2.11), the displacements were written as a Fourier series (due to the lattice periodicity) and in Eq. (2.12) further transformation was made in terms of the coordinates $\{Q_{\mathbf{q}j}\}$ and phonon eigenvectors $\{\mathbf{e}\left(\kappa|\mathbf{q}j'\right)\}$ to diagonalize the dynamical matrix defined by Eq. (2.22).

At this point, it is noted that the periodic boundary conditions restrict the possible values of the wave vector $\mathbf{q}$. The admissible values can be obtained as follows. Let

$$\mathbf{x}\left(mL\right) \equiv m_1 L\mathbf{a}_1 + m_2 L\mathbf{a}_2 + m_3 L\mathbf{a}_3, \qquad m_1, m_2, m_3 \in \mathbb{Z}, \tag{2.14}$$

Now, from the periodic boundary conditions it follows that

$$w_\alpha\left(l + mL, \kappa\right) = \frac{1}{N} \sum_{\mathbf{q}j} e_\alpha\left(\kappa|\mathbf{q}j\right) e^{i[\mathbf{q}\cdot\mathbf{x}(l)]} e^{i[\mathbf{q}\cdot\mathbf{x}(mL)]} Q_{\mathbf{q}j} = w_\alpha\left(l\kappa\right), \tag{2.15}$$

which implies that

$$e^{i[\mathbf{q}\cdot\mathbf{x}(mL)]} = 1. \tag{2.16}$$

These conditions are valid if the dot product between the wave vector and the translational vectors is $2\pi n$, $n \in \mathbb{Z}$. The wave vectors which satisfy the aforementioned condition belong to a reciprocal lattice. The reciprocal lattice translational vector can be defined in terms of the primitive reciprocal lattice translational vectors $\mathbf{b}^j$, namely

$$\mathbf{G}(h) \equiv \mathbf{G}\left(h_1\mathbf{b}^1, h_2\mathbf{b}^2, h_3\mathbf{b}^3\right) = h_1\mathbf{b}^1 + h_2\mathbf{b}^2 + h_3\mathbf{b}^3, \qquad h_1, h_2, h_3 \in \mathbb{Z}, \tag{2.17}$$

with

$$\mathbf{b}^1 = 2\pi\frac{\mathbf{a}_2\times\mathbf{a}_3}{|\mathbf{a}_1\cdot\mathbf{a}_2\times\mathbf{a}_3|}, \quad \mathbf{b}^2 = 2\pi\frac{\mathbf{a}_3\times\mathbf{a}_1}{|\mathbf{a}_1\cdot\mathbf{a}_2\times\mathbf{a}_3|}, \quad \mathbf{b}^3 = 2\pi\frac{\mathbf{a}_1\times\mathbf{a}_2}{|\mathbf{a}_1\cdot\mathbf{a}_2\times\mathbf{a}_3|}. \tag{2.18}$$

One can show that $\mathbf{a}_i\cdot\mathbf{b}^j = 2\pi\delta_{ij}$, which means that

$$\mathbf{x}(l)\cdot\mathbf{G}(h) = 2\pi\left(l_1h_1 + l_2h_2 + l_3h_3\right). \tag{2.19}$$

All distinct solutions for the displacements can be obtained if the wave vector values are restricted to the values given, for example, by

$$\mathbf{q}(h_1,h_2,h_3) \equiv \mathbf{q}(h) \equiv \mathbf{q} = \frac{h_1}{L}\mathbf{b}^1 + \frac{h_2}{L}\mathbf{b}^2 + \frac{h_3}{L}\mathbf{b}^3, \quad 0 \le h_j < L-1. \tag{2.20}$$

Thus, there is $L^3 = N$ different values for the integers h_1, h_2, h_3. In all cases considered in the present work, the wave vector mesh generated by Eq. (2.20) was used. In the actual calculations, QE and ShengBTE impose symmetry on the $\mathbf{q}$ meshes and there is no need to consider all the wave vectors included in Eq. (2.20) separately. Instead, one of the symmetry equivalent wave vectors is explicitly taken into account, while the effect of the others is included in the weighting function $W(\mathbf{q})$, which means that one replaces $1/N \to W(\mathbf{q})$ whenever there is a summation over $\mathbf{q}$.

Now the harmonic Hamiltonian H_0 is diagonalized. One may write after the substitution of Eq. 2.13 to Eq. 2.9

$$\begin{aligned}\Phi_2 &= \frac{1}{2N^2}\sum_{l,\kappa,\alpha}\sum_{l',\kappa',\beta}\sum_{\mathbf{q}j}\sum_{\mathbf{q}'j'} e_\alpha(\kappa|\mathbf{q}j)\, e^{i\mathbf{q}\cdot\mathbf{x}(l)} \\ &\quad \times D_{\alpha\beta}(l\kappa; l'\kappa')\, e_\beta(\kappa'|\mathbf{q}'j')\, e^{i\mathbf{q}'\cdot\mathbf{x}(l')} Q_{\mathbf{q}j}Q_{\mathbf{q}'j'} \\ &= \frac{1}{2N}\sum_{\mathbf{q},j,j'} Q^*_{\mathbf{q}j}Q_{\mathbf{q}j'}\sum_{\kappa,\alpha}\sum_{\kappa',\beta} e^*_\alpha(\kappa|\mathbf{q}j)\, D_{\alpha\beta}(\kappa\kappa'|\mathbf{q})\, e_\beta(\kappa'|\mathbf{q}j'),\end{aligned} \tag{2.21}$$

where the dynamical matrix is of the form

$$D_{\alpha\beta}(\kappa\kappa'|\mathbf{q}) \equiv \sum_l D_{\alpha\beta}(l\kappa; 0\kappa')\, e^{-i\mathbf{q}\cdot\mathbf{x}(l)}. \tag{2.22}$$

The dynamical matrix is Hermitian and the eigenvalue equation for this matrix can be written as

$$\omega_j^2(\mathbf{q})\, e_\alpha(\kappa|\mathbf{q}j) = \sum_{\kappa',\beta} D_{\alpha\beta}(\kappa\kappa'|\mathbf{q})\, e_\beta(\kappa'|\mathbf{q}j)\,. \tag{2.23}$$

In Eq. (2.23), $\omega_j(\mathbf{q})$ is the phonon eigenvalue (or phonon frequency) and $\mathbf{e}(\kappa|\mathbf{q}j')$ is the phonon eigenvector. Since the dynamical matrix is Hermitian, the eigenvectors can be chosen to satisfy

$$\sum_{\kappa,\alpha} e_\alpha(\kappa|\mathbf{q}j')\, e_\alpha^*(\kappa|\mathbf{q}j) = \delta_{jj'}, \tag{2.24}$$

$$\sum_{j} e_\alpha(\kappa|\mathbf{q}j)\, e_\beta^*(\kappa'|\mathbf{q}j) = \delta_{\alpha\beta}\delta_{\kappa\kappa'}. \tag{2.25}$$

If assumed that the displacements $w_\alpha(l\kappa)$ are real, it can be shown that $\mathbf{e}^*(\kappa|\mathbf{q}j) = \mathbf{e}(\kappa|-\mathbf{q}j)$, $\omega_j(-\mathbf{q}) = \omega_j(\mathbf{q})$ and $Q^*_{\mathbf{q}j} = Q_{-\mathbf{q}j}$. By using the results obtained so far, Eq. (2.21) can be written as

$$\Phi_2 = \frac{1}{2N}\sum_{\mathbf{q}=1}^{N}\sum_{j=1}^{3n} Q^*_{\mathbf{q}j} Q_{\mathbf{q}j}\omega_j^2(\mathbf{q})\,. \tag{2.26}$$

One may write in a similar way for the kinetic energy by noting that $p_\alpha^2(l\kappa)/M_\kappa = \dot{w}_\alpha^2(l\kappa)$ and after the calculation the harmonic Hamiltonian can be written as

$$H_0 = \frac{1}{2N}\sum_{\mathbf{q}=1}^{N}\sum_{j=1}^{3n}\left[Q^*_{\mathbf{q}j} Q_{\mathbf{q}j}\omega_j^2(\mathbf{q}) + \dot{Q}^*_{\mathbf{q}j}\dot{Q}_{\mathbf{q}j}\right]. \tag{2.27}$$

There are only diagonal terms in the harmonic Hamiltonian given by Eq. (2.27) and one may obtain the decoupled equations of motion when the Hamiltonian equations of motion are written for H_0. Further development in the lattice dynamical problem is established within the formalism of quantum mechanics in Sec. 2.2.1, which eventually allows the calculation of the quantities studied in the present work.

The actual calculation of the second-order IFCs and thus phonon eigenvalues and eigenvectors can be established by using the DFPT [17,18]. The preceding calculation is justified by the so-called harmonic approximation (a special case of an adiabatic approximation, see Sec. 2.5.1) [15]. In practice, the crystal structures are first optimized by the DFT together with the plane-wave basis and pseudopotentials from which the ground state electron density is obtained. Further, the second-order IFCs are obtained by applying the Hellmann-Feynman theorem [17, 47] (electron density *et cetera* needed). The used plane-wave basis sets, pseudopotentials and exchange-correlation energy approximations are listed in Articles I-III and the DFT method used is summarized in Sec. 2.5.2.

The calculation of the third-order IFCs can be conducted by applying the adiabatic approximation [15, 48]. In some special cases, the third-order IFCs have been calculated by using DFPT [19], but at the present, no open source code is available. Instead,

the third-order IFCs were calculated by using the finite-difference method, where the IFCs are obtained from the numerical derivatives of single point energies. Since the QE can calculate the force by applying the Hellmann-Feynman theorem [47,49], the finite differences are needed to calculate only the second-order numerical derivatives. This method is implemented in the ShengBTE program package [21, 22]. The adiabatic approximation justifies the preceding procedure provided the adiabatic approximation is valid for the description of the material considered. In particular, it is usually expected that the adiabatic approximation is valid for insulating and semiconducting crystals [42]. A more detailed description of the theoretical and computational techniques used to calculate the IFCs is given in Sec. 2.5.

2.2.1 Second quantization and phonons

The phonons can be considered as the collective excitations of a crystal lattice or in other words, the collective movement of the atoms comprising a crystal lattice. These excitations have similar properties as particles, for instance, phonons can have rather well defined energy. In this section, the second quantization [50] and occupation number representation is discussed in conjunction with phonons.

The occupation number representation is usually a rather convenient way to describe many-body systems in quantum mechanics and it turns out to be a quite useful technique in the lattice dynamical applications. Some principles of the method are summarized below. The many-body systems in quantum mechanics can be described by the spaces which are tensor products of the Hilbert spaces of one particle [51, 52]. If one considers a system of m identical particles, then the space which can be used to describe this system may be written as

$$\mathcal{H}^{\otimes m} = \underbrace{\mathcal{H} \otimes \cdots \otimes \mathcal{H}}_{\times m}, \tag{2.28}$$

where $\mathcal{H}$ is the single particle Hilbert space. If the number of particles is variable, then the space which describes the system is the so-called Fock space, which is a direct sum of tensor product spaces, namely [53]

$$\mathcal{F}(\mathcal{H}) = \oplus_{m=0}^{\infty} \mathcal{H}^{\otimes m} = \mathbb{C} \oplus \mathcal{H} \oplus (\mathcal{H} \otimes \mathcal{H}) \oplus \cdots . \tag{2.29}$$

The m particle states are described by the vectors $|\psi\rangle \in \mathcal{H}^{\otimes m}$ and any such state can be written as

$$|\psi\rangle = \sum_{i_1} \cdots \sum_{i_m} v_{i_1 \cdots i_m} \left|e_{i_1}^{(1)}\right\rangle \otimes \cdots \otimes \left|e_{i_m}^{(m)}\right\rangle, \tag{2.30}$$

where the basis is assumed to be discrete, the subscripts $\{i_j\}$ refer to basis states and the superscripts are particle labels. If the particles are identical, the latter may be omitted. Further, in Eq. (2.30), $v_{i_1 \cdots i_m}$ is the probability amplitude that there is one

particle in the state i_1, one particle in the state i_2,... and one particle in the state i_m. It is quite generally accepted that there are two classes of elementary particles in nature, namely, fermions and bosons. It turns out that the phonons are bosons and it seems that for bosons there are only symmetric states in nature. A system of identical bosons are thus described by symmetric spaces $\mathcal{H}_+^{\otimes m}$ and $\mathcal{F}_+(\mathcal{H})$. For instance, let $|\psi\rangle \in \mathcal{H}_+^{\otimes m}$, then

$$|\psi\rangle = \sum_{i_1,\ldots,i_m} v_{i_1\cdots i_m} \hat{S}_+ |e_{i_1}^{(1)}\rangle \otimes \cdots \otimes |e_{i_m}^{(m)}\rangle = \sum_{i_1,\ldots,i_m} v_{i_1\cdots i_m} \hat{S}_+ |e_{i_1} e_{i_2} \cdots e_{i_m}\rangle , \quad (2.31)$$

where the particle labels haven been neglected and the symmetrization operator is defined as

$$\hat{S}_+ \equiv \frac{1}{\sqrt{n!}} \sum_{\sigma_n} \hat{P}_{\sigma_n}, \quad (2.32)$$

where the summation is over all $n!$ permutations. There is some evidence that in the case of bosons, the system can be in the state in which several particles can be in the same state, that is, one could write for instance $v_{i_1 i_1 i_3 \cdots i_m}$. Therefore, in the case of bosons, one may say that $v_{i_1 i_2 \cdots i_m}$ is the probability amplitude that there is n_{i_1} particles in the state i_1, n_{i_2} particles in the state i_2, ... and n_{i_m} particles in the state i_m. Some of the $\left\{n_{i_j}\right\}$ may be zero or in an extreme case there could be $n_{i_j} = m$ and hence the other $\{n_{i_k}\}$ vanish. In the occupation number representation, the creation(annihilation) operators can be defined such that they create(annihilate) particles in the states, thus, these operators are maps (functions) within the Fock space and allow the description of various interaction processes. Indeed, the description of various interaction processes in terms of the creation and annihilation operators can be made in an arbitrary case since it can be shown [51] that any bosonic or fermionic operator can be written in terms of the creation and annihilation operators (including Hamiltonian). The symmetry(anti-symmetry) information of the states is included in the commutation(anti-commutation) relations of such operators. For example, the simple harmonic oscillator can be described with the mathematical construction discussed above. In this case the system may be described by the vectors belonging to symmetric Fock space (energy eigenbasis) [51]. The creation(annihilation) operator maps a ket $|n\rangle$ which belongs to an eigenvalue n to a ket which belongs to an eigenvalue $n+1(n-1)$. The same formalism can be used in the lattice dynamical problem, which is discussed below.

In the quantum mechanical treatment, the displacement $\mathbf{u}(l\kappa)$ and corresponding momentum $\mathbf{p}(l\kappa)$ are considered to be operators satisfying the following commutation relations (canonical quantization)

$$[\hat{u}_\alpha(l\kappa), \hat{u}_\beta(l'\kappa')]_- = [\hat{p}_\alpha(l\kappa), \hat{p}_\beta(l'\kappa')]_- = 0, \quad [\hat{u}_\alpha(l\kappa), \hat{p}_\beta(l'\kappa')]_- = i\hbar\delta_{ll'}\delta_{\kappa\kappa'}\delta_{\alpha\beta}. \quad (2.33)$$

The operators are denoted by the symbols with a hat placed on them. The displace-

ment given by Eq. (2.13) and the corresponding momentum may be written as

$$\hat{u}_\alpha(l\kappa) = \frac{1}{\sqrt{M_\kappa}N}\sum_{\mathbf{q}j} e_\alpha(\kappa|\mathbf{q}j)\, e^{i\mathbf{q}\cdot\mathbf{x}(l)}\hat{Q}_{\mathbf{q}j}, \tag{2.34}$$

$$\hat{p}_\alpha(l\kappa) = \frac{\sqrt{M_\kappa}}{N}\sum_{\mathbf{q}j} e_\alpha(\kappa|\mathbf{q}j)\, e^{i\mathbf{q}\cdot\mathbf{x}(l)}\frac{d}{dt}\hat{Q}_{\mathbf{q}j}. \tag{2.35}$$

The next step is similar to that taken in the simple harmonic oscillator case [51], that is, one defines $\hat{Q}_{\mathbf{q}j}$ and its time derivative as follows

$$\hat{Q}_{\mathbf{q}j} \equiv \left[\frac{\hbar}{2\omega_j(\mathbf{q})}\right]^{1/2}\left(\hat{a}_{\mathbf{q}j} + \hat{a}^\dagger_{-\mathbf{q}j}\right), \tag{2.36}$$

$$\frac{d}{dt}\hat{Q}_{\mathbf{q}j} \equiv -i\left[\frac{\hbar\omega_j(\mathbf{q})}{2}\right]^{1/2}\left(\hat{a}_{\mathbf{q}j} - \hat{a}^\dagger_{-\mathbf{q}j}\right). \tag{2.37}$$

and writes Eqs. (2.34) and (2.35) as

$$\hat{u}_\alpha(l\kappa) = \left(\frac{\hbar}{2N^2M_\kappa}\right)^{1/2}\sum_{\mathbf{q},j}\omega_j^{-1/2}(\mathbf{q})\, e^{i\mathbf{q}\cdot\mathbf{x}(l)}e_\alpha(\kappa|\mathbf{q}j)\left(\hat{a}_{\mathbf{q}j} + \hat{a}^\dagger_{-\mathbf{q}j}\right), \tag{2.38}$$

$$\hat{p}_\alpha(l\kappa) = -i\left(\frac{\hbar M_\kappa}{2N^2}\right)^{1/2}\sum_{\mathbf{q},j}\omega_j^{1/2}(\mathbf{q})\, e^{i\mathbf{q}\cdot\mathbf{x}(l)}e_\alpha(\kappa|\mathbf{q}j)\left(\hat{a}_{\mathbf{q}j} - \hat{a}^\dagger_{-\mathbf{q}j}\right), \tag{2.39}$$

where $\hat{a}^\dagger_{\mathbf{q}j}$ and $\hat{a}_{\mathbf{q}j}$ are the creation and annihilation operators for the phonon state $\mathbf{q}j$, respectively. The commutation relations for $\hat{a}^\dagger_{\mathbf{q}j}, \hat{a}_{\mathbf{q}j}$ follow from the commutation relations given by Eq. (2.33), namely

$$\left[\hat{a}^\dagger_{\mathbf{q}j}, \hat{a}^\dagger_{\mathbf{q}'j'}\right]_- = \left[\hat{a}_{\mathbf{q}j}, \hat{a}_{\mathbf{q}'j'}\right]_- = 0, \quad \left[\hat{a}_{\mathbf{q}j}, \hat{a}^\dagger_{\mathbf{q}'j'}\right]_- = \delta_{jj'}\Delta(\mathbf{q}-\mathbf{q}'). \tag{2.40}$$

Here

$$\Delta(\mathbf{q}-\mathbf{q}') = \frac{1}{N}\sum_l e^{i(\mathbf{q}-\mathbf{q}')\cdot\mathbf{x}(l)}, \tag{2.41}$$

which is unity if $\mathbf{q}-\mathbf{q}'$ is a translation vector of the reciprocal lattice (including zero) and otherwise zero. By denoting

$$\hat{A}_{\mathbf{q}j} = \hat{a}_{\mathbf{q}j} + \hat{a}^\dagger_{-\mathbf{q}j}, \quad \hat{B}_{\mathbf{q}j} = \hat{a}_{\mathbf{q}j} - \hat{a}^\dagger_{-\mathbf{q}j}, \quad \lambda \to \mathbf{q}j, \quad -\lambda \to -\mathbf{q}j, \tag{2.42}$$

and by using Eqs. (2.38) and (2.39) in the Hamiltonian $\hat{H} = \hat{H}_0 + \hat{H}_a$, one may write

$$\hat{H}_0 = \sum_\lambda \hbar\omega_\lambda\left(\frac{1}{2} + \hat{a}^\dagger_\lambda\hat{a}_\lambda\right) = \frac{1}{4}\sum_\lambda \hbar\omega_\lambda\left(\hat{A}^\dagger_\lambda\hat{A}_\lambda + \hat{B}^\dagger_\lambda\hat{B}_\lambda\right), \tag{2.43}$$

$$\hat{H}_a = \sum_\lambda V(\lambda)\,\hat{A}_\lambda + \sum_{n=3}\sum_{\lambda_1}\cdots\sum_{\lambda_n} V(\lambda_1;\ldots;\lambda_n)\,\hat{A}_{\lambda_1}\cdots\hat{A}_{\lambda_n}, \tag{2.44}$$

where

$$\begin{aligned} V\left(\mathbf{q}_1 j_1;\ldots;\mathbf{q}_n j_n\right) &= \frac{1}{n!N^n}\left(\frac{\hbar}{2}\right)^{n/2}\frac{\Delta\left(\mathbf{q}_1+\cdots+\mathbf{q}_n\right)}{\left[\omega_{j_1}\left(\mathbf{q}_1\right)\cdots\omega_{j_n}\left(\mathbf{q}_n\right)\right]^{1/2}} \\ &\times\sum_{\kappa_1,\alpha_1}\sum_{l_2,\kappa_2,\alpha_2}\cdots\sum_{l_n,\kappa_n,\alpha_n}\Phi_{\alpha_1\cdots\alpha_n}\left(0\kappa_1;l_2\kappa_2;\ldots;l_n'\kappa_n'\right) \\ &\times\frac{e_{\alpha_1}\left(\kappa_1|\mathbf{q}_1 j_1\right)}{M_{\kappa_1}^{1/2}}\cdots\frac{e_{\alpha_n}\left(\kappa_n|\mathbf{q}_n j_n\right)}{M_{\kappa_n}^{1/2}}e^{i[\mathbf{q}_2\cdot\mathbf{x}(l_2)+\cdots+\mathbf{q}_n\cdot\mathbf{x}(l_n)]}. \end{aligned} \tag{2.45}$$

From now on, the notations λ and $\mathbf{q}j$ are used interchangeably. Furthermore, the following notations are used $\omega_j\left(\mathbf{q}\right)=\omega\left(\lambda\right)=\omega_\lambda$. As mentioned earlier in this section, any operator can be written in terms of creation and annihilation operators and indeed this can be confirmed in the present case when Eqs. (2.43) and (2.44) are inspected. Usually, the eigenstates of the Hamiltonian $\hat{H}_0$ are considered to be stationary states of the system and $\hat{H}_a$ is treated as a perturbation. The preceding procedure is expected to produce reasonable results when the anharmonic Hamiltonian $\hat{H}_a$ is relatively small in comparison to $\hat{H}_0$.

When similar steps are made as in the simple harmonic oscillator case [51], it can be shown that the eigenstates of the Hamiltonian $\hat{H}_0$ can be written as

$$\left[\prod_{\mathbf{q}}^{N}\prod_{j}^{3n}\left(n_{\mathbf{q}j}!\right)^{-1/2}\left(\hat{a}_{\mathbf{q}j}^{\dagger}\right)^{n_{\mathbf{q}j}}\right]|0\rangle=|n_{\mathbf{q}_1 j_1}\cdots n_{\mathbf{q}_N j_{3n}}\rangle\,, \tag{2.46}$$

where $|0\rangle$ is the vacuum state and $|n_{\mathbf{q}_1 j_1}\cdots n_{\mathbf{q}_N j_{3n}}\rangle$ is the state with $n_{\mathbf{q}_1 j_1}$ phonons in the phonon state $\mathbf{q}_1 j_1$ *et cetera*. A space in which $|n_{\mathbf{q}_1 j_1}\cdots n_{\mathbf{q}_N j_{3n}}\rangle$ belongs is different from those referred so far and it belongs to a tensor product space in which the individual spaces in the tensor product are symmetrized Fock spaces and the Fock space which describes the system is the direct sum of these tensor product spaces. As in the simple harmonic oscillator case, the following relations hold for the creation and annihilation operators

$$\begin{aligned} \hat{a}_{\mathbf{q}j}^{\dagger}|n_{\mathbf{q}_1 j_1}\cdots n_{\mathbf{q}_N j_{3n}}\rangle &= \left(n_{\mathbf{q}j}+1\right)^{1/2}|n_{\mathbf{q}_1 j_1}\cdots n_{\mathbf{q}j}+1\cdots n_{\mathbf{q}_N j_{3n}}\rangle\,, \\ \hat{a}_{\mathbf{q}j}|n_{\mathbf{q}_1 j_1}\cdots n_{\mathbf{q}_N j_{3n}}\rangle &= \left(n_{\mathbf{q}j}\right)^{1/2}|n_{\mathbf{q}_1 j_1}\cdots n_{\mathbf{q}j}-1\cdots n_{\mathbf{q}_N j_{3n}}\rangle\,. \end{aligned} \tag{2.47}$$

Thus, $\hat{a}_{\mathbf{q}j}^{\dagger}$ and $\hat{a}_{\mathbf{q}j}$ are one-body operators which act only on vectors of one subspace in the tensor product leaving the others unchanged (identity operator for other spaces in the tensor product). Now, one may say that when $\hat{a}_{\mathbf{q}j}^{\dagger}$ acts on the eigenket of the harmonic Hamiltonian belonging to the eigenvalue $n_{\mathbf{q}j}$, another eigenket is obtained which belong to the eigenvalue $n_{\mathbf{q}j}+1$. By using the relations given in Eq. (2.47), one may write

$$\hat{H}_0|n_{\mathbf{q}_1 j_1}\cdots n_{\mathbf{q}_N j_{3n}}\rangle=\sum_{\mathbf{q}}^{N}\sum_{j}^{3n}\hbar\omega_j\left(\mathbf{q}\right)\left(\frac{1}{2}+n_{\mathbf{q}j}\right)|n_{\mathbf{q}_1 j_1}\cdots n_{\mathbf{q}_N j_{3n}}\rangle\,, \tag{2.48}$$

where $\hbar\omega_j(\mathbf{q})/2$ is the vacuum energy. Thus, $\hat{a}^\dagger_{\mathbf{q}j}$ increases the energy of the state $\mathbf{q}j$ by an amount $\hbar\omega_j(\mathbf{q})$ and it is said that one phonon is added on the state $\mathbf{q}j$. One cannot annihilate a phonon from the vacuum, therefore $\hat{a}_{\mathbf{q}j}|0\rangle = 0$. Further, kets belonging to different phonon numbers are orthonormal, which can be stated mathematically as

$$\langle n_{\mathbf{q}_N j_{3n}} \cdots n_{\mathbf{q}_1 j_1} | m_{\mathbf{q}_1 j_1} \cdots m_{\mathbf{q}_N j_{3n}} \rangle = \delta_{n_{\mathbf{q}_1 j_1} m_{\mathbf{q}_1 j_1}} \cdots \delta_{n_{\mathbf{q}_N j_{3N}} m_{\mathbf{q}_N j_{3N}}}. \tag{2.49}$$

The properties of the creation and annihilation operators given by Eqs. (2.40) and (2.47) are essential when the expressions for quantities such as the lifetimes of phonons are derived.

The definition of an operator $\hat{O}$ in the Heisenberg picture is

$$\hat{O}_H(t) \equiv e^{i\hat{H}t/\hbar}\hat{O}e^{-i\hat{H}t/\hbar}. \tag{2.50}$$

Within the harmonic approximation, the creation $\hat{a}^\dagger_{\mathbf{q}j,H}(t)$ and annihilation $\hat{a}_{\mathbf{q}j,H}(t)$ operators in the Heisenberg picture have the equations of motion

$$i\hbar\frac{d}{dt}\hat{a}_{\mathbf{q}j,H}(t) = \left[\hat{a}_{\mathbf{q}j,H}(t), \hat{H}_0\right]_-, \qquad i\hbar\frac{d}{dt}\hat{a}^\dagger_{\mathbf{q}j,H}(t) = \left[\hat{a}^\dagger_{\mathbf{q}j,H}(t), \hat{H}_0\right]_-, \tag{2.51}$$

when the Hamiltonian $\hat{H}_0$ has no explicit time dependence. In the present case, operators in the interaction picture are equivalent since the Hamiltonian $\hat{H}_0$ is used. By using the commutation rules given by Eq. (2.40), one may write

$$i\hbar\frac{d}{dt}\hat{a}_{\mathbf{q}j,H}(t) = \hbar\omega_j(\mathbf{q})\,\hat{a}_{\mathbf{q}j,H}(t), \qquad i\hbar\frac{d}{dt}\hat{a}^\dagger_{\mathbf{q}j,H}(t) = -\hbar\omega_j(\mathbf{q})\,\hat{a}^\dagger_{\mathbf{q}j,H}(t), \tag{2.52}$$

which are separable equations with the following solutions (here, the operators can be treated as numbers for each t)

$$\hat{a}_{\mathbf{q}j,H}(t) = \hat{a}_{\mathbf{q}j}e^{-i\omega_j(\mathbf{q})t}, \quad \hat{a}^\dagger_{\mathbf{q}j,H}(t) = \hat{a}^\dagger_{\mathbf{q}j}e^{i\omega_j(\mathbf{q})t}. \tag{2.53}$$

The integration was made over the interval $[0, t]$ and thus

$$\hat{a}_{\mathbf{q}j,H}(0) = \hat{a}_{\mathbf{q}j}, \quad \hat{a}^\dagger_{\mathbf{q}j,H}(0) = \hat{a}^\dagger_{\mathbf{q}j}. \tag{2.54}$$

2.2.2 Expansion of potential energy with respect to macroscopical variables

In order to calculate different physical quantities of a crystal such as the elastic properties, the following expansion of the Hamiltonian is made (see Refs. [15, 54] and

Article IV).

$$\begin{aligned}\hat{H}_p &= \sum_{m=1}\sum_{n_1=0}\cdots\sum_{n_m=0}\sum_{\alpha_1^{(1,1)}}\cdots\sum_{\alpha_{n_m}^{(m,h_m)}}\sum_{k_1=0}\sum_{\bar{\lambda}_{k_1}}\cdots\sum_{k_m=0}\sum_{\bar{\lambda}_{k_m}} \\ &\times g_{\bar{\lambda}_{k_m}}^{\alpha_1^{(1,1)}\cdots\alpha_{n_m}^{(m,h_m)}} f_{\alpha_1^{(1,1)}\cdots\alpha_1^{(1,h_1)}}\cdots f_{\alpha_{n_1}^{(1,1)}\cdots\alpha_{n_1}^{(1,h_1)}}\cdots \\ &\times f_{\alpha_1^{(2,1)}\cdots\alpha_1^{(2,h_2)}}\cdots f_{\alpha_{n_2}^{(2,1)}\cdots\alpha_{n_2}^{(2,h_2)}}\cdots f_{\alpha_1^{(m,1)}\cdots\alpha_1^{(m,h_m)}} \\ &\times\cdots f_{\alpha_{n_m}^{(m,1)}\cdots\alpha_{n_m}^{(m,h_m)}}\hat{A}_{\lambda_1}\cdots\hat{A}_{\lambda_{k_1}}\cdots\hat{A}_{\lambda_{1_m}}\cdots\hat{A}_{\lambda_{k_m}}, \end{aligned} \tag{2.55}$$

where the notation given by Eq. (2.60) is used and

$$\left\{f_{\alpha_{n_m}^{(m,1)}\cdots\alpha_{n_m}^{(m,h_m)}}\right\}, \tag{2.56}$$

is the set of mth macroscopic parameters with h_m indices. In expanding $\hat{H}_p$, it is first assumed that the Hamiltonian is a function of the macroscopic parameters and then a power expansion in these parameters is written. Then it is assumed that the coefficients g (indices neglected) of the preceding expansion are functions of the displacements $\hat{\mathbf{u}}(l\kappa)$ [and thus functions of the operators $\hat{A}_\lambda$, see Eq. (2.42)] and the second expansion is made in the displacements. Examples of such macroscopic parameters are the infinitesimal strain parameters (considered in Article IV) and electric field components. For instance, the expansion in terms of the infinitesimal strain parameters can be written as

$$\hat{H}_s = \sum_{m=1}\frac{1}{m!}\sum_{\bar{\mu}_m}\sum_{\bar{\nu}_m}\sum_{n=0}\sum_{\bar{\lambda}_n} V_{\bar{\mu}_m\bar{\nu}_m}\left(\bar{\lambda}_n\right)\bar{u}_{\mu_m\nu_m}\hat{A}_{\lambda_1}\cdots\hat{A}_{\lambda_n}. \tag{2.57}$$

where

$$\begin{aligned} V_{\mu_1\nu_1\cdots\mu_m\nu_m}(\lambda_1;\lambda_2;\cdots;\lambda_n) &= \frac{1}{n!}\sum_{\kappa_1,\alpha_1}\sum_{l_2\kappa_2,\alpha_2}\cdots\sum_{l_n\kappa_n,\alpha_n}\sum_{l_1'\kappa_1'}\sum_{l_2'\kappa_2'}\cdots\sum_{l_m'\kappa_m'} \\ &\times\Delta(\mathbf{q}_1+\mathbf{q}_2+\cdots+\mathbf{q}_n) \\ &\times\Phi_{\alpha_1\cdots\alpha_n\mu_1\cdots\mu_m}(0\kappa_1;l_2\kappa_2;\cdots;l_n\kappa_n;l_1'\kappa_1';\cdots;l_m'\kappa_m') \\ &\times T_{\alpha_1}(\lambda_1|0\kappa_1)\,T_{\alpha_2}(\lambda_2|l_2\kappa_2)\cdots T_{\alpha_n}(\lambda_n|l_n\kappa_n) \\ &\times x_{\nu_1}(l_1'\kappa_1')\,x_{\nu_2}(l_2'\kappa_2')\cdots x_{\nu_m}(l_m'\kappa_m'), \end{aligned} \tag{2.58}$$

and

$$T_\alpha(\lambda|l\kappa) = \left(\frac{\hbar}{2M_\kappa}\right)^{1/2}\omega_\lambda^{-1/2}e^{i\mathbf{q}\cdot\mathbf{x}(l)}e_\alpha(\kappa|\lambda). \tag{2.59}$$

In Eq. (2.57), the following notations are used

$$\begin{aligned}
\sum_{\bar{\mu}_m} &\equiv \sum_{\mu_1}\cdots\sum_{\mu_m}, \quad \sum_{\bar{\nu}_m} \equiv \sum_{\nu_1}\cdots\sum_{\nu_m}, \\
\bar{\mu}_m &\equiv \mu_1\cdots\mu_m, \quad \bar{\nu}_m \equiv \nu_1\cdots\nu_m, \\
\bar{u}_{\mu_m\nu_m} &\equiv u_{\mu_1\nu_1}\cdots u_{\mu_m\nu_m}, \\
\bar{\lambda}_n &\equiv \lambda_1;\lambda_2;\cdots;\lambda_n, \quad \sum_{\bar{\lambda}_n} \equiv \sum_{\lambda_1}\cdots\sum_{\lambda_n}, \\
V_{\bar{\mu}_m\bar{\nu}_m}\left(\bar{\lambda}_n\right) &\equiv V_{\mu_1\nu_1\cdots\mu_m\nu_m}\left(\lambda_1;\lambda_2;\cdots;\lambda_n\right). \qquad (2.60)
\end{aligned}$$

The total lattice Hamiltonian is now assumed to be of the following form

$$\hat{H}_d = \hat{H}_0 + \hat{H}_a + \hat{H}_s = \hat{H}_0 + \hat{H}_{int}, \qquad (2.61)$$

where $\hat{H}_0$ and $\hat{H}_a$ are given by Eqs. 2.43 and 2.44, respectively. The Hamiltonian $\hat{H}_d$ is used to derive the results of Article IV and the many-body perturbation theory used to derive these results is summarized in Sec. 2.4.

2.2.3 Physical interpretation of phonon eigenvectors

In this section, a physical interpretation of the phonon eigenvectors and the phase factors (like $e^{i\mathbf{q}\cdot\mathbf{x}(l)}$), is given. The interpretation is represented in Article IV and to the author's knowledge, no such similar interpretation in the lattice dynamical context has been given in the literature before. However, in the relativistic quantum field theory, a similar interpretation is given to unit spinors of spin-1/2 fields in the expansion of quantum field operators, which are in turn analogous to the polarization vectors of spin-1 fields [55].

Let $\{|l,\kappa,\alpha\rangle\}$ form a complete set (a basis) such that

$$\sum_{l,\kappa,\alpha} |l,\kappa,\alpha\rangle\langle\alpha,\kappa,l| = \hat{\mathbb{1}}. \qquad (2.62)$$

Then, one may write for the harmonic potential energy

$$\hat{\Phi}_2 = \frac{1}{2}\sum_{l,\kappa,\alpha}\sum_{l',\kappa',\beta}\Phi_{\alpha\beta,2}\left(l\kappa;l'\kappa'\right)|l,\kappa,\alpha\rangle\langle\beta,\kappa',l'|, \qquad (2.63)$$

where

$$\Phi_{\alpha\beta,2}\left(l\kappa;l'\kappa'\right) \equiv \langle\alpha,\kappa,l|\hat{\Phi}_2|l',\kappa',\beta\rangle. \qquad (2.64)$$

By comparing Eqs. 2.63, 2.64 and 2.9, one may identify

$$\Phi_{\alpha\beta,2}\left(l\kappa;l'\kappa'\right) = D_{\alpha\beta}\left(l\kappa;l'\kappa'\right), \qquad (2.65)$$

and

$$|l,\kappa,\alpha\rangle\langle\beta,\kappa',l'| = \hat{w}_\alpha(l\kappa)\,\hat{w}_\beta(l'\kappa'). \tag{2.66}$$

Further, one may write Eq. 2.63 as

$$\begin{aligned}\hat{\Phi}_2 &= \frac{1}{2}\sum_{l,\kappa,\alpha}\sum_{l',\kappa',\beta}\Phi_{\alpha\beta,2}(l\kappa;l'\kappa')\,|l,\kappa,\alpha\rangle\langle\beta,\kappa',l'| \\ &= \frac{1}{2N^2}\sum_{l,\kappa,\alpha}\sum_{l',\kappa',\beta}\sum_{\mathbf{q},j}\sum_{\mathbf{q}',j'}\langle j,\mathbf{q}|l,\kappa,\alpha\rangle\,D_{\alpha\beta}(l\kappa;l'\kappa')\,\langle\beta,\kappa',l'|\mathbf{q}',j'\rangle \\ &\quad\times|\mathbf{q},j\rangle\langle j',\mathbf{q}'|. \end{aligned}\tag{2.67}$$

Here, the notation is inexact for the quantities $\langle\mathbf{q},j|l,\kappa,\alpha\rangle$. The kets $|l,\kappa,\alpha\rangle$ and $|j,\mathbf{q}\rangle$ should belong to a space with equal dimensions and this is indeed the case when l and $\mathbf{q}$ is considered. The mode index has the values $j = 1,2,\ldots,3n$, and thus, to be more precise, one has to use a common index for the indices κ,α, which (as a pair) have $3n$ different values. For the sake of notational consistency with the eigenvectors $\mathbf{e}(\kappa|\mathbf{q}j)$ and dynamical matrix, the indices are written separately.

Now, a comparison of Eqs. 2.21 and 2.67 shows that one may identify

$$\langle\mathbf{q},j|l,\kappa,\alpha\rangle = e_\alpha(\kappa|\mathbf{q}j)\,e^{i\mathbf{q}\cdot\mathbf{x}(l)}, \tag{2.68}$$

and

$$|\mathbf{q},j\rangle\langle j',\mathbf{q}'| = \hat{Q}_{\mathbf{q}j}\hat{Q}_{\mathbf{q}'j'}. \tag{2.69}$$

By using quantum mechanical interpretation [51], the quantities, $\langle\mathbf{q},j|l,\kappa,\alpha\rangle$ in Eq. 2.68 can be considered as the probability amplitudes of $\{j'\}$ having the value j (for each $\mathbf{q}$) when $\{l',\kappa',\alpha'\}$ certainly have the values l,κ,α. In a similar way, one may consider

$$|\langle j,\mathbf{q}|l,\kappa,\alpha\rangle|^2 = |\langle j,\mathbf{q}|\kappa,\alpha\rangle|^2 = |e_\alpha(\kappa|\mathbf{q}j)|^2, \tag{2.70}$$

as the probability of $\{j'\}$ having the value j (for each $\mathbf{q}$) when $\{\kappa',\alpha'\}$ certainly have the values κ,α or the probability of $\{\kappa',\alpha'\}$ having the values κ,α when $\{j'\}$ certainly have the value j (for each $\mathbf{q}$). The probability is not affected by the phase factor $e^{i\mathbf{q}\cdot\mathbf{x}(l)}$ and thus, it is not affected by the cell index l (only phase difference matters). By using the present notation, the conditions for eigenvectors given by Eqs. 2.24 and 2.25 show that these probabilities are normalized (cell index l neglected)

$$\sum_\kappa|\langle j,\mathbf{q}|\kappa\rangle|^2 = \sum_j|\langle j,\mathbf{q}|\kappa,\alpha\rangle|^2 = 1, \tag{2.71}$$

where $|\langle j,\mathbf{q}|\kappa\rangle|^2 = |\mathbf{e}(\kappa|\mathbf{q}j)|^2$. In other words, one may interpret $|\mathbf{e}(\kappa|\mathbf{q}j)|^2$ as the probability that the atom κ vibrates in the phonon mode $\mathbf{q}j$. The interpretation given here is used in the analysis of the numerical results.

2.3 Description of lattice thermal conductivity

The lattice thermal conductivity $\kappa_{\alpha\beta}$ can be defined through the phenomenological Fourier relation

$$J_\alpha = -\sum_\beta \kappa_{\alpha\beta} \frac{\partial T}{\partial x_\beta}, \tag{2.72}$$

where J_α is the αth Cartesian component of the heat flux. The description of the lattice thermal conductivity by theoretical means is a rather challenging task since the crystal lattice is not in thermal equilibrium. Usually, it is assumed that the temperature behave rather smoothly as a function of position and thus one may assume that there is a local equilibrium in different parts of the crystal lattice. This simplifies the treatment. In the approach used in the present work, the following form for the heat flux is assumed

$$\mathbf{J} = \frac{1}{V} \sum_{\mathbf{q},j} \hbar\omega_j(\mathbf{q})\, \mathbf{v}(\mathbf{q}j)\, n_{\mathbf{q}j}. \tag{2.73}$$

where V is the volume of the unit cell, $n_{\mathbf{q}j}$ is the non-equilibrium phonon distribution function and $\mathbf{v}(\mathbf{q}j)$ is the phonon group velocity for the state labeled by $\mathbf{q}j$. However, it has been shown that the $\mathbf{J}$ given by Eq. (2.73) is a special case of more general heat flux [56]. All the other terms included in $\mathbf{J}$, except $n_{\mathbf{q}j}$, are known from the harmonic approximation. In the BTE approach [25, 57, 58], $n_{\mathbf{q}j}$ is approximated by

$$n_\lambda \approx \bar{n}_\lambda(\hbar\omega_\lambda + \mathbf{F}_\lambda \cdot \nabla T) = \frac{1}{e^{(\hbar\omega_\lambda + \mathbf{F}_\lambda \cdot \nabla T)\beta} - 1} \approx \bar{n}_\lambda + \left.\frac{\partial \bar{n}_\lambda}{\partial \hbar\omega'_\lambda}\right|_{\omega'_\lambda = \omega_\lambda} \mathbf{F}_\lambda \cdot \nabla T. \tag{2.74}$$

In Eq. (2.74), $\bar{n}_\lambda$ is the so-called Bose-Einstein distribution function [see Eq. (2.88) of Sec. 2.4.1]. When this approximate expression is used in Eq. (2.73), one can identify the lattice thermal conductivity to be

$$\kappa_{\alpha\beta} = \frac{\hbar}{k_B T V} \sum_\lambda \omega_\lambda v_\alpha(\lambda)\, \bar{n}_\lambda(\bar{n}_\lambda + 1)\, F_{\beta,\lambda}. \tag{2.75}$$

The unknown quantity $\mathbf{F}_\lambda$ can be solved iteratively by using the linearized BTE [22, 58–60] for the approximate distribution function n_λ. A summarized derivation for the iterative solution of $\mathbf{F}_\lambda$ was shown in Article II and the result can be written as

$$\begin{aligned} F_{\alpha,\lambda} &= \frac{1}{X_\lambda} \sum_{\lambda'} \sum_{\lambda''} \left[\Gamma^{\lambda''}_{\lambda\lambda'} (F_{\alpha,\lambda''} - F_{\alpha,\lambda'}) + \Gamma^{\lambda'\lambda''}_{\lambda} (F_{\alpha,\lambda'} + F_{\alpha,\lambda''}) \right] \\ &\quad + \frac{\hbar\omega_\lambda v_\alpha(\lambda)}{T X_\lambda} \bar{n}_\lambda(\bar{n}_\lambda + 1), \end{aligned} \tag{2.76}$$

where

$$X_\lambda \equiv \sum_{\lambda'} \sum_{\lambda''} \left(\Gamma^{\lambda''}_{\lambda\lambda'} + \Gamma^{\lambda'\lambda''}_{\lambda} \right) + \sum_{\lambda'} \Gamma^{\lambda'}_{\lambda}, \tag{2.77}$$

In Eqs. (2.76) and (2.77), $\Gamma_{\lambda}^{\lambda'\lambda''}$ is the scattering rate for a process in which a phonon labeled by λ vanishes and two phonons λ', λ'' are created, while $\Gamma_{\lambda\lambda'}^{\lambda''}$ is the scattering rate for an opposite process. Moreover, $\Gamma_{\lambda}^{\lambda'}$ is the scattering rate for a process in which a phonon labeled by λ vanishes and a phonon λ' is created. For example, $\Gamma_{\lambda}^{\lambda'}$ could be a scattering rate related to two phonon processes caused by the isotopic scattering [22, 61]. These scattering rates can be obtained from the so-called Golden rule or from the imaginary part of the phonon self-energy [62] (Sec. 2.4.2). The so-called generalized RTs are related to the $F_{\alpha,\lambda}$s through the relation [60]

$$\tau_{\alpha}(\lambda) = \frac{TF_{\alpha,\lambda}}{\hbar\omega_{\lambda}v_{\alpha}(\lambda)}, \tag{2.78}$$

and with these results, Eq. (2.75) can be written as

$$\kappa_{\alpha\beta} = \frac{1}{V}\sum_{\lambda} v_{\alpha}(\lambda)\, v_{\beta}(\lambda)\, c_{v}(\lambda)\, \tau_{\beta}(\lambda), \tag{2.79}$$

where the harmonic heat capacity at constant volume (strain) is of the form

$$c_{v}(\lambda) = k_{B}\beta^{2}\hbar^{2}\omega_{\lambda}^{2}\bar{n}_{\lambda}(\bar{n}_{\lambda}+1). \tag{2.80}$$

All the other quantities in Eq. (2.79), except $\tau_{\beta}(\lambda)$, can be obtained within the harmonic approximation. That is, in order to calculate the scattering rates $\Gamma_{\lambda}^{\lambda'\lambda''}$ and $\Gamma_{\lambda\lambda'}^{\lambda''}$, the third-order IFCs are needed. The computational details and convergence of the lattice thermal conductivity with respect to $\mathbf{q}$ mesh size was discussed in Articles II and III.

It is usually expected that the scattering rates $\Gamma_{\lambda}^{\lambda'\lambda''}, \Gamma_{\lambda\lambda'}^{\lambda''}$ are rather small at relatively low temperatures (such as temperatures below 50 K). Therefore, at low temperatures, other scattering mechanisms are usually the ones which mainly lower the lattice thermal conductivity. In ShengBTE, the isotopic scattering included is a rather rough approximation. Thus, the accuracy for the isotopic scattering rates is probably not comparable to the accuracy obtained for the scattering rates $\Gamma_{\lambda}^{\lambda'\lambda''}, \Gamma_{\lambda\lambda'}^{\lambda''}$. Indeed, this was verified in Article II (see also Sec. 3.3), where the experimental and computational results for *d*-Si were compared at low temperatures.

Before the iterative solution of the Boltzmann equation was established, various RT models were developed to describe the phonon scattering. To get the overall picture behind the relaxation time approximations, let

$$F_{\alpha,\lambda}^{0} \equiv \frac{\hbar\omega_{\lambda}v_{\alpha}(\lambda)}{TX_{\lambda}}\bar{n}_{\lambda}(\bar{n}_{\lambda}+1). \tag{2.81}$$

and

$$F_{\alpha,\lambda}^{(nd)} \equiv \frac{1}{X_{\lambda}}\sum_{\lambda'}\sum_{\lambda''}\left[\Gamma_{\lambda\lambda'}^{\lambda''}\left(F_{\alpha,\lambda''}-F_{\alpha,\lambda'}\right)+\Gamma_{\lambda}^{\lambda'\lambda''}\left(F_{\alpha,\lambda'}+F_{\alpha,\lambda''}\right)\right]. \tag{2.82}$$

Now, Eq. (2.76) can be written as $F_{\alpha,\lambda} = F^{(nd)}_{\alpha,\lambda} + F^{0}_{\alpha,\lambda}$. If one assumes that $F_{\alpha,\lambda'} = F_{\alpha,\lambda''} = 0$ for each $\lambda', \lambda'' \neq \lambda$, then $F_{\alpha,\lambda} = F^{0}_{\alpha,\lambda}$. The corresponding RT may be written as [Eq. (2.78)]

$$\tau^{0}_{\alpha}(\lambda) \equiv \frac{TF^{0}_{\alpha,\lambda}}{\hbar\omega_{\lambda} v_{\alpha}(\lambda)}, \tag{2.83}$$

which is called single mode relaxation time (SMRT) and if one uses this approximation to solve the RT, the approximation made is called single mode relaxation time approximation. The quantity $F_{\alpha,\lambda}$ is a measure of the deviation of phonon energy from the harmonic value. In SMRT the deviations $F_{\alpha,\lambda'} = F_{\alpha,\lambda''} = 0$ and thus all the other states are assumed to be in equilibrium except λ, from which the name SMRT originates. In SMRT, the RTs of the states are assumed to be independent. In general, as Eq. (2.76) shows, the preceding is not valid and the deviations of states from the equilibrium change the RTs of the other states. In times when the iterative solution of the BTE was not available, various approximations were developed to go beyond SMRT approximation, that is, approximations for $F^{(nd)}_{\alpha,\lambda}$ were developed. In Ref. [57], different approximations are discussed including the Klemens' [63], Callaway's [64] and Srivastava's [65–67] model.

2.4 Many-body perturbation theory applied on lattice dynamics

The method of many-body Green's functions and many-body perturbation theory are rather convenient methods in solving problems on various systems. In addition to condensed matter problems [13, 14, 40, 62, 68–74], the method is applied in the relativistic quantum field theory [55, 75–77]. There are several seemingly different many-body Green's function formalisms such as the zero temperature, real and imaginary time (temperature) Green's functions. These different techniques are treated together within the contour formalism discussed for instance in Refs. [14, 74]. The Green's functions can be used to calculate several different quantities of interest in many-body systems such as the ensemble average of an arbitrary operator or the ground and excited states of a system [12, 13]. The Green's functions are named after the British mathematical physicist George Green.

In the present work, mostly the imaginary time Green's functions were considered and in Article IV, the method of many-body Green's functions is used to derive the thermodynamical and elastic properties of crystals. In this section, the method is summarized and few example derivations of the results given in Article IV are shown. As already mentioned, the imaginary time Green's functions are related to the real time Green's functions. Sometimes the calculations are made by using the imaginary time Green's functions and the other Green's functions can be obtained by changing

time (or frequency) variables in an appropriate way. In Sec. 2.4.2 the determination of the retarded real time Green's function is performed by using the imaginary time Green's function formalism in order to obtain the lifetime of a phonon state.

2.4.1 Harmonic ensemble averages

In this section, few results for harmonic ensemble averages are given. These results are used in the actual calculations represented in Articles I-IV. The results of this section can be found for example from Refs. [15, 46, 78, 79]. An ensemble average of an operator $\hat{O}$ in canonical ensemble, can be written as

$$\left\langle \hat{O} \right\rangle = Z^{-1} \sum_{n} \langle n | e^{-\beta \hat{H}} \hat{O} | n \rangle \,, \tag{2.84}$$

where

$$Z = \sum_{n} \langle n | e^{-\beta \hat{H}} | n \rangle = Tr \left[e^{-\beta \hat{H}} \right], \tag{2.85}$$

and $|n\rangle$ is an eigenstate of the Hamiltonian $\hat{H}$. The harmonic ensemble average is denoted as

$$\left\langle \hat{O} \right\rangle_0 = Z_0^{-1} \sum_{n} \langle n | e^{-\beta \hat{H}_0} \hat{O} | n \rangle \,, \tag{2.86}$$

where the eigenstates and the summations over n can be written as (Sec. 2.2.1)

$$|n\rangle \equiv |n_{\mathbf{q}_1 j_1} \cdots n_{\mathbf{q}_N j_{3n}} \rangle \,, \quad \sum_{n} \equiv \sum_{n_{\mathbf{q}_1 j_1}=0}^{\infty} \cdots \sum_{n_{\mathbf{q}_N j_{3n}}=0}^{\infty} . \tag{2.87}$$

For example, by using the results of Sec. 2.2.1, an ensemble average of $\hat{n}_{\mathbf{q}j} = \hat{a}^{\dagger}_{\mathbf{q}j} \hat{a}_{\mathbf{q}j}$ can be written as

$$\langle \hat{n}_{\mathbf{q}j} \rangle_0 = \frac{1}{e^{\beta \hbar \omega_j(\mathbf{q})} - 1} \equiv \bar{n}_{\mathbf{q}j}, \tag{2.88}$$

which is the Bose-Einstein distribution function. By using Eqs. (2.43) and (2.88), one can write

$$\left\langle \hat{H}_0 \right\rangle_0 = \sum_{\mathbf{q},j} \hbar \omega_j(\mathbf{q}) \left(\bar{n}_{\mathbf{q}j} + \frac{1}{2} \right). \tag{2.89}$$

In a similar way, by using Eqs. (2.38), (2.39) and the result

$$\left\langle \hat{a}_{\mathbf{q}j} \hat{a}^{\dagger}_{\mathbf{q}j} \right\rangle_0 = \bar{n}_{\mathbf{q}j} + 1, \tag{2.90}$$

one may write for the displacement-displacement and momentum-momentum ensemble averages

$$\begin{aligned} \langle \hat{u}_\alpha(l\kappa)\, \hat{u}_\beta(l'\kappa') \rangle_0 &= \frac{\hbar}{2N (M_\kappa M_{\kappa'})^{1/2}} \sum_{\mathbf{q},j} e_\alpha(\kappa|\mathbf{q}j)\, e^*_\beta(\kappa'|\mathbf{q}j)\, \omega_j^{-1}(\mathbf{q}) \\ &\times \; e^{i\mathbf{q}\cdot[\mathbf{x}(l)-\mathbf{x}(l')]} (2\bar{n}_{\mathbf{q}j} + 1) \,, \end{aligned} \tag{2.91}$$

$$\begin{aligned}\left\langle \hat{p}_{\alpha}\left(l\kappa\right)\hat{p}_{\beta,H}\left(l'\kappa'\right)\right\rangle_{0} &= \frac{\hbar\left(M_{\kappa}M_{\kappa'}\right)^{1/2}}{2N}\sum_{\mathbf{q},j}e_{\alpha}\left(\kappa|\mathbf{q}j\right)e_{\beta}^{*}\left(\kappa'|\mathbf{q}j\right)\omega_{j}\left(\mathbf{q}\right)\\ &\times\ e^{i\mathbf{q}\cdot\left[\mathbf{x}(l)-\mathbf{x}(l')\right]}\left(2\bar{n}_{\mathbf{q}j}+1\right). \end{aligned} \tag{2.92}$$

For a physical interpretation, a special case of Eq. (2.91) is $\left\langle \hat{u}_{\alpha}^{2}\left(l\kappa\right)\right\rangle_{0}$, which is the mean square displacement of the atom $l\kappa$ from the equilibrium position $\mathbf{x}\left(l\kappa\right)$ in the direction α. The harmonic Helmholtz free energy can be expressed as

$$\begin{aligned}F_{0} &= -\beta^{-1}\ln Z_{0}=-\beta^{-1}\ln\left(\prod_{\mathbf{q}}^{N}\prod_{j}^{3n}\frac{e^{-\frac{1}{2}\beta\hbar\omega_{j}(\mathbf{q})}}{1-e^{-\beta\hbar\omega_{j}(\mathbf{q})}}\right)\\ &= \beta^{-1}\sum_{\mathbf{q},j}\left[\frac{1}{2}\beta\hbar\omega_{j}\left(\mathbf{q}\right)+\ln\left(1-e^{-\beta\hbar\omega_{j}(\mathbf{q})}\right)\right]. \end{aligned} \tag{2.93}$$

The definition of isothermal and adiabatic elastic constants can be made by expanding the Helmholtz free energy and internal energy to Taylor series in strains η_{ij} and temperature, that is [45, 78, 80]

$$\begin{aligned}F = \quad & F_{\eta_0}+\frac{\partial F}{\partial T'}T+\sum_{\mu,\nu=1}^{3}\frac{\partial F}{\partial\eta'_{\mu\nu}}\eta_{\mu\nu}+\sum_{\mu,\nu=1}^{3}\frac{\partial^{2}F}{\partial\eta'_{\mu\nu}\partial T'}\eta_{\mu\nu}T\\ & +\frac{1}{2}\sum_{\mu_1,\nu_1,\mu_2,\nu_2,l=1}^{3}\frac{\partial^{2}F}{\partial\eta'_{\mu_1\nu_1}\partial\eta'_{\mu_2\nu_2}}\eta_{\mu_1\nu_1}\eta_{\mu_2\nu_2}+\cdots,\\ U = \quad & U_{\eta_0}+\frac{\partial U}{\partial T'}T+\sum_{\mu,\nu=1}^{3}\frac{\partial U}{\partial\eta'_{\mu\nu}}\eta_{\mu\nu}+\sum_{\mu,\nu=1}^{3}\frac{\partial^{2}U}{\partial\eta'_{\mu\nu}\partial T'}\eta_{\mu\nu}T\\ & +\frac{1}{2}\sum_{\mu_1,\nu_1,\mu_2,\nu_2,l=1}^{3}\frac{\partial^{2}U}{\partial\eta'_{\mu_1\nu_1}\partial\eta'_{\mu_2\nu_2}}\eta_{\mu_1\nu_1}\eta_{\mu_2\nu_2}+\cdots, \end{aligned} \tag{2.94}$$

where the finite strain parameters may be written in terms of the infinitesimal strain parameters as

$$\eta_{\mu\nu}=\frac{1}{2}\left(u_{\mu\nu}+u_{\nu\mu}+\sum_{\epsilon}u_{\epsilon\mu}u_{\epsilon\nu}\right). \tag{2.95}$$

The coefficients in Eq. 2.94 are

$$\frac{\partial F}{\partial T}=-S,\quad \frac{\partial F}{\partial\eta_{\mu\nu}}=\sigma_{\mu\nu}^{T},\quad \frac{\partial U}{\partial T}=C_{\eta},\quad \frac{\partial U}{\partial\eta_{\mu\nu}}=\sigma_{\mu\nu}^{A}, \tag{2.96}$$

where S is the entropy, C_{η} the heat capacity at constant strain (volume), $\sigma_{\mu\nu}^{T}$ the isothermal stress and $\sigma_{\mu\nu}^{A}$ the adiabatic stress. Moreover, the kth-order adiabatic and isothermal elastic constants may be written as

$$\frac{\partial^{k}F}{\partial\eta_{\mu_1\nu_1}\cdots\partial\eta_{\mu_k\nu_k}}=c_{\mu_1\nu_1\cdots\mu_k\nu_k}^{T},\quad \frac{\partial^{k}U}{\partial\eta_{\mu_1\nu_1}\cdots\partial\eta_{\mu_k\nu_k}}=c_{\mu_1\nu_1\cdots\mu_k\nu_k}^{A}. \tag{2.97}$$

Now, the free energy F_0 can be used to derive other thermodynamical and elastic properties (within QHA) as it is done in Article IV, for example

$$\begin{aligned}
S_0 &= \frac{\beta}{T}\frac{\partial F_0}{\partial \beta} = \sum_\lambda \frac{\hbar\omega_\lambda}{T}\left(\bar{n}_\lambda + \frac{1}{2}\right) - k_B \sum_\lambda \ln\left(\left[\bar{n}_\lambda\left(\bar{n}_\lambda+1\right)\right]^{-1/2}\right), \\
U_0 &= \sum_\lambda \hbar\omega_\lambda\left(\bar{n}_\lambda + \frac{1}{2}\right) = \sum_\lambda U_0\left(\lambda\right), \\
C_{\eta,0} &= \frac{\partial U_0}{\partial T} = k_B \sum_\lambda \left[\hbar\omega_\lambda\beta\right]^2 \bar{n}_\lambda\left(\bar{n}_\lambda+1\right) = \sum_\lambda c_\eta\left(\lambda\right), \\
\frac{\partial^2 F_0}{\partial\eta_{\mu\nu}\partial\eta_{\mu'\nu'}} &= c^T_{\mu\nu\mu'\nu',0} = -\sum_\lambda\left[U_0\left(\lambda\right)\gamma_{\mu\nu\mu'\nu'}\left(\lambda\right) - T c_\eta\left(\lambda\right)\gamma_{\mu\nu}\left(\lambda\right)\gamma_{\mu'\nu'}\left(\lambda\right)\right], \\
\gamma_{\mu_1\nu_1\cdots\mu_n\nu_n}\left(\lambda\right) &= -\frac{1}{\omega_\lambda}\frac{\partial^n\omega_\lambda}{\partial\eta_{\mu_1\nu_1}\partial\eta_{\mu_2\nu_2}\cdots\partial\eta_{\mu_n\nu_n}},
\end{aligned} \tag{2.98}$$

where S_0 is the harmonic entropy, U_0 is the harmonic internal energy, $C_{\eta,0}$ is the harmonic heat capacity at constant strain, $c^T_{\mu\nu\mu'\nu',0}$ is the second-order isothermal elastic constant (within QHA) and $\gamma_{\mu_1\nu_1\cdots\mu_n\nu_n}\left(\lambda\right)$ is the so-called generalized Grüneisen parameter. In the expression of $c^T_{\mu\nu\mu'\nu',0}$ given by Eq. (2.98), the static lattice contribution is neglected. The CTE within the QHA can be written as [78] (subscript 0 neglected)

$$\frac{\partial\eta_{\mu_1\nu_1}}{\partial T} = \alpha_{\mu_1\nu_1} = \sum_{\mu_2,\nu_2=1}^{3} s^T_{\mu_1\nu_1\mu_2\nu_2}\sum_\lambda c_v\left(\lambda\right)\gamma_{\mu_2\nu_2}\left(\lambda\right). \tag{2.99}$$

Here, $s^T_{\mu_1\nu_1\mu_2\nu_2}$ is the tensor inverse of the tensor $c^T_{\mu_1\nu_1\mu_2\nu_2}$, namely

$$\sum_{\mu_2,\nu_2=1}^{3} c^T_{\mu_1\nu_1\mu_2\nu_2} s^T_{\mu_2\nu_2\mu_3\nu_3} = \delta_{\mu_1\mu_3}\delta_{\nu_1\nu_3}. \tag{2.100}$$

The inversion of $s^T_{\mu_1\nu_1\mu_2\nu_2}$ and $c^T_{\mu_1\nu_1\mu_2\nu_2}$ is discussed, for example, in Ref. [79]. In the case of cubic crystal structures, for example, one may write

$$\begin{aligned}
s^T_{1111} &= \frac{c^T_{1111}+c^T_{1122}}{\left(c^T_{1111}-c^T_{1122}\right)\left(c^T_{1111}+2c^T_{1122}\right)}, \\
s^T_{1122} &= -\frac{c^T_{1122}}{\left(c^T_{1111}-c^T_{1122}\right)\left(c^T_{1111}+2c^T_{1122}\right)}, \\
s^T_{2323} &= 1/c^T_{2323}.
\end{aligned} \tag{2.101}$$

A special case of Eq. (2.99) was used in the numerical calculations conducted in Article I for cubic structures, where only the static lattice contribution to bulk modulus B_T was taken into account, namely

$$\alpha_V = \frac{1}{B_T V}\sum_\lambda c_v\left(\lambda\right)\gamma\left(\lambda\right), \tag{2.102}$$

In Eq. (2.102), α_V is the volumetric CTE and B_T is the isothermal bulk modulus defined in the case of cubic crystals as [78, 79]

$$\frac{1}{B_T} \equiv 3\left(s^T_{1111} + 2s^T_{1122}\right) = \frac{3}{c^T_{1111} + 2c^T_{1122}}. \tag{2.103}$$

Further, $\gamma(\lambda)$ is the volumetric Grüneisen parameter [81]

$$\gamma(\lambda) \equiv -\frac{V}{\omega_\lambda}\frac{\partial \omega_\lambda}{\partial V}. \tag{2.104}$$

Since only the static lattice contribution to B_T was included, the temperature dependence of B_T was neglected in Article I. In Article IV, expressions, for instance, for the CTE was derived by applying many-body perturbation theory. The CTE have a connection to lattice thermal conductivity and this is discussed in Article III (see also Sec. 3.2).

2.4.2 Green's functions and phonon self-energy

The evaluation of the perturbation expansion which is used to derive the results of Article IV (considered in Sec. 2.4.3) can be made by using some results from the theory of the many-body Green's functions [12–14, 54, 62, 68–70, 72–74], namely

$$\begin{aligned}
G_0(\lambda\tau|\lambda'\tau') &\equiv \left\langle \mathcal{T}\left\{\hat{A}_{\lambda,I}(\tau)\,\hat{A}_{\lambda',I}(\tau')\right\}\right\rangle_0 = G_0(\lambda\tau|\lambda' 0) \\
&= \theta(\tau)\left\langle \hat{A}_{\lambda,I}(\tau)\,\hat{A}_{\lambda',I}(0)\right\rangle_0 + \theta(-\tau)\left\langle \hat{A}_{\lambda',I}(0)\,\hat{A}_{\lambda,I}(\tau)\right\rangle_0 \\
&= \delta_{\lambda(-\lambda')}\theta(\tau)\left[e^{\hbar\omega_\lambda\tau}\bar{n}_\lambda + e^{-\hbar\omega_\lambda\tau}(\bar{n}_\lambda+1)\right] \\
&\quad +\delta_{\lambda(-\lambda')}\theta(-\tau)\left[e^{-\hbar\omega_\lambda\tau}\bar{n}_\lambda + e^{\hbar\omega_\lambda\tau}(\bar{n}_\lambda+1)\right], \\
G_0(\lambda\tau|\lambda'\tau) &= \delta_{\lambda(-\lambda')}(2\bar{n}_\lambda+1), \quad \delta_{\lambda(-\lambda')} = \delta_{jj'}\Delta(\mathbf{q}+\mathbf{q}'), \\
G_0(\lambda\tau|\lambda 0) &\equiv G_0(\lambda\tau) = \sum_{n=-\infty}^{\infty} G_0(\lambda|\omega_n)\,e^{i\omega_n\tau}, \\
G_0(\lambda|\omega_n) &= \frac{2\omega_\lambda}{\beta\hbar\left[\omega_\lambda^2+\omega_n^2\right]}, \quad \omega_n = \frac{2\pi n}{\beta\hbar}, \\
G_0(\lambda|\omega_n) &= \frac{1}{\beta}\int_0^\beta G_0(\lambda\tau|\lambda' 0)\,e^{-i\omega_n\tau}.
\end{aligned} \tag{2.105}$$

In Eq. (2.105), $\theta(\tau)$ is the Heaviside step function, the time ordering $\mathcal{T}\{\cdots\}$ is defined by the second row and the operators are in the interaction picture

$$\hat{A}_{\lambda,I}(\tau) = e^{\tau\hat{H}_0}\hat{A}_\lambda e^{-\tau\hat{H}_0}. \tag{2.106}$$

The method of many-body Green's functions can be used to derive expressions for the lifetimes of phonons, as it is done in Ref. [62]. This can be done by evaluation of the Fourier transform of the interacting one-body Green's function

$$\begin{aligned} G\left(\lambda\tau|\lambda'\right) &\equiv \left\langle \mathcal{T}\left\{\hat{A}_{\lambda}\left(\tau\right)\hat{A}_{\lambda'}\left(0\right)\right\}\right\rangle \\ &= \sum_{k=0}^{\infty}\frac{\left(-1\right)^{k}}{k!}\left\langle \mathcal{T}\left\{\left[\prod^{k}\int_{0}^{\beta}d\tau_{k}\hat{H}_{a}\left(\tau_{k}\right)\right]\hat{A}_{\lambda,I}\left(\tau\right)\hat{A}_{\lambda',I}\left(0\right)\right\}\right\rangle_{0,c}. \end{aligned} \tag{2.107}$$

where the subscript c indicates that only the so-called connected terms in the expansion are taken into account. A derivation of such perturbation expansion can be found, for example, from Refs. [13, 14]. A similar expansion was also used to derive the results of Article IV. A derivation of the aforementioned expansion is given in Sec. 2.4.3. The ensemble averages in the perturbation expansion given by Eq. (2.107) can be simplified by using Wick's Theorem of the following form [54, 74, 82]

$$\left\langle \mathcal{T}\left\{\hat{A}_{\lambda_1}\cdots\hat{A}_{\lambda_{2n}}\right\}\right\rangle_{0,c} = \sum_{k=2}^{2n}\left\langle \mathcal{T}\left\{\hat{A}_{\lambda_1}\hat{A}_{\lambda_k}\right\}\right\rangle_{0}\left\langle \mathcal{T}\left\{\prod_{l\neq 1,k}^{2n}\hat{A}_{\lambda_l}\right\}\right\rangle_{0,c}. \tag{2.108}$$

For instance, one may write for the ensemble average of four operators

$$\begin{aligned} \left\langle \mathcal{T}\left\{\hat{A}_{\lambda_1}\cdots\hat{A}_{\lambda_4}\right\}\right\rangle_{0,c} &= \left\langle \mathcal{T}\left\{\hat{A}_{\lambda_1}\hat{A}_{\lambda_2}\right\}\right\rangle_{0}\left\langle \mathcal{T}\left\{\hat{A}_{\lambda_3}\hat{A}_{\lambda_4}\right\}\right\rangle_{0} \\ &\quad + \left\langle \mathcal{T}\left\{\hat{A}_{\lambda_1}\hat{A}_{\lambda_3}\right\}\right\rangle_{0}\left\langle \mathcal{T}\left\{\hat{A}_{\lambda_2}\hat{A}_{\lambda_4}\right\}\right\rangle_{0} \\ &\quad + \left\langle \mathcal{T}\left\{\hat{A}_{\lambda_1}\hat{A}_{\lambda_4}\right\}\right\rangle_{0}\left\langle \mathcal{T}\left\{\hat{A}_{\lambda_2}\hat{A}_{\lambda_3}\right\}\right\rangle_{0}. \end{aligned} \tag{2.109}$$

Further, one may use the following symmetry properties of the coefficients [the notation from Eq. (2.60) is used]

$$\begin{aligned} V\left(\lambda_1;\lambda_2;\ldots;\lambda_n\right) &= V\left(\lambda_2;\lambda_1;\ldots;\lambda_n\right) = \cdots, \\ V_{\bar{\mu}_m\bar{\nu}_m}\left(\lambda_1;\lambda_2;\ldots;\lambda_n\right) &= V_{\bar{\mu}_m\bar{\nu}_m}\left(\lambda_2;\lambda_1;\ldots;\lambda_n\right) = \cdots, \end{aligned} \tag{2.110}$$

to identify identical terms in the expansion. In some cases, the preceding symmetry relations may lead to a rather significant reduction of computational requirements. In Ref. [62], the following terms in the expansion of $G\left(\lambda\tau|\lambda'\right)$ were included

$$\begin{aligned} G\left(\lambda\tau|\lambda'\right) &\approx -\int_{0}^{\beta}d\tau_1\left\langle \mathcal{T}\left\{\hat{H}_4\left(\tau_1\right)\hat{A}_{\lambda,I}\left(\tau\right)\hat{A}_{\lambda',I}\left(0\right)\right\}\right\rangle_{0,c} \\ &\quad + \frac{1}{2}\int_{0}^{\beta}d\tau_1\int_{0}^{\beta}d\tau_2\left\langle \mathcal{T}\left\{\hat{H}_3\left(\tau_1\right)\hat{H}_3\left(\tau_2\right)\hat{A}_{\lambda,I}\left(\tau\right)\hat{A}_{\lambda',I}\left(0\right)\right\}\right\rangle_{0,c}, \end{aligned} \tag{2.111}$$

where $\hat{H}_3$ and $\hat{H}_4$ are the third and fourth-order Hamiltonian terms given in Eq. (2.44), respectively. After the substitution of the Hamiltonians and applying Wick's

Theorem given by Eq. (2.108), the Fourier transform of Eq. (2.111) can be written as (here $\lambda \to \mathbf{q}_1 j_1$, $\lambda' \to \mathbf{q}_2 j_2$)

$$\begin{aligned} G\left(\mathbf{q}_1 j_1; \mathbf{q}_2 j_2 | \omega_n\right) &= -12\beta \sum_{\mathbf{q}_3, j_3} V\left(\mathbf{q}_1 j_1; \mathbf{q}_2 j_2; \mathbf{q}_3 j_3; -\mathbf{q}_3 j_3\right) \left(2\bar{n}_{\mathbf{q}_3 j_3} + 1\right) \\ &\times G_0\left(\mathbf{q}_1 j_1 | \omega_n\right) G_0\left(\mathbf{q}_2 j_2 | \omega_n\right) \\ &+18\beta^2 \sum_{\mathbf{q}_1', j_1'} \sum_{\mathbf{q}_2', j_2'} V\left(\mathbf{q}_1 j_1; \mathbf{q}_2 j_2; \mathbf{q}_1' j_1'\right) V\left(-\mathbf{q}_1' j_1'; \mathbf{q}_2' j_2'; -\mathbf{q}_2' j_2'\right) \\ &\times G_0\left(\mathbf{q}_1 j_1 | \omega_n\right) G_0\left(\mathbf{q}_2 j_2 | \omega_n\right) \left(2\bar{n}_{\mathbf{q}_2' j_2'} + 1\right) G_0\left(\mathbf{q}_1' j_1' | \omega_{n'} = 0\right) \\ &+18\beta^2 \sum_{\mathbf{q}_1', j_1'} \sum_{\mathbf{q}_2', j_2'} V\left(\mathbf{q}_1 j_1; \mathbf{q}_1' j_1'; \mathbf{q}_2' j_2'\right) \\ &\times V\left(\mathbf{q}_2 j_2; -\mathbf{q}_1' j_1'; -\mathbf{q}_2' j_2'\right) G_0\left(\mathbf{q}_1 j_1 | \omega_n\right) G_0\left(\mathbf{q}_2 j_2 | \omega_n\right) \\ &\times \sum_{n', n''=-\infty}^{\infty} G_0\left(\mathbf{q}_1' j_1' | \omega_{n'}\right) G_0\left(\mathbf{q}_2' j_2' | \omega_{n''}\right) \delta_{-n+n'+n''}. \end{aligned} \tag{2.112}$$

In obtaining Eq. (2.112), the following result was used

$$\int_0^\beta d\tau e^{i\omega_n \tau} = \beta \delta_{n0}. \tag{2.113}$$

The aim is to write the expression for $G\left(\mathbf{q}_1 j_1 j_2 | \omega_n\right)$ in such a way that one can sum certain terms up to infinite order and beyond the approximation given by Eq. (2.111). In particular, it can be shown that $G\left(\mathbf{q}_1 j_1; \mathbf{q}_2 j_2 | \omega_n\right)$ may be written as [62]

$$G\left(\mathbf{q}_1 j_1 j_2 | \omega_n\right) = \delta_{j_1 j_2} G_0\left(\mathbf{q}_1 j_1 | \omega_n\right) + G_0\left(\mathbf{q}_1 j_1 | \omega_n\right) \sum_{j_1'} \Sigma\left(\mathbf{q}_1 j_1 j_1' | \omega_n\right) G\left(\mathbf{q}_1 j_1' j_2 | \omega_n\right), \tag{2.114}$$

where $G\left(\mathbf{q}_1 j_1 j_2 | \omega_n\right) \equiv G\left(\mathbf{q}_1 j_1; \mathbf{q}_1 j_2 | \omega_n\right)$ and the proper phonon self-energy is defined as

$$\begin{aligned} \Sigma\left(\mathbf{q}_1 j_1 j_1' | \omega_n\right) &\equiv -12\beta \sum_{\mathbf{q}_3, j_3} V\left(-\mathbf{q}_1 j_1; \mathbf{q}_1 j_1'; \mathbf{q}_3 j_3; -\mathbf{q}_3 j_3\right) \left(2\bar{n}_{\mathbf{q}_3 j_3} + 1\right) \\ &+18\beta^2 \sum_{\mathbf{q}_1'', j_1''} \sum_{\mathbf{q}_2', j_2'} V\left(-\mathbf{q}_1 j_1; \mathbf{q}_1'' j_1''; \mathbf{q}_2' j_2'\right) V\left(\mathbf{q}_1 j_1'; -\mathbf{q}_1'' j_1''; -\mathbf{q}_2' j_2'\right) \\ &\times \sum_{n', n''=-\infty}^{\infty} G_0\left(\mathbf{q}_1'' j_1'' | \omega_{n'}\right) G_0\left(\mathbf{q}_2' j_2' | \omega_{n''}\right) \delta_{-n+n'+n''}. \end{aligned} \tag{2.115}$$

It should be noted that Eq. (2.114) goes beyond the approximation given by Eq. (2.111), that is, Eq. (2.111) is included in Eq. (2.114) and iteration produces higher-order terms. For example, one may iterate Eq. (2.114) and write

$$\begin{aligned} G\left(\mathbf{q}_1 j_1 j_2 | \omega_n\right) &= \delta_{j_1 j_2} G_0\left(\mathbf{q}_1 j_1 | \omega_n\right) + G_0\left(\mathbf{q}_1 j_1 | \omega_n\right) \Sigma\left(\mathbf{q}_1 j_1 j_2 | \omega_n\right) G_0\left(\mathbf{q}_1 j_2 | \omega_n\right) \\ &+G_0\left(\mathbf{q}_1 j_1 | \omega_n\right) \sum_{j_1'} \Sigma\left(\mathbf{q}_1 j_1 j_1' | \omega_n\right) G_0\left(\mathbf{q}_1 j_1' | \omega_n\right) \\ &\times \Sigma\left(\mathbf{q}_1 j_1' j_2 | \omega_n\right) G_0\left(\mathbf{q}_1 j_2 | \omega_n\right) + \cdots. \end{aligned} \tag{2.116}$$

If one considers only the diagonal terms in the phonon self-energy, that is $\Sigma(\mathbf{q}_1 j_1 j_1') \to \Sigma(\mathbf{q}jj) \equiv \Sigma(\mathbf{q}j)$, then Eq. (2.114) may be written as

$$\begin{aligned} G(\mathbf{q}jj'|\omega_n) &\approx \delta_{jj'} G_0(\mathbf{q}j|\omega_n) \sum_{n=0}^{\infty} \left[G_0(\mathbf{q}j|\omega_n)\Sigma(\mathbf{q}j|\omega_n)\right]^n \\ &= \frac{\delta_{jj'} G_0(\mathbf{q}j|\omega_n)}{1 - G_0(\mathbf{q}j|\omega_n)\Sigma(\mathbf{q}j|\omega_n)} \\ &= \frac{2\omega_j(\mathbf{q})}{\beta\hbar} \frac{\delta_{jj'}}{\omega_j^2(\mathbf{q}) + \omega_n^2 - \frac{2\omega_j(\mathbf{q})}{\beta\hbar}\Sigma(\mathbf{q}j|\omega_n)}, \end{aligned} \tag{2.117}$$

where the infinite series is convergent for

$$|G_0(\mathbf{q}j|\omega_n)\Sigma(\mathbf{q}j|\omega_n)| < 1. \tag{2.118}$$

The non-diagonal terms in the phonon self-energy ($j_1 \neq j_1'$), which were neglected in Eq. (2.117), are sometimes called polarization mixing terms. The result for the summation in Eq. (2.115) is given in Appendix A by Eq. (A.31), thus

$$\begin{aligned} \Sigma(\mathbf{q}jj'|\omega_n) &= -12\beta \sum_{\mathbf{q}_1, j_1} V(-\mathbf{q}j; \mathbf{q}j'; \mathbf{q}_1 j_1; -\mathbf{q}_1 j_1)(2\bar{n}_{\mathbf{q}_1 j_1} + 1) \\ &\quad + 18\frac{\beta}{\hbar} \sum_{\mathbf{q}_1'', j_1''} \sum_{\mathbf{q}_2', j_2'} V(-\mathbf{q}j; \mathbf{q}_1 j_1; \mathbf{q}_2 j_2) V(\mathbf{q}j'; -\mathbf{q}_1 j_1; -\mathbf{q}_2 j_2) \\ &\quad \times \left[\frac{\bar{n}_{\mathbf{q}_2 j_2} + \bar{n}_{\mathbf{q}_1 j_1} + 1}{\omega_{j_1}(\mathbf{q}_1) + \omega_{j_2}(\mathbf{q}_2) + i\omega_n} - \frac{\bar{n}_{\mathbf{q}_1 j_1} + \bar{n}_{\mathbf{q}_2 j_2} + 1}{-\omega_{j_1}(\mathbf{q}_1) - \omega_{j_2}(\mathbf{q}_2) + i\omega_n} \right. \\ &\quad \left. + \frac{\bar{n}_{\mathbf{q}_1 j_1} - \bar{n}_{\mathbf{q}_2 j_2}}{-\omega_{j_1}(\mathbf{q}_1) + \omega_{j_2}(\mathbf{q}_2) + i\omega_n} - \frac{\bar{n}_{\mathbf{q}_1 j_1} - \bar{n}_{\mathbf{q}_2 j_2}}{\omega_{j_1}(\mathbf{q}_1) - \omega_{j_2}(\mathbf{q}_2) + i\omega_n} \right]. \end{aligned} \tag{2.119}$$

The retarded self-energy provides the phonon lifetime and energy shift and can be obtained by replacing $i\omega_n \to \omega + i\epsilon$, $\omega, \epsilon \in \mathbb{R}$ and by taking the limit $\epsilon \to 0$. Then, by using

$$\lim_{\epsilon^+ \to 0} \frac{1}{\omega - x \pm i\epsilon} = \frac{1}{(\omega - x)_P} \mp i\pi\delta(\omega - x), \quad \frac{1}{(\omega - x)_P} = \lim_{\epsilon^+ \to 0} \frac{\omega - x}{(\omega - x)^2 + \epsilon^2}, \tag{2.120}$$

one may, in order to divide the self-energy into real and imaginary parts, write Eq. (2.119) as ($j = j'$)

$$-\frac{1}{\beta\hbar} \lim_{\epsilon^+ \to 0} \Sigma(\lambda|\omega_\lambda \pm i\epsilon) = \Delta(\lambda|\omega) \mp i\Gamma(\lambda|\omega), \tag{2.121}$$

where

$$\begin{aligned}
\Delta(\lambda|\omega) &\equiv \frac{12}{\hbar}\sum_{\lambda'} V(\lambda;-\lambda;\lambda';-\lambda')(2\bar{n}_{\lambda'}+1) \\
&\quad -18\frac{1}{\hbar^2}\sum_{\lambda'}\sum_{\lambda''}|V(-\lambda;\lambda';\lambda'')|^2 \\
&\quad \times\left[\frac{\bar{n}_{\lambda'}+\bar{n}_{\lambda''}+1}{(\omega+\omega_{\lambda'}+\omega_{\lambda''})_P} - \frac{\bar{n}_{\lambda'}+\bar{n}_{\lambda''}+1}{(\omega-\omega_{\lambda'}-\omega_{\lambda''})_P}\right. \\
&\quad \left.+\frac{\bar{n}_{\lambda'}-\bar{n}_{\lambda''}}{(\omega-\omega_{\lambda'}+\omega_{\lambda''})_P} - \frac{\bar{n}_{\lambda'}-\bar{n}_{\lambda''}}{(\omega+\omega_{\lambda'}-\omega_{\lambda''})_P}\right], \\
\Gamma(\lambda|\omega) &\equiv -18\frac{\pi}{\hbar^2}\sum_{\lambda'}\sum_{\lambda''}|V(-\lambda;\lambda';\lambda'')|^2 \\
&\quad \times\{(\bar{n}_{\lambda'}+\bar{n}_{\lambda''}+1)\,\delta[\omega-\omega_{\lambda'}-\omega_{\lambda''}] \\
&\quad +2(\bar{n}_{\lambda'}-\bar{n}_{\lambda''})\,\delta[\omega+\omega_{\lambda'}-\omega_{\lambda''}]\}. \qquad (2.122)
\end{aligned}$$

The retarded Green's function can be written as

$$G^R(\mathbf{q}jj'|\omega) \approx \frac{2\omega_j(\mathbf{q})}{\beta\hbar}\frac{\delta_{jj'}}{\omega^2+\omega_j^2(\mathbf{q})+2\omega_j(\mathbf{q})\{\Delta(\mathbf{q}j|\omega)+i\Gamma(\mathbf{q}j|\omega)\}}. \qquad (2.123)$$

The real part of the retarded self-energy $\Delta(\lambda|\omega_\lambda)$, represents the shift of the phonon eigenvalue ω_λ caused by the third and fourth-order anharmonic Hamiltonian while the imaginary part $\Gamma(\lambda|\omega_\lambda)$ is proportional to the reciprocal of the lifetime of a phonon state λ [62]. The imaginary part of the retarded self-energy is used in the zeroth-order solution of the linearized BTE in the ShengBTE program [22].

To summarize, the Green's functions give information about the states of a many-body system. For instance, the poles of the non-interacting Green's function $G_0(\mathbf{q}j|\omega_n)$ are the harmonic phonon eigenvalues ω_λ, while the poles of the interacting Green's function are shifted by an amount $2\omega_j(\mathbf{q})\{\Delta(\mathbf{q}j|\omega)+i\Gamma(\mathbf{q}j|\omega)\}$ and are complex, in general. By approximating the interacting Green's function as in Eq. (2.123), some particular class of interactions are taken into account up to infinite-order as can be seen from Eq. (2.117). This particular class of interactions is generated by the phonon self-energy $\Sigma(\mathbf{q}j|\omega_n)$, which is a special case of Eq. (2.119). If the approximation given by Eq. (2.123) does not describe the system appropriately, one may have to include the polarization mixing in order to obtain reliable results.

2.4.3 Evaluation of the perturbation expansion

Here the evaluation of the perturbation expansion used in Article IV is summarized. The present method is based on the imaginary time Green's function formalism [40,

41, 54]. The starting point is to find a suitable form for the partition function to be used in the perturbative calculations and to obtain such a form, one may write

$$e^{-\beta\hat{H}_d} = e^{-\beta\left(\hat{H}_0+\hat{H}_{int}\right)} = e^{-\beta\hat{H}_0}\hat{S}\left(\beta\right), \quad \hat{S}\left(\beta\right) = e^{-\beta\hat{H}_{int}}, \tag{2.124}$$

since $\hat{H}_0$ and $\hat{H}_{int}$ commute. With this notation, the partition function may be written as

$$Z = Z_0\left\langle\hat{S}\left(\beta\right)\right\rangle_0. \tag{2.125}$$

The ensemble average in Eq. (2.125) can be written as [Eq. (2.86)]

$$\left\langle\hat{S}\left(\beta\right)\right\rangle_0 = Z_0^{-1}\sum_n \langle n|e^{-\beta\hat{H}_0}\hat{S}\left(\beta\right)|n\rangle. \tag{2.126}$$

and after differentiation of $\hat{S}\left(\beta\right)$ with respect to β

$$\frac{\partial}{\partial\beta}\hat{S}\left(\beta\right) = -\hat{H}_{int}\left(\beta\right)\hat{S}\left(\beta\right). \tag{2.127}$$

It can be seen from Eq. 2.124 that $\hat{S}\left(0\right) = 1$. Then, by integration and iteration of Eq. 2.127, one obtains

$$\hat{S}\left(\beta\right) = 1 - \sum_{h=1}^{\infty}\frac{\left(-1\right)^h}{h!}\int_0^\beta d\tau_1\cdots\int_0^\beta d\tau_h\mathcal{T}\left\{\hat{H}_{int}\left(\tau_1\right)\cdots\hat{H}_{int}\left(\tau_h\right)\right\}, \tag{2.128}$$

where

$$\hat{S}\left(\beta\right) = e^{-\beta\hat{H}_{int}}, \quad \hat{H}_{int}\left(\tau_i\right) = e^{\tau_i\hat{H}_0}\hat{H}_{int}e^{-\tau_i\hat{H}_0}, \tag{2.129}$$

and the time-ordering means that

$$\mathcal{T}\left\{\hat{H}_{int}\left(\tau_1\right)\cdots\hat{H}_{int}\left(\tau_h\right)\right\} = \hat{H}_{int}\left(\tau_1\right)\cdots\hat{H}_{int}\left(\tau_h\right), \quad \tau_1 \geq \ldots \geq \tau_h. \tag{2.130}$$

The interaction Hamiltonian $\hat{H}_{int}\left(\tau_i\right)$ is given by Eq. (2.61), that is $\hat{H}_{int} = \hat{H}_a + \hat{H}_s$. Now, by using Eqs. 2.125 and 2.128, the perturbation expansion for the partition function can be written as

$$Z = Z_0\sum_{h=0}^{\infty}\frac{\left(-1\right)^h}{h!}\int_0^\beta d\tau_1\cdots\int_0^\beta d\tau_h\left\langle\mathcal{T}\left\{\hat{H}_{int}\left(\tau_1\right)\cdots\hat{H}_{int}\left(\tau_h\right)\right\}\right\rangle_0, \tag{2.131}$$

and the Helmhotz free energy may be expressed as

$$F = \Phi_0 - \frac{1}{\beta}\ln Z_0 - \frac{1}{\beta}\ln\left\langle\hat{S}\left(\beta\right)\right\rangle_0 = F_0 + \tilde{F}_A. \tag{2.132}$$

where F_0 is given by Eq. (2.93) and $\tilde{F}_A$ is the last term after the first equality in Eq. 2.132. One can show by using, for instance, combinatorial arguments that only the connected terms need to be included in the expansion of $\tilde{F}_A$ and one may write [41,54]

$$\tilde{F}_A = -\frac{1}{\beta}\left\langle\hat{S}\left(\beta\right)\right\rangle_{0,c}. \tag{2.133}$$

As in Article IV, all the anharmonic elastic and thermodynamical quantities considered can be written in terms of the harmonic ensemble average $\hat{S}(\beta)$, namely

$$\begin{aligned}
\tilde{U}_A &= -\frac{\partial}{\partial\beta}\left\langle \hat{S}(\beta)\right\rangle_{0,c}, \\
\tilde{S}_A &= \frac{1}{T\beta}\left\langle \hat{S}(\beta)\right\rangle_{0,c} - \frac{1}{T}\frac{\partial}{\partial\beta}\left\langle \hat{S}(\beta)\right\rangle_{0,c} = \frac{1}{T}\left(\tilde{U}_A - \tilde{F}_A\right), \\
\tilde{C}_{A,\eta} &= \frac{\beta}{T}\frac{\partial^2}{\partial\beta^2}\left\langle \hat{S}(\beta)\right\rangle_{0,c}, \\
\tilde{c}^T_{\mu_1\nu_1\cdots\mu_k\nu_k} &= -\frac{1}{\beta}\left.\frac{\partial^k\left\langle \hat{S}(\beta)\right\rangle_{0,c}}{\partial u_{\mu_1\nu_1}\cdots\partial u_{\mu_k\nu_k}}\right|_{u_{\mu_1\nu_1}=0,\ldots,u_{\mu_k\nu_k}=0}, \\
\tilde{c}^A_{\mu_1\nu_1\cdots\mu_k\nu_k} &= -\frac{\partial}{\partial\beta}\left.\frac{\partial^k\left\langle \hat{S}(\beta)\right\rangle_{0,c}}{\partial u_{\mu_1\nu_1}\cdots\partial u_{\mu_k\nu_k}}\right|_{u_{\mu_1\nu_1}=0,\ldots,u_{\mu_k\nu_k}=0}.
\end{aligned} \tag{2.134}$$

where $\tilde{U}_A$ is the anharmonic part of internal energy, $\tilde{S}_A$ the anharmonic part of entropy, $\tilde{C}_{A,\eta}$ the anharmonic part of heat capacity at constant strain, $\tilde{c}^T_{\mu_1\nu_1\cdots\mu_k\nu_k}$ the kth-order isothermal and $\tilde{c}^A_{\mu_1\nu_1\cdots\mu_k\nu_k}$ the kth-order adiabatic elastic constants. Thus, one may calculate all the quantities considered here in terms of the ensemble average taken over the quantity $\hat{S}(\beta)$. This makes the actual calculations rather consistent since one can consider the elastic and thermal properties of a crystal by means of the same perturbation expansion. The CTE can be written as [78] [see also Eqs. (2.99)-(2.101)]

$$\alpha_{\mu\nu} = -\sum_{\gamma,\delta=1}^{3} s^T_{\mu\nu\gamma\delta}\frac{\partial\sigma^T_{\gamma\delta}}{\partial T} = \frac{1}{T}\sum_{\gamma,\delta=1}^{3} s^T_{\mu\nu\gamma\delta}\left(\sigma^A_{\gamma\delta} - \sigma^T_{\gamma\delta}\right), \tag{2.135}$$

which can be evaluated by using the quantities included in Eq. (2.134).

The following steps are made to evaluate the integrals over the ensemble averages as in Eq. 2.131: the ensemble averages are simplified by using Wick's Theorem given by Eq. 2.108, the resulting Green's functions are written in terms of their Fourier series given in Eq. 2.105 and finally the integrals are simplified by using Eq. (2.113). The resulting summations can be calculated by applying the residue theorem as shown in Appendix A. Terms in the expansion can be represented with algebraic expressions or alternatively by diagrams (see Sec. 3.4). Terms of the perturbation expansion considered in Article IV were

$$\left\langle \hat{S}(\beta)\right\rangle_{0,c,h=1} = -\int_0^\beta d\tau_1\left\langle \mathcal{T}\left\{\hat{H}_a(\tau_1) + \hat{H}_s(\tau_1)\right\}\right\rangle_{0,c}, \tag{2.136}$$

$$\begin{aligned}\left\langle \hat{S}(\beta)\right\rangle_{0,c,h=2} = \quad & \frac{1}{2}\int_0^\beta d\tau_1 \int_0^\beta d\tau_2 \left\langle \mathcal{T}\left\{\hat{H}_a(\tau_1)\,\hat{H}_a(\tau_2)\right\}\right\rangle_{0,c} \\ & + \frac{1}{2}\int_0^\beta d\tau_1 \int_0^\beta d\tau_2 \left\langle \mathcal{T}\left\{\hat{H}_s(\tau_1)\,\hat{H}_s(\tau_2)\right\}\right\rangle_{0,c} \\ & + \int_0^\beta d\tau_1 \int_0^\beta d\tau_2 \left\langle \mathcal{T}\left\{\hat{H}_s(\tau_2)\,\hat{H}_a(\tau_1)\right\}\right\rangle_{0,c}, \end{aligned} \tag{2.137}$$

and

$$\begin{aligned}\left\langle \hat{S}(\beta)\right\rangle_{0,c,h=3} = \quad & -\frac{1}{6}\int_0^\beta d\tau_1 \int_0^\beta d\tau_2 \int_0^\beta d\tau_3 \left\langle \mathcal{T}\left\{\hat{H}_a(\tau_1)\,\hat{H}_a(\tau_2)\,\hat{H}_a(\tau_3)\right\}\right\rangle_{0,c} \\ & -\frac{1}{2}\int_0^\beta d\tau_1 \int_0^\beta d\tau_2 \int_0^\beta d\tau_3 \left\langle \mathcal{T}\left\{\hat{H}_a(\tau_1)\,\hat{H}_a(\tau_2)\,\hat{H}_s(\tau_3)\right\}\right\rangle_{0,c} \\ & -\frac{1}{2}\int_0^\beta d\tau_1 \int_0^\beta d\tau_2 \int_0^\beta d\tau_3 \left\langle \mathcal{T}\left\{\hat{H}_s(\tau_1)\,\hat{H}_s(\tau_2)\,\hat{H}_a(\tau_3)\right\}\right\rangle_{0,c} \\ & -\frac{1}{6}\int_0^\beta d\tau_1 \int_0^\beta d\tau_2 \int_0^\beta d\tau_3 \left\langle \mathcal{T}\left\{\hat{H}_s(\tau_1)\,\hat{H}_s(\tau_2)\,\hat{H}_s(\tau_3)\right\}\right\rangle_{0,c}. \end{aligned} \tag{2.138}$$

While the first order term, Eq. (2.136), was considered as a whole, only some terms of Eqs. (2.137) and (2.138) were taken into account. Few example calculations for Eqs. (2.137) and (2.138) are established in Appendix C.

2.5 Interatomic force constants and density functional theory

The IFCs have been quite central quantities in the discussion so far, but not much have been about mentioned how IFCs are actually calculated. In this section, a summary of the methods applied is given. In Sec. 2.5.1, the quantum many-body problem is discussed and the adiabatic approximation is considered. The DFT applied in the present work in order to calculate the IFCs is considered In Sec. 2.5.2.

2.5.1 General notes and adiabatic approximation

In a non-relativistic case, a state which describes a quantum mechanical system can be obtained by solving the Schrödinger equation [51]

$$i\hbar\frac{\partial}{\partial t}\left|\Psi\right\rangle = \hat{H}\left|\Psi\right\rangle = E\left|\Psi\right\rangle, \tag{2.139}$$

where $\hat{H}$ is the Hamiltonian of the system and the same equation holds for a particular representation chosen. For example, the present many-body system is the lattice

comprising n electrons and k nuclei for which the wave function in the position representation may be written as $\Psi(\mathbf{r}_1, \ldots, \mathbf{r}_n, \mathbf{R}_1, \ldots, \mathbf{R}_k)$. The ket $|\Psi\rangle$ or the wave function obtained by solving Eq. (2.139) can be used to calculate the expected value of an observable $\hat{O}$. In the case of electrons, for instance, the kets and wave functions are anti-symmetrized such that the anti-symmetrized m-body wave function can be written as [compare to Eqs. (2.31) and (2.32)]

$$\Psi^{(-)}_{i_1 \cdots i_m} = \hat{S}_- \Psi_{i_1 \cdots i_m}, \quad \hat{S}_- \equiv \frac{1}{\sqrt{n!}} \sum_{\sigma_n} (-1)^{N(\sigma_n)} \hat{P}_{\sigma_n}, \tag{2.140}$$

where $N(\sigma_n)$ is the number of inversions in the permutation σ_n. Due to the complexity of Eq. (2.139) in the case of many-body systems, some approximate methods are needed to solve the Schrödinger equation. In one of the simplest approximations, called the Hartree-Fock approximation, one assumes that the Hamiltonian does not contain two-body interactions, except in some average sense [see Eq. (2.158)], and that the wave function can be written as [12]

$$\Psi^{(-)}_{i_1 \cdots i_m} = \hat{S}_- \Psi_{i_1} \cdots \Psi_{i_m}. \tag{2.141}$$

The right hand side of Eq. (2.141) is sometimes called the Slater determinant. To make a comparison, in the case of discrete basis, a general m-body state can be written as (Sec. 2.2.1, anti-symmetrization neglected)

$$|\Psi\rangle = \sum_{i_1, \ldots, i_m} \Psi_{i_1 \cdots i_m} |e^{(1)}_{i_1}\rangle \otimes \cdots \otimes |e^{(m)}_{i_m}\rangle \tag{2.142}$$

and in the special case of Eq. (2.141), this state becomes

$$|\Psi\rangle \approx \sum_{i_1, \ldots, i_m} \Psi_{i_1} \cdots \Psi_{i_m} |e^{(1)}_{i_1}\rangle \otimes \cdots \otimes |e^{(m)}_{i_m}\rangle . \tag{2.143}$$

If a quantum state can be written in the form given by Eq. (2.143) [or Eq. (2.141)], it is said to be separable, otherwise it is said to be entangled [83]. Therefore, the Hartree-Fock approximation assumes that the states are separable, which is not the case in general. Sometimes the Hartree-Fock approximation does not describe the system appropriately due to simplifications made and more rigorous methods are needed. However, when calculating better approximations for the wave function, the computational cost increases rather rapidly as a function of system size and some alternative methods may be needed in order to describe the many-body quantum systems. In addition to the calculation of the many-body wave function, there are several alternative ways to calculate observable quantities for a many-body quantum systems. One approach is to use the many-body Green's function method [13, 14, 40, 62,68–74,84] discussed in the lattice dynamical context in Sec. 2.4. Another and rather extensively used method in the computational study of many-body quantum systems is the DFT [85–88], which is applied also in the present work [17] (see Sec. 2.5.2).

Before even choosing the approximate method in order to solve the Schrödinger equation, the wave function is usually simplified by some other means. In the case of crystal lattices, for example, due to the rather large mass difference between electrons and nuclei, the wave function can be written within the so-called adiabatic approximation as follows [15, 42, 48]

$$\Psi_n\left(\underline{\mathbf{r}}, \underline{\mathbf{R}}\right) \approx \Psi_n\left(\underline{\mathbf{r}}, \underline{\tilde{\mathbf{R}}}\right) \approx \chi\left(\underline{\mathbf{u}}\right) \theta_n\left(\underline{\mathbf{r}}, \underline{\tilde{\mathbf{R}}}\right), \tag{2.144}$$

where

$$\underline{\mathbf{r}} \equiv \mathbf{r}_1, \ldots, \mathbf{r}_n, \quad \underline{\tilde{\mathbf{R}}} \equiv \tilde{\mathbf{R}}_1, \ldots, \tilde{\mathbf{R}}_k, \quad \underline{\mathbf{u}} \equiv \mathbf{u}_1, \ldots, \mathbf{u}_k. \tag{2.145}$$

In Eqs. (2.144) and (2.145), the tilde placed on the $\underline{\mathbf{R}} = \underline{\mathbf{x}} + \underline{\mathbf{u}}$ indicates that the nuclei coordinates are treated as parameters and the subscript n refers to some particular electronic state. Further, $\{\mathbf{u}_i\}$ are the displacements of the nuclei from their equilibrium positions $\{\mathbf{x}_i\}$. A special case of the adiabatic approximation is the harmonic approximation [15, 42] in which

$$\Psi_n\left(\underline{\mathbf{r}}, \underline{\mathbf{R}}\right) \approx \Psi_n\left(\underline{\mathbf{r}}, \underline{\tilde{\mathbf{R}}}\right) \approx \varphi\left(\underline{\mathbf{u}}\right) \phi_n\left(\underline{\mathbf{r}}, \underline{\tilde{\mathbf{x}}}\right), \tag{2.146}$$

where the electronic wave function depends only on the parametric equilibrium positions $\underline{\tilde{\mathbf{x}}}$ instead of the instantaneous positions $\underline{\tilde{\mathbf{R}}}$ of the nuclei. Within the adiabatic approximation, the Schrödinger equation for electrons with fixed $\underline{\tilde{\mathbf{R}}}$ can be written as

$$\hat{H}_{ad}\theta_n\left(\underline{\mathbf{r}}, \underline{\tilde{\mathbf{R}}}\right) = E_{ad}\theta_n\left(\underline{\mathbf{r}}, \underline{\tilde{\mathbf{R}}}\right), \quad \hat{H}_{ad} = \hat{H}_e + \hat{H}_{en} + \hat{H}_{nn}, \tag{2.147}$$

where $\hat{H}_e$ is the electron-electron interaction Hamiltonian with the kinetic energy of electrons included, $\hat{H}_{en}$ is the electron-nuclei interaction Hamiltonian and $\hat{H}_{nn}$ is the nuclei-nuclei interaction Hamiltonian. Within this approximation, the nuclei are fixed to their instantaneous positions and the kinetic energy of the nuclei vanishes. Thus, the second-order partial derivatives of E_{ad} with respect to the nuclei coordinates, evaluated at the equilibrium positions, can be used to calculate the second-order IFCs included in the harmonic Hamiltonian $\hat{H}_0$ [Eq. (2.6)]. To obtain the second-order derivatives the Hellmann-Feynman theorem [47] may be used with the DFT and DFPT [17]. Since the adiabatic approximation is valid for the instantaneous positions $\underline{\tilde{\mathbf{R}}}$ of the nuclei, one may use finite differences to calculate estimates for the higher-order IFCs as well. The validity of the adiabatic approximation is considered in Refs. [15, 42] and it is usually expected to hold in the case of insulators and semiconductors.

2.5.2 Density functional theory

The DFT allows the calculation of various observables of a system without the knowledge of the many-body wave function, which usually makes the numerical computations more feasible. Let the Hamiltonian of the system be $\hat{H} = \hat{T} + \hat{V} + \hat{W}$, where $\hat{T}$

is the kinetic energy of electrons, $\hat{V}$ is the external potential and $\hat{W}$ is the electron-electron interaction potential. The external potential in the present case could be the interaction between the fixed nuclei and electrons. The Schrödinger equation can be written as

$$\left(\hat{T}+\hat{V}+\hat{W}\right)|\psi\rangle = E\,|\psi\rangle\,, \tag{2.148}$$

and it can be shown that the external potential may be written in the form

$$\hat{V} = \int d\mathbf{r}\hat{n}\left(\mathbf{r}\right)v\left(\mathbf{r}\right). \tag{2.149}$$

In Eq. (2.149), $\hat{n}\left(\mathbf{r}\right)$ is the electron density operator. The form of the operator given by Eq. (2.149) is quite general because, when one (assumed to be diagonal) and two-body interactions are included an arbitrary operator (in non-relativistic quantum mechanics) can be written in terms of the creation and annihilation operators as [14, 51]

$$\hat{O} = \int d\mathbf{r}o_1\left(\mathbf{r}\right)\hat{\psi}^{\dagger}\left(\mathbf{r}\right)\hat{\psi}\left(\mathbf{r}\right) + \frac{1}{2}\int d\mathbf{r}\int d\mathbf{r}'o_2\left(\mathbf{r},\mathbf{r}'\right)\hat{\psi}^{\dagger}\left(\mathbf{r}\right)\hat{\psi}^{\dagger}\left(\mathbf{r}'\right)\hat{\psi}\left(\mathbf{r}'\right)\hat{\psi}\left(\mathbf{r}\right), \tag{2.150}$$

where $\hat{\psi}^{\dagger}\left(\mathbf{r}\right)\hat{\psi}\left(\mathbf{r}\right) = \hat{n}\left(\mathbf{r}\right)$. The operators $\hat{\psi}^{\dagger}\left(\mathbf{r}\right)$ and $\hat{\psi}\left(\mathbf{r}\right)$ satisfy the commutation (anti-commutation) relations in the case of bosons (fermions), namely

$$\left[\hat{\psi}\left(\mathbf{r}\right),\hat{\psi}^{\dagger}\left(\mathbf{r}'\right)\right]_{\pm} = \delta\left(\mathbf{r}-\mathbf{r}'\right). \tag{2.151}$$

For instance, in the case of fermions, Eq. (2.150) can be written in terms of densities as follows

$$\hat{O} = \int d\mathbf{r}o_1\left(\mathbf{r}\right)\hat{n}\left(\mathbf{r}\right) - \frac{1}{2}\int d\mathbf{r}o_2\left(\mathbf{r},\mathbf{r}\right)\hat{n}\left(\mathbf{r}\right) + \frac{1}{2}\int d\mathbf{r}\int d\mathbf{r}'o_2\left(\mathbf{r},\mathbf{r}'\right)\hat{n}\left(\mathbf{r}\right)\hat{n}\left(\mathbf{r}'\right). \tag{2.152}$$

Now, the Hohenberg-Kohn theorem [89] states that there is a bijective map (function) between potentials and ground state wave functions and a bijective map between the ground state wave functions and ground state electron densities. A ground state $|\psi_0\rangle$ is defined to be a state with the lowest energy. Since a bijective map is also invertible, the ground state wave function can be calculated, in principle, by using the ground state density *et cetera*. The ground state expected value of an observable can be written as $O = \langle\psi_0|\hat{O}|\psi_0\rangle$ and in particular for energy

$$E_{\tilde{v}} = F + \int d\mathbf{r}n\left(\mathbf{r}\right)\tilde{v}\left(\mathbf{r}\right), \quad F \equiv \langle\psi_0|\hat{T}+\hat{W}|\psi_0\rangle\,. \tag{2.153}$$

Here, F is the Hohenberg-Kohn functional and $\tilde{v}\left(\mathbf{r}\right)$ is a fixed external potential at $\mathbf{r}$. Since the so-called Rayleigh-Ritz variational principle states that the expected value of the energy is greater or equal to the ground state energy $E_{v,0}$, namely $\langle\psi|E_v|\psi\rangle \geq E_{v,0}$, one may use the calculus of variations to obtain an expression for the energy. The ground state energy can be found when

$$\frac{\delta E_{\tilde{v}}}{\delta n\left(\mathbf{r}\right)} = k \Leftrightarrow \frac{\delta F}{\delta n\left(\mathbf{r}\right)} = k - \tilde{v}\left(\mathbf{r}\right), \quad k \in \mathbb{R}. \tag{2.154}$$

However, the form of the functional F is not known and in the practical implementations it is approximated in various ways.

The actual implementations of the DFT are sometimes, as in the present work, based on the Kohn-Sham scheme [90]. Within the Kohn-Sham scheme, the electron density of the interacting system can be calculated by using the eigenstates of the Hamiltonian $\hat{H}_s = \hat{T} + \hat{V}_s$, where the external potential $\hat{V}_s$ is assumed to be known. The Schrödinger equation for this Hamiltonian, $\hat{H}_s \left|\Psi_s\right\rangle = E_s \left|\Psi_s\right\rangle$, can be written separately for each eigenstate, that is

$$\left[-\frac{\hbar^2}{2m_e}\nabla^2_{\mathbf{r}} + v_s\left(\mathbf{r}\right)\right]\varphi_n\left(\mathbf{r}\sigma\right) = \epsilon_n \varphi_n\left(\mathbf{r}\sigma\right). \tag{2.155}$$

The approximate ground state wave function can be represented as a Slater determinant of the eigenfunctions $\varphi_n\left(\mathbf{r}\sigma\right)$ and the electron density at $\mathbf{r}$ may be written in terms of the single particle wave functions

$$n\left(\mathbf{r}\right) = \sum_{\sigma}\sum_{n}\left|\varphi_n\left(\mathbf{r}\sigma\right)\right|^2. \tag{2.156}$$

The wave functions $\{\varphi_n\left(\mathbf{r}\sigma\right)\}$ are sometimes called the Kohn-Sham orbitals. The interactions are included by defining the Hohenberg-Kohn functional as a sum of kinetic energy of the non-interacting system $\hat{T}_s$, Hartree energy E_h and exchange-correlation energy E_{xc}, namely

$$F \equiv T_s + E_h + E_{xc}. \tag{2.157}$$

The kinetic energy can be calculated from the expected value $T_s = \langle\Psi_s|\hat{T}|\Psi_s\rangle$ and the Hartree energy is given by [compare to Eq. (2.152)]

$$E_h = \frac{1}{2}\int d\mathbf{r}\int d\mathbf{r}' w\left(\mathbf{r},\mathbf{r}'\right) n\left(\mathbf{r}\right) n\left(\mathbf{r}'\right), \tag{2.158}$$

while the form of the exchange-correlation energy is unknown in general and various approximations are needed. After using Eq. (2.157) in Eq. (2.154), one may write ($k = 0$)

$$v_s\left(\mathbf{r}\right) = \tilde{v}\left(\mathbf{r}\right) + v_H\left(\mathbf{r}\right) + v_{xc}\left(\mathbf{r}\right), \tag{2.159}$$

where

$$v_s\left(\mathbf{r}\right) = -\frac{\delta T_s}{\delta n\left(\mathbf{r}\right)}, \quad v_H\left(\mathbf{r}\right) = \frac{\delta E_h}{\delta n\left(\mathbf{r}\right)} = \int d\mathbf{r}' w\left(\mathbf{r},\mathbf{r}'\right) n\left(\mathbf{r}'\right), \quad v_{xc}\left(\mathbf{r}\right) = \frac{\delta E_{xc}}{\delta n\left(\mathbf{r}\right)}. \tag{2.160}$$

Now, the expression for $v_s\left(\mathbf{r}\right)$ given by Eq. (2.160) can be used in Eq. (2.155) and provided the expression for the exchange-correlation energy and potential is known, the electron density can be solved. In Article I, the local density approximation (LDA) [85–87, 90–92] for the exchange-correlation energy was used, while a generalized gradient approximation (GGA) [93–96] was used in Articles II and III. In the

local spin density approximation (LSDA), the exchange-correlation energy is assumed to be of the following form

$$E_{xc}^{LSDA} = \int d\mathbf{r} \epsilon_{xc} \left[n_{\downarrow} \left(\mathbf{r} \right), n_{\uparrow} \left(\mathbf{r} \right) \right] n \left(\mathbf{r} \right), \tag{2.161}$$

where $\epsilon_{xc} \left[n_{\downarrow} \left(\mathbf{r} \right), n_{\uparrow} \left(\mathbf{r} \right) \right]$ is the exchange-correlation energy at $\mathbf{r}$ of the homogenous electron gas. Given Eqs. (2.152), (2.157), (2.158) and (2.161), the present approach gives a rather general form for the Hohenberg-Kohn functional apart from the approximation made for the exchange-correlation energy $\epsilon_{xc} \left[n_{\downarrow} \left(\mathbf{r} \right), n_{\uparrow} \left(\mathbf{r} \right) \right]$. As the name implies, the system from which $\epsilon_{xc} \left[n_{\downarrow} \left(\mathbf{r} \right), n_{\uparrow} \left(\mathbf{r} \right) \right]$ is obtained is a box of interacting electrons with constant density. In GGAs, one assumes that there are density variations in the system of interacting electrons, the exchange-correlation energy is expanded in the density variations and eventually in density gradients and one obtains approximations of different order. GGAs are usually expected to be more suitable for describing systems with stronger electron density variations. Thus, in order to calculate observables within DFT, it is not necessary to calculate the many-body wave function, which leads to the reduction of the computational cost.

After the approximation for the E_{xc} is given, the Kohn-Sham equations can be solved as follows. An initial guess for the electron density is given, the potential $v_s \left(\mathbf{r} \right)$ is calculated and after that the Kohn-Sham equation is solved to obtain the wave functions $\{ \varphi_n \left(\mathbf{r} \sigma \right) \}$ and the electron density through Eq. (2.156). The obtained electron density is used to calculate the potential $v_s \left(\mathbf{r} \right)$ and the described procedure is continued to self-consistency, which is achieved for example, when the energy difference of subsequent iterations is smaller than the predetermined cut-off value. To obtain the initial guess for the electron density it is useful to have some initial form for the wave functions $\{ \varphi_n \left(\mathbf{r} \sigma \right) \}$. In the present work, plane wave basis sets were used to describe the wave functions. In numerical calculations, some finite set of basis functions is used. The number of basis functions is sometimes determined by establishing several calculations with a different number of basis functions and by making a compromise between the accuracy and computational cost. The so-called pseudopotential method [97–100] can be used to further decrease the computational cost by neglecting the explicit effect of the electrons which are relatively close to the nuclei. That is, only the valence electrons are described by the wave functions and the effect of the rest of the electrons are included in the pseudopotentials, which are effective potentials induced by the nuclei and inner electrons. Based on the quantities obtained from DFT calculations, such as the energy of the system, the second and higher-order IFCs can be calculated by applying DFPT [17, 101–104].

3 Results and discussion

3.1 Phonon spectrum

In the present work, the phonon spectrum of seven different silicon clathrate frameworks (I, II, IV, V, VII, VIII, H, Article I), two different Zintl clathrates ($[Si_{19}P_4]Cl_4$, $Na_4[Al_4Si_{19}]$, Article III), and the silicon diamond structure (*d*-Si, Articles I and II) was studied. It is known [16, 17], that the DFT and DFPT methods provide relatively accurate results for the harmonic phonon eigenvalues. The experimental and computational results for *d*-Si were compared in Articles I-II and the maximum difference between the experimental and the computed phonon eigenvalues were 7%-11% depending on the plane-wave basis sets, pseudopotentials and exchange-correlation energy functionals used in the calculations. In Article I, all calculations were conducted by using the LDA to describe the exchange-correlation energy, while in Articles II and III the GGA was used instead. In the actual measurements of the phonon eigenstates, the anharmonicity of the crystal lattice is included and the resulting states observed do not have well determined harmonic energy. Further, as shown in Sec. 2.4.2, the anharmonic IFCs cause temperature dependent shifts on the harmonic phonon eigenvalues. This effect was neglected in the present work.

All silicon clathrate frameworks considered in Article I, except the framework VII, were found to have a rather similar phonon spectrum from which similar thermal properties, such as the heat capacity and CTE follow. Few distinctive features arose, however. For instance, the silicon clathrate framework V was found to possess two phonon band gaps, while the other silicon clathrate frameworks, excluding VII, were found to have only one phonon band gap. As an example, the phonon dispersion relations along high symmetry paths in the first Brillouin zone for the silicon clathrates VII are shown in Fig. 3.1. In obtaining the results depicted in Fig. 3.1, the same pseudopotential and plane-wave basis set was used as in Articles II and III (GGA applied with the same computational details), while the applied $\mathbf{k}$ and $\mathbf{q}$ samplings were the same as in Article I. The results obtained with GGA and LDA approaches are otherwise quite similar except for the lowest energy optical modes. In Article I, the lowest energy optical modes for VII were found to have values near 10 cm^{-1} when $\mathbf{q} \to 0$, while the minimum values for these modes obtained with the method used in Articles II and III are approximately 60 cm^{-1}. The preceding can be verified from Fig. 3.1. The CTE values calculated with the GGA and LDA methods are compared in Sec. 3.2. Even though the lowest optical modes of VII have smaller values in the long

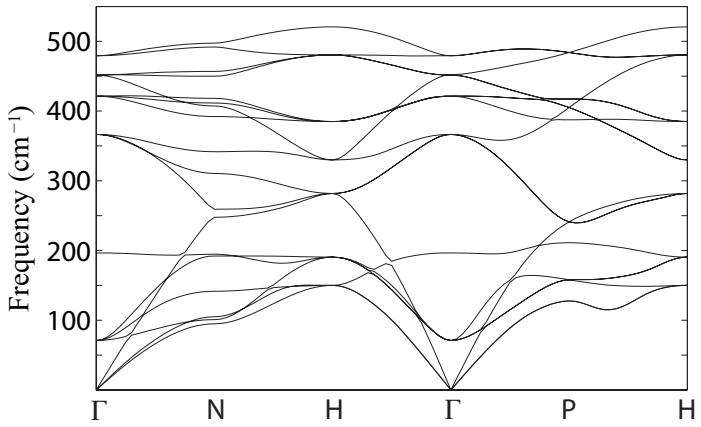

Figure 3.1: Phonon dispersion relations along high symmetry paths in the first Brillouin zone for the silicon clathrate framework VII calculated with the method used in Articles II and III.

wave length limit than obtained for the other cubic silicon clathrate frameworks, there is no visible flattening of the acoustic modes. In the actual measurements, the strict values of energy shown in dispersion curves are absent. Instead, some distribution of energy values is found and if the anharmonic interactions are sufficiently weak the distribution can be of the Lorentzian form, the width of the Lorentzian being related to the lifetime (or zeroth-order RT) of a particular state [62]. The aforementioned distribution is temperature dependent.

The silicon clathrate framework VIII (Si_{23}) is taken to be as the representative of the silicon clathrate frameworks. The phonon dispersion relations for Si_{23}, $[Si_{19}P_4]Cl_4$ and $Na_4[Al_4Si_{19}]$ are shown in Fig. 3.2. As discussed in Article III, the acoustic modes of the clathrate $Na_4[Al_4Si_{19}]$ have rather different dispersion than obtained for Si_{23} and $[Si_{19}P_4]Cl_4$. In comparison to $[Si_{19}P_4]Cl_4$, it seems that the highest and lowest energy phonon states of $Na_4[Al_4Si_{19}]$ have smaller values. Since the wave vector dependence is the same in both cases, it is useful to consider the dynamical matrix at $\mathbf{q} = 0$, thus from Eq. (2.22) it follows that

$$D_{\alpha\alpha'}\left(\kappa\kappa'|0\right) = \sum_{l'} \frac{\Phi_{\alpha\alpha'}\left(l\kappa; l'\kappa'\right)}{\sqrt{M_\kappa M_{\kappa'}}} = \sum_{l'} D_{\alpha\alpha'}\left(0\kappa; l'\kappa'\right), \tag{3.1}$$

or

$$D_{\alpha\alpha'}\left(\kappa\kappa'|0\right) \equiv D\left(\varsigma\varsigma'|0\right), \quad \varsigma \equiv \alpha\kappa, \quad \varsigma' \equiv \alpha'\kappa'. \tag{3.2}$$

The corresponding eigenvalues can be obtained from Eq. (2.23). One way to estimate the phonon eigenvalues is the method of Gerschgorin circles [105] applied on $D\left(\varsigma\varsigma'|0\right)$. The method of Gerschgorin circles states that the eigenvalues ω^2 of $D\left(\varsigma\varsigma'|0\right)$ are contained in the following union

$$r_{\varsigma_1} \cup r_{\varsigma_2} \cup \cdots \cup r_{\varsigma_{3n}}, \tag{3.3}$$

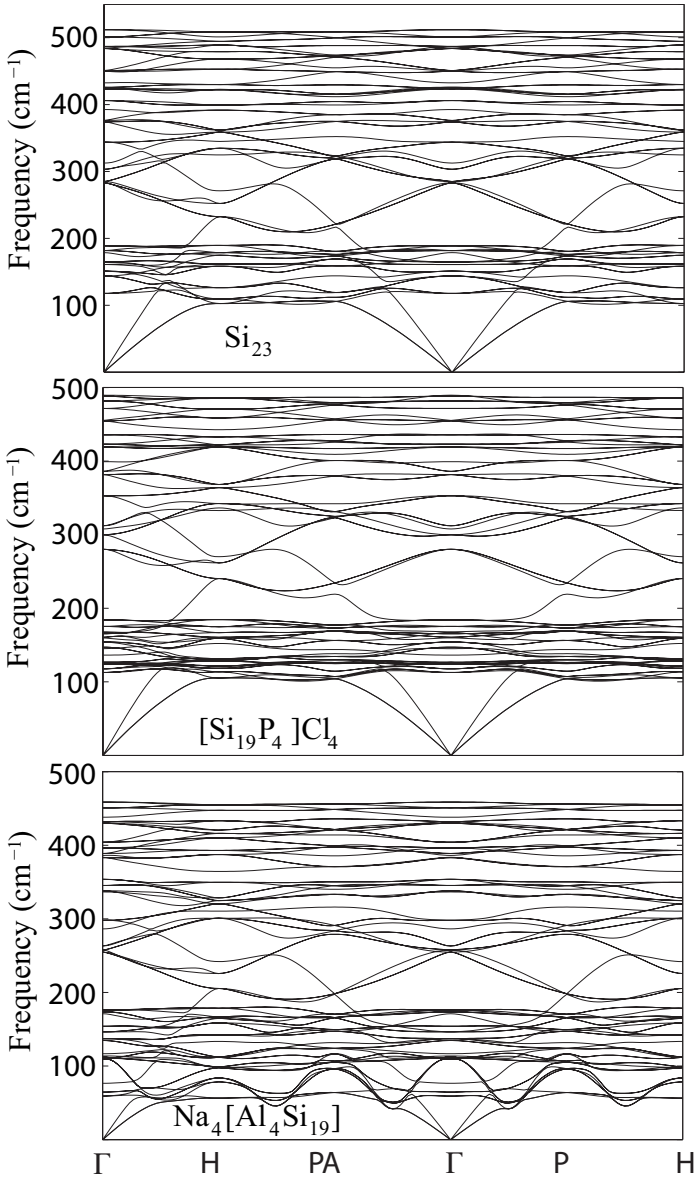

Figure 3.2: Phonon dispersion relations along high symmetry paths in the first Brillouin zone for Si_{23}, $[Si_{19}P_4]Cl_4$ and $Na_4[Al_4Si_{19}]$. Copyright © 2016, American Physical Society.

where

$$\left|\omega^2 - D\left(\varsigma\varsigma|0\right)\right| \leq r_\varsigma, \quad r_\varsigma = \sum_{\varsigma'=1,\varsigma\neq\varsigma'}^{3n} D\left(\varsigma\varsigma'|0\right). \tag{3.4}$$

Since the eigenvalues of the dynamical matrix are real, the Gerschgorin circles are in fact intervals on the real axis. First, all the diagonal elements $D\left(\varsigma\varsigma|0\right)$ in the case of the clathrate $[Si_{19}P_4]Cl_4$ are higher than obtained for $Na_4[Al_4Si_{19}]$. The ratio of the diagonal elements is within the interval $[1.21, 1.49]$. Further, the length of the intervals, r_ς, are larger for the clathrate $[Si_{19}P_4]Cl_4$ and the ratio is within the interval $[1.16, 2.50]$ the largest values being obtained for the guest atoms Na/Cl. Both of these observations favor the smaller phonon eigenvalues to be obtained for the clathrate $Na_4[Al_4Si_{19}]$. In particular, the lengths r_{ς_g} centered at $D\left(\varsigma_g\varsigma_g|0\right)$ are so small that there is no overlap between the diagonal elements $D\left(\varsigma_f\varsigma_f|0\right)$ and the intervals r_{ς_g}. Here, the subscripts g and f refer to the guest (Na/Cl) and framework atoms (P/Al/Si), respectively. However, the overlap of these intervals is obtained since the lengths r_{ς_f} centered at $D\left(\varsigma_f\varsigma_f|0\right)$ overlap with the diagonal elements $D\left(\varsigma_g\varsigma_g|0\right)$. The results thus indicate, that in order to minimize the energy of the lowest phonon states it is favorable to minimize the diagonal elements $D\left(\varsigma\varsigma|0\right)$ and perhaps the length of the intervals r_ς as well.

It was found in Article III, that the difference in the second-order IFCs in the clathrates $[Si_{19}P_4]Cl_4$ and $Na_4[Al_4Si_{19}]$ leads to a more local characteristics of the acoustic modes in $Na_4[Al_4Si_{19}]$. The localization was measured with the participation ratio (PR) defined as [106–109]

$$PR\left(\lambda\right) \equiv \frac{\left[\sum_\kappa \left|\mathbf{e}\left(\kappa|\lambda\right)\right|^2 M_\kappa^{-1}\right]^2}{N_a \sum_\kappa \left|\mathbf{e}\left(\kappa|\lambda\right)\right|^4 M_\kappa^{-2}}. \tag{3.5}$$

In Eq. (3.5), N_a is the number of atoms within the unit cell. The more local character the phonon state possesses, the value of $PR\left(\lambda\right)$ approaches N_a^{-1}. The opposite is indicated by the $PR\left(\lambda\right)$ values near to unity. Similar deductions can be made from the quantities $\left|\mathbf{e}\left(\kappa|\lambda\right)\right|^2$ by using a physical interpretation given in Sec. 2.2.3. Measured with these quantities, a state λ with a more local character have the $\left|\mathbf{e}\left(\kappa|\lambda\right)\right|^2$ value near to unity for some κ. It is expected that in the localized mode, an atom κ vibrates in isolation such that the displacement of other atoms decays faster than exponentially as a function of distance from the atom κ. If the probability $\left|\mathbf{e}\left(\kappa|\lambda\right)\right|^2$ that an atom $l\kappa$ vibrates in the phonon mode λ is unity, the probability for the other atoms to vibrate in the phonon mode λ is zero (Sec. 2.2.3), which would make this mode rather localized. The PR values for Si_{23}, $[Si_{19}P_4]Cl_4$ and $Na_4[Al_4Si_{19}]$ together with the atom projected density of states $\rho_\kappa\left(\omega\right) = 1/N \sum_\lambda \left|\mathbf{e}\left(\kappa|\lambda\right)\right|^2 \delta\left(\omega - \omega_\lambda\right)$ are shown in Fig. 3.3. As already mentioned, the clathrate $Na_4[Al_4Si_{19}]$ has acoustic modes with more local characteristics and as the $\rho_\kappa\left(\omega\right)$ values indicate, the probability that the guest atoms Cl/Na contribute to the low energy acoustic modes is higher than for the other atoms in these structures. Sometimes these kind of phonon modes, observed at the low

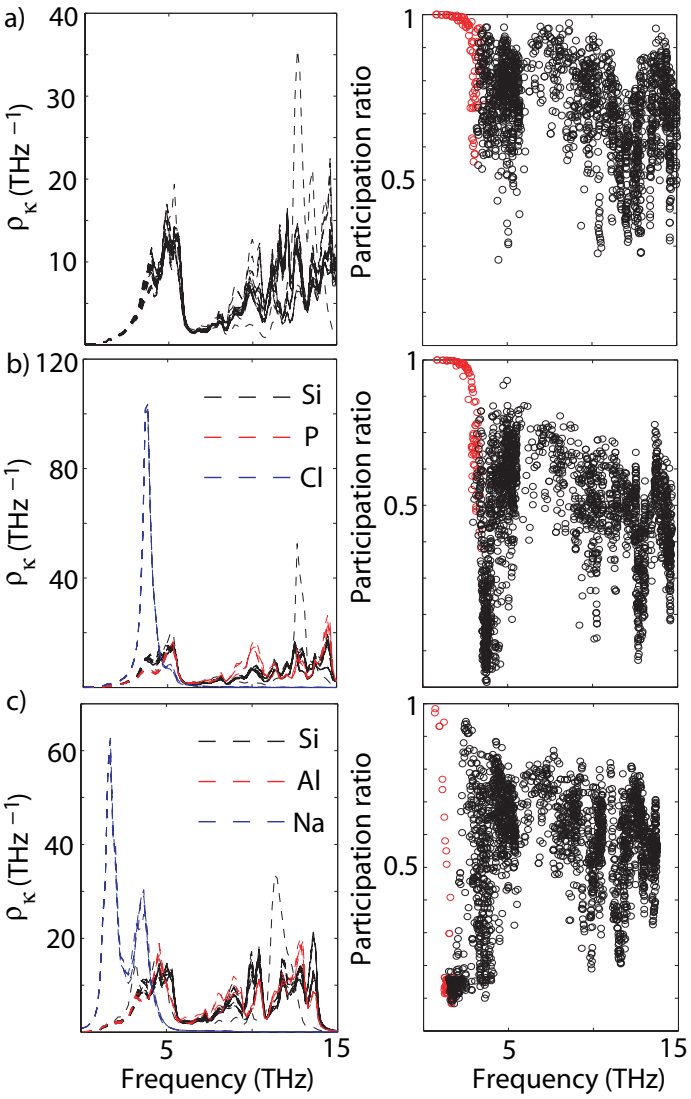

Figure 3.3: The atom projected density of states $\rho_\kappa(\omega)$ and participation ratio for each structure. (a) Si_{23}, (b) $[Si_{19}P_4]Cl_4$ and (c) $Na_4[Al_4Si_{19}]$. The participation ratio values for the acoustic modes are drawn in red.

frequencies in $Na_4[Al_4Si_{19}]$, are called resonance modes [110]. It is usually expected that the atoms which mainly contribute to these modes are either heavier or coupled rather weakly to the lattice when compared with the other atoms in the structure [110] and it appears that the latter condition may hold in the present case. There seems to be a connection between the lower phonon energies and local characteristics of these phonon states. Further studies are needed to find possible reasons for this behavior.

3.2 Thermal expansion

The CTE of the silicon clathrate frameworks I, II, IV, V, VII, VIII, and H was studied in Article I. In particular, the differing NTE of the framework VII was considered. The calculated linear and volumetric CTEs as a function of temperature for *d*-Si and seven different silicon clathrate frameworks is depicted in Fig. 3.4. For *d*-Si, also the experimental values obtained in Ref. [111] are shown. The values shown in Fig. 3.4 were calculated by using Eq. (2.102) and $\alpha_L = \alpha_V/3$ (valid for cubic structures). The calculated CTE values for *d*-Si are lower than the experimental ones at all temperatures considered. One reason, which may lower the calculated CTE is that the temperature dependence of the bulk modulus B_T and thus the elastic constants is neglected. Experiments have shown that for *d*-Si, all the second-order elastic constants and bulk modulus have decreasing values as a function of temperature. At 300 K, for instance, the experimental bulk modulus value is approximately 97.8 GPa [112, 113]. On the other hand at 100 K, the experimental bulk modulus is about 99.2 GPa [112]. The computed value for the bulk modulus used in the calculation of the CTE was 96.5 GPa in the case of *d*-Si, which is the static lattice contribution at 0 K. The calculated value is already lower than the experimental one, but larger CTE values are obtained provided the calculated bulk modulus has similar dependence on the temperature as obtained by experiments. In some cases, the anharmonic IFCs may have some measurable significance in calculating the temperature dependence of the bulk modulus, since the anharmonic IFCs contribute to the elastic constants as the results of Ref. [54] and Article IV show, for example.

All the studied silicon clathrate frameworks, except VII, were found to have a rather similar CTE as a function of temperature, as can be verified from Fig. 3.4. A temperature range where the NTE occurred was found to be approximately 100 K wide in these cases, while in the case of VII, the NTE temperature range was about 300 K wide. The results shown in Fig. 3.4 are similar to those obtained in Ref. [39] by using GGA. In order to compare the CTE for VII obtained by using the LDA and GGA, the calculation of CTE with the same plane wave pseudopotentials used in Articles II and III was established. Further, instead of using the finite difference method to calculate the Grüneisen parameters, a perturbative approach to calculate the parameters was used [see Eq. (3.6)]. This approach is implemented in the ShengBTE program

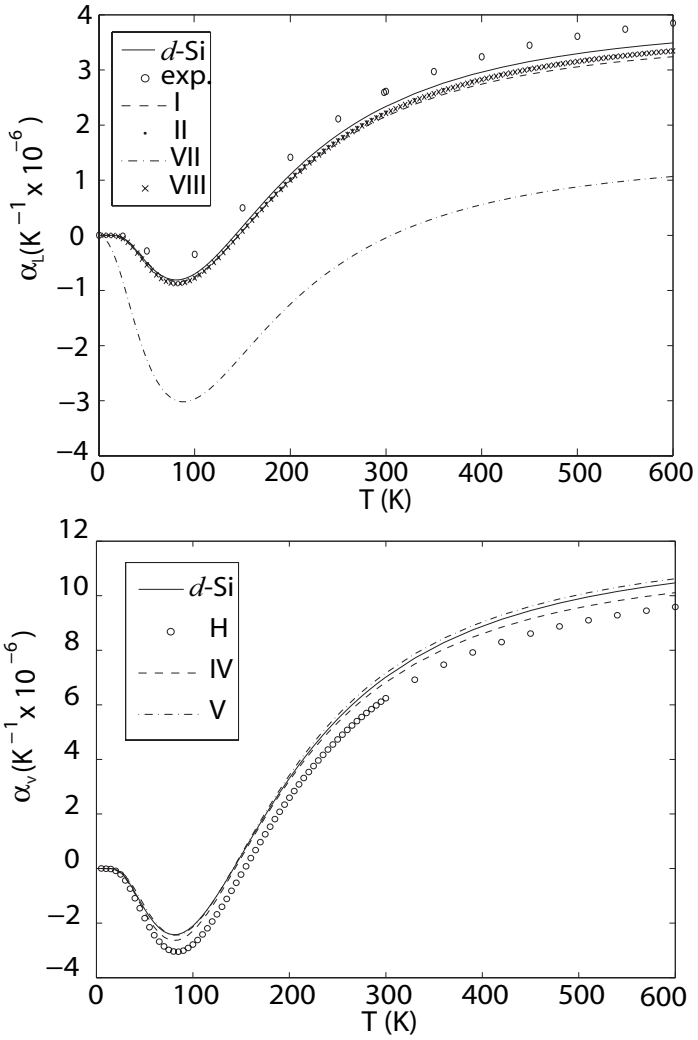

Figure 3.4: Top: Linear CTE for the studied cubic structures. The experimental values for d-Si are indicated with circles [111]. Bottom: Volumetric CTE for the studied hexagonal structures, d-Si is included as a reference.

package. By using the preceding method, the NTE temperature range was found to be about 255 K wide, which is less than obtained with LDA used in Article I. The minimum value of the CTE was found to be approximately the same and it occurred at ∼95 K.

Since the Grüneisen parameters in the present approach were taken to be independent of temperature, only temperature dependent quantity in the calculation of the CTE was the heat capacity $c_v(\lambda)$. Further, when Eq. (2.102) is considered, the only quantity which makes the CTE contribution of a particular state negative is the Grüneisen parameter $\gamma(\lambda)$. The Grüneisen parameter values were found to have a rather different kind of distribution in the case of the silicon clathrate framework VII, than in the other cases and this is the quantity which can be used to explain some of the differences in CTE between VII and the other structures. The Grüneisen parameters is related to the third-order IFCs through the relation [54]

$$\gamma_{\mu\nu}(\lambda) = -\sum_{j'=4}^{3n} \frac{12V_{\mu\nu}(0j')\,V(0j';\lambda;-\lambda)}{\hbar^2\omega_{0j'}\omega_\lambda} - \frac{2V_{\mu\nu}(\lambda;-\lambda)}{\hbar\omega_\lambda}, \tag{3.6}$$

In Eq. (3.6), the coefficients $V(\lambda;\lambda';\lambda'')$ and $V_{\mu\nu}(\lambda;\lambda')$ are given by Eqs. (2.45) and (2.58), respectively. Furthermore, in the case of cubic crystals, one may write $\gamma(\lambda) = \gamma_{\mu\mu}(\lambda)/3$. In the open source program package ShengBTE (version 1.0.2), only the second term in Eq. (3.6) is taken into account, the other being non-zero in general for crystals where the position of every atom is not determined by the symmetry [54]. From Eq. (2.58) it follows that one may write for the coefficients

$$\begin{aligned} V_{\mu\mu}(\lambda;-\lambda) &= \frac{\hbar}{4\omega_\lambda}\sum_{\kappa,\alpha}\sum_{l',\kappa',\alpha'}\sum_{l'',\kappa''}\Phi_{\alpha\alpha'\mu}(0\kappa;l'\kappa';l''\kappa'') \\ &\quad\times\frac{e_\alpha(\kappa|\lambda)\,e^*_{\alpha'}(\kappa'|\lambda)}{\sqrt{M_\kappa M_{\kappa'}}}e^{-i\mathbf{q}\cdot\mathbf{x}(l')}x_\mu(l''\kappa'')\,. \end{aligned} \tag{3.7}$$

The atomic masses M_κ are the same in all cases and makes no difference between the silicon clathrate frameworks. Further, since the silicon clathrate frameworks VII and VIII have body-centered cubic Bravais lattices, the exponential factors $e^{-i\mathbf{q}\cdot\mathbf{x}(l')}$ are the same in both cases and cannot be used to explain the differences in the Grüneisen parameter distributions in these structures (VIII has similar distribution than the other studied structures excluding VII). As the acoustic modes at relatively small wave vector values in VII are not particularly flat in comparison to the other structures, the factor $1/\omega_\lambda$ in Eq. (3.7) cannot be used either to explain the difference. What is left to explain the difference in the Grüneisen parameter distributions is the following factor

$$\Phi_{\alpha\alpha'\mu}(0\kappa;l'\kappa';l''\kappa'')\,e_\alpha(\kappa|\lambda)\,e^*_{\alpha'}(\kappa'|\lambda)\,x_\mu(l''\kappa'')\,. \tag{3.8}$$

For phonon states with more local character, the eigenvectors components $e_\alpha(\kappa|\lambda)$ are expected to have larger values when compared with the states with less local character.

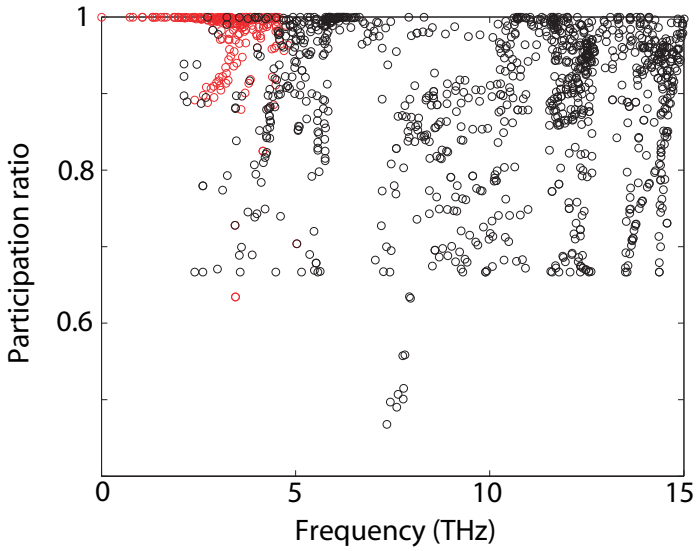

Figure 3.5: The participation ratio for the silicon clathrate framework VII. The values for the acoustic modes are drawn in red.

As stated in Sec. 2.2.3, $\mathbf{e}(\kappa|\lambda)$ can be considered as the probability amplitude that the atom $l = 0, \kappa$ vibrates in the phonon mode λ. In Fig. 3.5, the PR as a function of frequency is depicted for VII in order to compare the localization and thus the possible effect of the eigenvector components on Eq. (3.8) in VII and VIII. The smallest PR value for the acoustic modes is about 0.62 which indicates that the modes are relatively delocalized, which is a similar result as obtained for VIII (see Fig. 3.3). Therefore it seems that the differing Grüneisen parameter distribution for the acoustic modes in the case of VII is probably due to the differing third-order IFCs through the factor $\Phi_{\alpha\alpha'\mu}(0\kappa; l'\kappa'; l''\kappa'')\, x_\mu(l''\kappa'')$. With the preceding in mind, it appears that the third-order IFCs may have a relatively large role in explaining the anomalous NTE behaviour of the structure VII.

In particular, it seems that the anharmonicity in the silicon clathrate framework VII and in the clathrate $Na_4[Al_4Si_{19}]$ arise mostly for different reasons. In the case of $Na_4[Al_4Si_{19}]$ (Article III), rather large absolute values of $\gamma(\lambda)$ were found. However, the Grüneisen parameters for acoustic modes were found to be positive, while in the case of VII most of the corresponding values were negative. The preceding indicates that the CTE for $Na_4[Al_4Si_{19}]$ is relatively large when compared with Si_{23} and $[Si_{19}P_4]Cl_4$, but positive. Further, it was found that the anharmonicity in $Na_4[Al_4Si_{19}]$ is mostly due to differing harmonic quantities. The anharmonicity in VII, on the other hand, appears to be mostly due to the third-order IFCs. Thus, further comparative study of these structures may give answers to questions such as: why the anharmonicity observed in $Na_4[Al_4Si_{19}]$ does not lead to NTE, what is the role of NTE on the lattice thermal conductivity or how to maximize the third-order IFCs and at the same

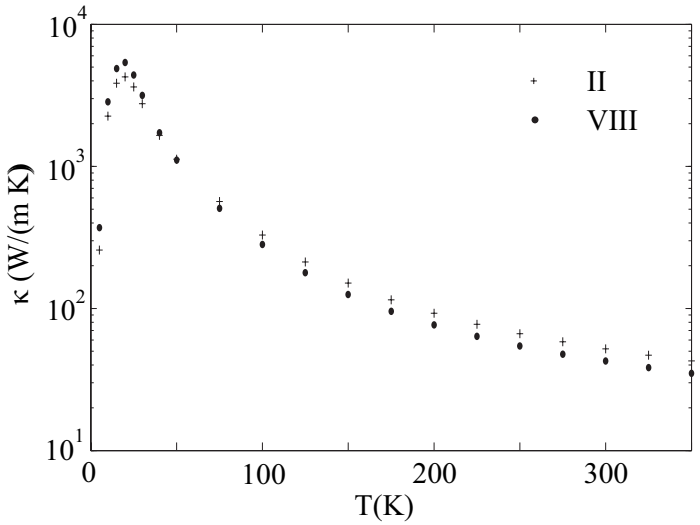

Figure 3.6: The calculated lattice thermal conductivity of the clathrate structures II and VIII (Si_{23}).

time the effect of harmonic quantities on the anharmonicity.

3.3 Lattice thermal conductivity

The lattice thermal conductivity of the silicon clathrate frameworks II and VIII was studied in Article II. The validity of the method was tested by comparing the calculated lattice thermal conductivity of *d*-Si with experimental results [114] within the temperature range 5-300 K. The lattice thermal conductivity values obtained for *d*-Si were in agreement with the earlier computational results [60, 115]. Within the temperature range 100-300 K the maximum difference between the experimental and computational results is 4%-13% (the largest difference is at 125 K). A possible reason for these rather large differences at lower temperatures is, for example, the description of isotopic scattering, since the expressions used are expected to be valid only for relatively weak perturbations and long wavelengths [61]. It was also justified in Article II that the difference at temperatures below 100 K may not be solely explained by the absence of boundary scattering in the model used, since the crystal size in the experiments was about 2 mm. The calculated lattice thermal conductivity values of the clathrate structures II and VIII (Si_{23}) are depicted in Fig. 3.6. At 300 K, the lattice thermal conductivities were approximately 52 and 43 W/(m K) for the silicon clathrate frameworks II and VIII, respectively. It was concluded that the difference may be partly due to the differing coefficients $V(\lambda; \lambda'; \lambda'')$. Further, the lattice thermal conductivity of the silicon clathrate framework II was found to be about twenty

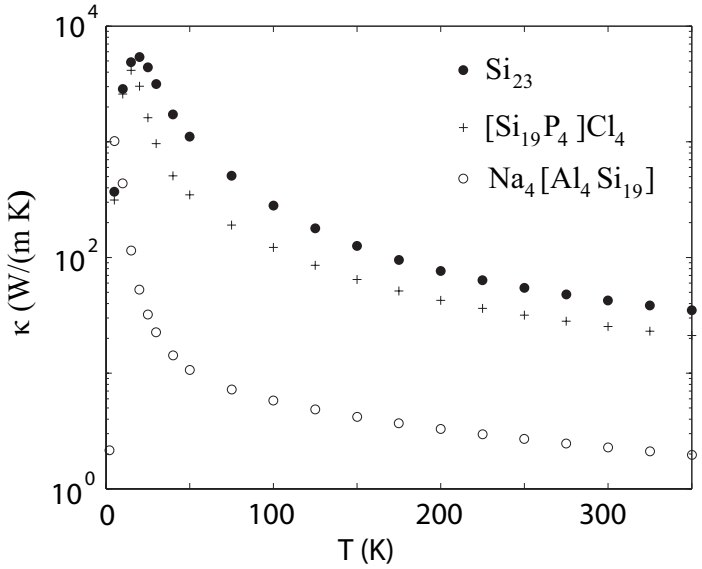

Figure 3.7: The calculated lattice thermal conductivity values for the structures Si_{23} (VIII), $[Si_{19}P_4]Cl_4$ and $Na_4[Al_4Si_{19}]$. Copyright © 2016, American Physical Society.

times higher than measured previously for polycrystalline samples at 300 K [116]. For a better comparison, the lattice thermal conductivity values measured for single crystals are needed.

The calculated lattice thermal conductivity values obtained in Article III are shown in Fig. 3.7. At 300 K, the calculated lattice thermal conductivities obtained for Si_{23} (VIII), $[Si_{19}P_4]Cl_4$ and $Na_4[Al_4Si_{19}]$ are approximately 43 W/(m K), 25 W/(m K) and 2 W/(m K), respectively. It was found that the clathrate $Na_4[Al_4Si_{19}]$ possesses lower lattice thermal conductivity due to smaller RTs and phonon group velocities. The RTs were found to be smaller due to larger three-phonon phase space and differing second-order IFCs, which change the phonon spectrum such that the anharmonicity increases. The third-order IFCs were found to have a rather similar distribution in all structures considered in Article III.

The lattice thermal conductivity of the semiconducting clathrates has been investigated quite intensively in recent years [39, 108, 109, 116–134]. Several different mechanisms have been proposed to explain the reduced lattice thermal conductivity values in these clathrates and lattice thermal conductivity values as low as ~ 1 W/m K at 150 K have been obtained experimentally for some silicon clathrates [1, 123], by using a single crystal samples. Some experimental and computational studies have given different explanations for the reasons behind the reduction of the lattice thermal conductivity in semiconducting clathrates [108, 109]. For instance, in Ref. [109] for the clathrate $Ba_8Ga_{16}Ge_{30}$ the reduction was suggested to arise mainly from rather short

RTs, while in Ref. [108] it was summarized that the reduction of the lattice thermal conductivity of the Ba_8Si_{46} clathrate is mostly due to the harmonic phonon spectrum (not dominated by the scattering processes). As already mentioned, when compared with $[Si_{19}P_4]Cl_4$, it seems that in the case of $Na_4[Al_4Si_{19}]$, the reduction in the lattice thermal conductivity appears to be mainly due to the shorter RTs, which in turn are shorter mostly due to the different harmonic phonon spectrum. Eventually, the differing harmonic phonon spectrum of these structures arise due to the mass reduced second-order IFCs. It also seems that similar mechanisms cause a rather low lattice thermal conductivity of $BaCo_4Sb_{12}$ and $YbFe_4Sb_{12}$ skutterudites [135, 136]

There are several shortcomings in the method used to calculate the lattice thermal conductivity and some of these issues were discussed in Article II. One issue is the same as encountered in amorphous solids [137, 138], namely, when the mean free path (MFP) of a phonon $mfp(\lambda) = \tau(\lambda)|\mathbf{v}(\lambda)|$ becomes shorter than the shortest distance between the atoms comprising the crystal. Since the aforementioned harmonic phonons do not exist a contradiction is encountered. In Article II it was discovered that in the case of the silicon clathrate framework VIII at 300 K, the percentage of $\mathbf{q}$-points violating the criterion $mfp(\lambda) < a$ (a is the lattice constant of the primitive unit cell) is about 2% for acoustical modes and 2%-96% for optical modes. Thus, strictly speaking, some of the phonon states are not well defined in the present perturbative approach. In other words, the states violating the criterion are not stationary, but are instead time dependent. The effect of the preceding may be identified when more rigorous methods are used to describe these systems in more detail.

It has been shown that the form of the energy flux used [Eq. (2.73)] is a special case of a more general energy flux, which may be written as [56]

$$\begin{aligned}\hat{\mathbf{J}}' &= \frac{1}{V}\sum_{l,\kappa}\frac{\hat{\mathbf{p}}(l\kappa)}{M_\kappa}\hat{H} + \frac{1}{V}\sum_{l,\kappa,l',\kappa'}\left[\hat{\mathbf{u}}(l\kappa) - \hat{\mathbf{u}}(l'\kappa')\right]\frac{1}{i\hbar}\left[\frac{\hat{\mathbf{p}}^2(l\kappa)}{2M_\kappa}, \hat{H}_{a0}\right]_- \\ &\quad + \frac{1}{V}\sum_{l,\kappa,l',\kappa'}\left[\mathbf{x}(l\kappa) - \mathbf{x}(l'\kappa')\right]\frac{1}{i\hbar}\left[\frac{\hat{\mathbf{p}}^2(l\kappa)}{2M_\kappa}, \hat{H}_{a0}\right]_-, \end{aligned} \tag{3.9}$$

where

$$\hat{H}_{a0} = \frac{1}{2}\sum_{l,\kappa,\alpha}\sum_{l',\kappa',\beta}\Phi_{\alpha\beta}(l\kappa; l'\kappa')\,\hat{u}_\alpha(l\kappa)\,\hat{u}_\beta(l'\kappa') + \hat{H}_a. \tag{3.10}$$

In Eq. (3.10), the first term on the right hand side is the potential energy part of the harmonic Hamiltonian $\hat{H}_0$ and $\hat{H}_a$ is given by Eq. (2.44). The first term on the right hand side of Eq. (3.9) is the lattice Hamiltonian $\hat{H} = \hat{H}_0 + \hat{H}_a$ times the velocity $\hat{\mathbf{p}}(l\kappa)/M_\kappa$ of an atom $l\kappa$ and it is usually expected to be rather small in crystals [137], but to our acknowledge, there is no known proof that this is true for arbitrary crystals. The relative contribution of the second and third term on the right hand side of Eq. (3.9) is determined by the following terms $\mathbf{x}(l\kappa) - \mathbf{x}(l'\kappa')$ and $\hat{\mathbf{u}}(l\kappa) - \hat{\mathbf{u}}(l'\kappa')$. If the relative displacements of the atoms $l\kappa$ and $l'\kappa'$ is relatively large, the second term may

have some significance, but it is usually expected to be rather small in crystals [56]. On the other hand, atoms vibrating in the so-called resonance modes are expected to have relatively large mean square displacements [110] and therefore in crystals in which such resonance modes exist, the second term may have some larger significance.

The energy flux used in the present work [Eq. (2.73)] can be obtained from Eq. (3.9) by using the following steps. First, the energy flux given by Eq. (3.9) is approximated as

$$\hat{\mathbf{J}}' \approx \frac{1}{V} \sum_{l,\kappa,l',\kappa'} \left[\mathbf{x}\left(l\kappa\right) - \mathbf{x}\left(l'\kappa'\right)\right] \frac{1}{i\hbar} \left[\frac{\hat{\mathbf{p}}^2\left(l\kappa\right)}{2M_\kappa}, \hat{H}_{a0}\right]_- . \tag{3.11}$$

Then, $\hat{H}_a$ is neglected in the expression given by Eq. (3.10) giving

$$\hat{\mathbf{J}}' \approx \frac{1}{V} \sum_{l,\kappa,l',\kappa'} \left[\mathbf{x}\left(l\kappa\right) - \mathbf{x}\left(l'\kappa'\right)\right] \frac{1}{i\hbar} \left[\frac{\hat{\mathbf{p}}^2\left(l\kappa\right)}{2M_\kappa}, \hat{H}_{p0}\right]_- , \tag{3.12}$$

where $\hat{H}_{p0}$ denotes the potential energy part of the harmonic Hamiltonian. After using the expansions given by Eqs. (2.34) and (2.35), by applying the commutation relations for the creation and annihilation operators and imposing some further simplifications on the resulting expression (discussed in Ref. [56]) one obtains the energy flux $\hat{\mathbf{J}}$ given by Eq. (2.73). Thus, the energy flux used to calculate the lattice thermal conductivity in the present work is a special case of the last term on the right hand side of Eq. (3.9) and there are more general harmonic energy fluxes than used here. Moreover, if the anharmonicity of a crystal is sufficiently strong, the anharmonic energy fluxes may have some significance in the calculation of lattice thermal conductivity. In the case of some particular triangular lattices, the lowest-order anharmonic energy fluxes have been shown to make even larger contribution to the lattice thermal conductivity than the harmonic ones [139]. To the author's knowledge, there is no *ab initio* lattice thermal conductivity computations applied on real materials so far by using the anharmonic heat fluxes. Since the harmonic heat flux already contains such contributions that are not taken into account in the present approaches, these contributions should not be discarded in general, unless it can be shown that such contributions are in practice insignificant. The preceding, however, can be rather difficult to verify without explicit computations due to the complexity of the systems.

The present method also neglects the effect of thermal expansion, which makes the IFCs temperature dependent. *Ab initio* calculations of the lattice thermal conductivity have already been established for PbTe and the results show that in some materials the effect of thermal expansion on the lattice thermal conductivity may be rather significant [31]. There is also some development in the computational methods that allow the calculation of anharmonic properties beyond the present perturbative approach [19]. Application of such methods on the lattice thermal conductivity calculations of semiconducting clathrates, for example, may provide some further insights

about the lattice thermal conductivity in these materials and can be used to test the validity of the present results.

One further issue causing some numerical inaccuracy is the way by which the ShengBTE program package treats the third-order IFCs. The second-order IFCs in the QE program package are obtained by Fourier transforming the dynamical matrix $D_{\alpha\beta}(\kappa\kappa'|\mathbf{q})$ by using arbitrary $\mathbf{q}$ meshes. However, $\mathbf{q}$ meshes used are usually smaller than $(10, 10, 10)$, say, for materials with unit cells larger than that of d-Si (two atoms per primitive unit cell). After the calculation with (n_1, n_2, n_3) mesh is completed, the QE program package uses Fourier interpolation to obtain the dynamical matrix in a mesh (n_1', n_2', n_3'), which is denser than the original one. One obtains the second-order IFCs by (discrete) Fourier transform within a cell, which consists of $n_1' \times n_2' \times n_3'$ unit cells [18]. In Ref. [19], the third-order IFCs have been treated in a similar way. In ShengBTE, a different approach is used in order to calculate the third-order IFCs (the program thirdorder.py included in the ShengBTE distribution [21]): ShengBTE creates a super cell (m_1, m_2, m_3) and then forms displacement patterns for single point DFT calculations from which all the different third-order IFCs up to some cut off value are calculated by using finite differences and by taking the symmetry into account. In the calculation of the RTs, for example, the third-order Hamiltonian [Eqs. (2.44) and (2.44)] is used and what is needed is the Fourier transform of the third-order IFCs. The issue is that the ShengBTE program uses the third-order IFCs obtained within a super cell (m_1, m_2, m_3) with arbitrary $\mathbf{q}$ meshes. The preceding procedure is different from that used with the second-order IFCs implemented in the QE and this causes some errors in the calculations. In the case of the clathrates, it was not possible to test the convergence with respect to the super cell size due to the computational requirements.

3.4 Elastic and thermal properties

In Article IV, the elastic and thermal properties of crystals with arbitrary symmetry were considered by using many-body perturbation theory. There have been several works discussing these properties by applying different techniques [15,41,45,54,68,69, 140–145], but to the author's knowledge no such a systematic approach established in Article IV exist. For instance, generic expressions for kth-order elastic constants were derived up to third-order [$h = 3$, Eq. (2.128)] and to various orders in IFCs. The adiabatic and isothermal stress with the second-order isothermal elastic constants are essential when the CTE is calculated by using Eq. (2.135), for example. The higher-order elastic constants, on the other hand, can be useful in the study of physical acoustics and non-linear elasticity of crystals [146,147]. Present computational methods allow the calculation of the elastic constants for arbitrary crystals and elastic constants up to fourth-order have been computed for some crystalline materials [148].

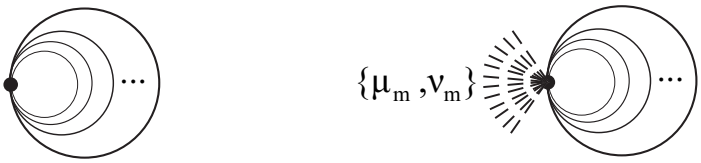

Figure 3.8: The first order diagrams considered in Article IV.

However, the computations as established in Refs. [148–150], for example, take only the so-called static terms into account and thus neglect the effect of the vibrations of the lattice (phonons), which may have some importance in some cases. Both of these effects are taken into account when the perturbative approach applied in Article IV is used. In the situation when the anharmonic forces are sufficiently strong, the perturbation theory with a few lowest-order terms, used in the present approach, may not describe the system in sufficient detail and more rigorous methods are probably needed. An example of such method is the self-consistent theory for phonons described, for instance, in Refs. [71, 151–153].

All diagrams considered in Article IV are depicted in Figs. 3.8-3.10. Some of the diagrams shown in Figs. 3.8-3.10 have been given earlier by using diagrams or algebraic expressions. The third and higher-order elastic constants have not been considered in such a systematic manner before by applying the present approach. For example, in Ref. [142], only the static contribution to the third-order elastic constant was considered, while in Ref. [54] only one contribution to the isothermal third-order elastic constant was taken into account and was represented as a diagram. All diagrams represented in Ref. [41] (diagrams related to elastic constants or stresses) were also shown in Ref. [54]. In Ref. [54], two algebraic expressions corresponding to stress contributions were given. The stress diagrams considered in Ref. [54] were a special case of Fig. 3.8, special cases of diagrams h), k) and m) in Fig. 3.9 and one third-order diagram. Furthermore, in Ref. [54], three different algebraic expressions were given for the second-order isothermal elastic constants, while diagrams included were special cases of Fig. 3.8, special cases of diagrams e), f), h), i), j), l), m) and n) shown in Fig. 3.9 and special cases of diagrams e), f), g) and m) shown in Fig. 3.10.

To get some understanding how the diagrams shown in Figs. 3.8-3.10 arise, few examples are considered. To first-order ($h = 1$), the isothermal elastic constants may be

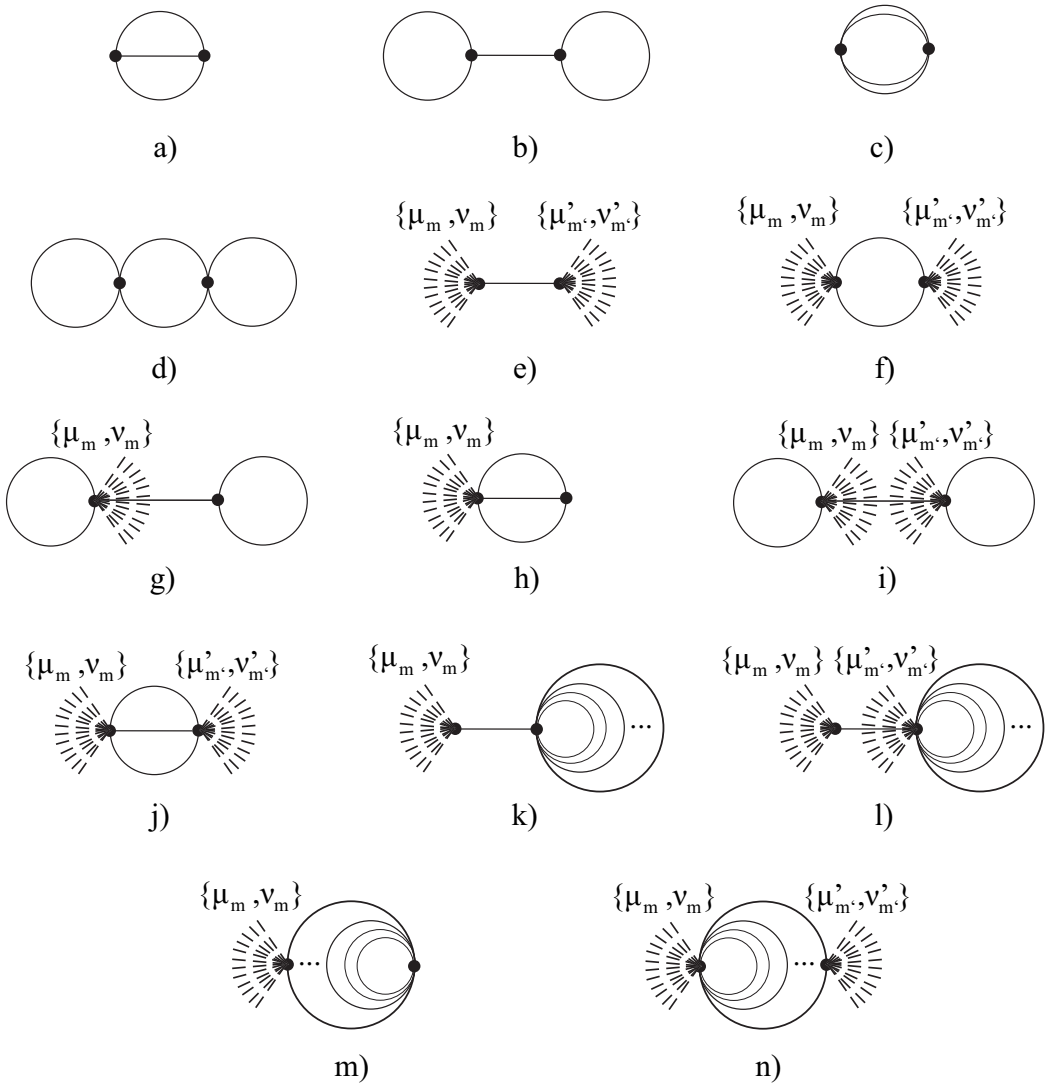

Figure 3.9: Some second-order diagrams considered in Article IV.

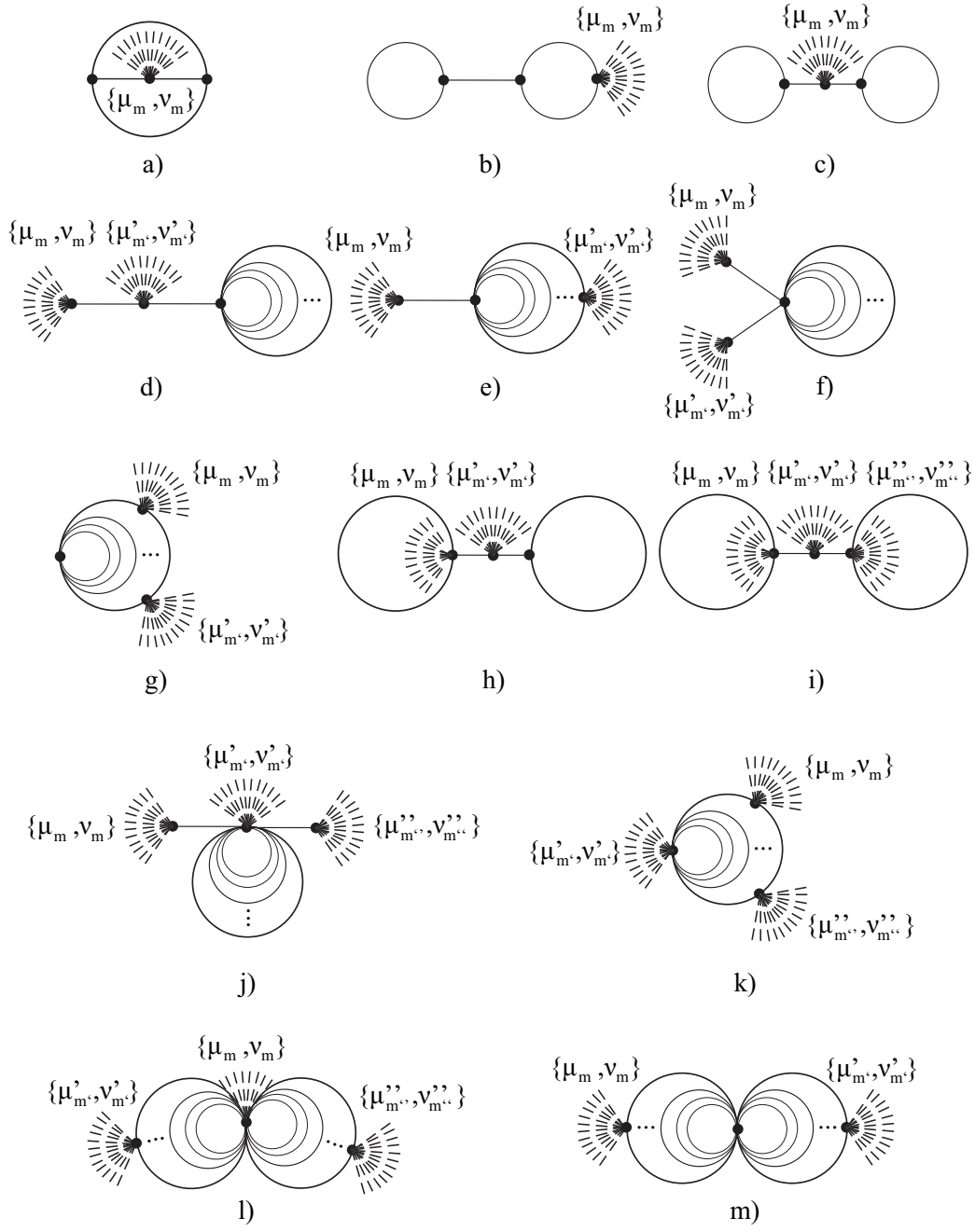

Figure 3.10: Some third-order diagrams considered in Article IV.

written as [Eqs. (2.128), (2.133) and (2.134)]

$$\begin{aligned}
\tilde{c}^{T,(1)}_{\bar{\mu}_m\bar{\nu}_m} &= \frac{1}{\beta}\int_0^\beta d\tau_1 \sum_{n=2m'}\sum_{\bar{\lambda}_n}\frac{1}{m!}V_{\bar{\mu}_m\bar{\nu}_m}\left(\bar{\lambda}_n\right)\left\langle\mathcal{T}\left\{\hat{A}_{\lambda_1}(\tau_1)\cdots\hat{A}_{\lambda_n}(\tau_1)\right\}\right\rangle_{0,c} \\
&= \sum_{n=2m'}\sum_{\bar{\lambda}_n}\frac{1}{m!}V_{\bar{\mu}_m\bar{\nu}_m}\left(\bar{\lambda}_n\right)\prod_{k=1\wedge k=\,odd}^{n-1}(k) \\
&\quad\times\sum_{n_1=-\infty}^{\infty}G_0\left(\lambda_1|\omega_{n_1}\right)\delta_{\lambda_1-\lambda_2}\cdots\sum_{n_{n-1}=-\infty}^{\infty}G_0\left(\lambda_{n-1}|\omega_{n_{n-1}}\right)\delta_{\lambda_{n-1}(-\lambda_n)} \\
&= \sum_{n=2m'}\sum_{\bar{\lambda}_{n/2}}\frac{1}{m!}V_{\bar{\mu}_m\bar{\nu}_m}\left(\bar{\lambda}_{n/2};-\bar{\lambda}_{n/2}\right)\prod_{k=1\wedge k=\,odd}^{n-1}(k) \\
&\quad\times\sum_{n_1=-\infty}^{\infty}G_0\left(\lambda_1|\omega_{n_1}\right)\cdots\sum_{n_{n/2}=-\infty}^{\infty}G_0\left(\lambda_{n/2}|\omega_{n_{n/2}}\right), \qquad (3.13)
\end{aligned}$$

where $m' \in \mathbb{N}$ and Wick's Theorem is used. Further, the notation introduced in Secs. 2.2.2 and 2.4.2 is used. The lowest-order case ($n = 0$) is $V_{\bar{\mu}_m\bar{\nu}_m}/m!$ and the corresponding diagram is a special case of the second diagram in Fig. 3.8, that is a dot and a fan of dashed lines. The number of dashed lines in the fan depends on the order of the elastic constants considered, the lowest-order case ($m = 1$) being the isothermal stress. The next case is $n = 2$, which can be written as

$$\sum_{\lambda}\frac{1}{m!}V_{\bar{\mu}_m\bar{\nu}_m}(\lambda;-\lambda)\sum_{n=-\infty}^{\infty}G_0\left(\lambda|\omega_n\right) = \frac{2}{m!}\sum_{\lambda}V_{\bar{\mu}_m\bar{\nu}_m}(\lambda;-\lambda)\left(\bar{n}_\lambda+\frac{1}{2}\right). \qquad (3.14)$$

The corresponding diagram is a dot connected with a fan of dashed lines and circle which intersects the dot. Each circle in Fig. 3.8 represents a Green's function $\sum_{n=-\infty}^{\infty}G_0\left(\lambda|\omega_n\right)$. The number of outgoing lines from a dot gives the number of phonon labels included in the coefficients $V_{\bar{\mu}_m\bar{\nu}_m}\left(\bar{\lambda}_n\right)$ or $V\left(\bar{\lambda}_n\right)$. The vertices describing the coefficients $V\left(\bar{\lambda}_n\right)$ are otherwise the same as the vertices describing the strained coefficients $V_{\bar{\mu}_m\bar{\nu}_m}\left(\bar{\lambda}_n\right)$, except that in the former case, there is no fan of dashed lines. The lines between two vertices arise from the terms like

$$\sum_{n_1=-\infty}^{\infty}G_0\left(\lambda_1|\omega_{n_1}\right)\delta_{\lambda_1-\lambda_2}, \qquad (3.15)$$

where λ_1 and λ_2 belong to different coefficients such that after the summation over λ_2, say, two different coefficients share the same label λ_1. Another example is diagram n) of Fig. 3.9, the algebraic expression for this diagram can be written as ($m+m' = l$,

which is the order of the elastic constant)

$$
\begin{aligned}
&-\frac{1}{\beta}\sum_{\lambda_1,\lambda_2}\sum_{m,m'=1}\frac{1}{m!m'!}\sum_{\bar{\mu}_m,\bar{\nu}_m}\sum_{\bar{\mu}'_{m'},\bar{\nu}'_{m'}}\sum_{n'=1}\sum_{\bar{\lambda}'_{2n'}} V_{\bar{\mu}_m\bar{\nu}_m}(\lambda_1;\lambda_2)\, V_{\bar{\mu}'_{m'}\bar{\nu}'_{m'}}\left(\bar{\lambda}'_{2n'}\right)\\
&\times n'\delta_{\lambda_1(-\lambda'_1)}\delta_{\lambda_2(-\lambda'_2)}\delta_{\lambda'_3(-\lambda'_4)}\delta_{\lambda'_5(-\lambda'_6)}\cdots\delta_{\lambda'_{2n'-1}(-\lambda'_{2n'})}\\
&\times\int_0^\beta d\tau_1\int_0^\beta d\tau_2\sum_{n_1,n_2=-\infty}^{\infty} G_0(\lambda_1|\omega_{n_1})\, e^{i\omega_{n_1}(\tau_1-\tau_2)} G_0(\lambda_2|\omega_{n_2})\, e^{i\omega_{n_2}(\tau_1-\tau_2)}\\
&\times\prod_{k=1\wedge k=odd}^{2n'-3} k\sum_{n_3=-\infty}^{\infty} G_0(\lambda'_3|\omega_{n_3})\cdots\sum_{n_{2n'-1}=-\infty}^{\infty} G_0\left(\lambda'_{2n'-1}|\omega_{n_{2n'-1}}\right). \qquad (3.16)
\end{aligned}
$$

The summations in Eq. (3.16) can be simplified by using the method described in Appendix A. When the summations over the labels $\lambda'_1, \lambda'_2, \lambda'_4, \lambda'_6, \ldots$ are established, it can be seen that the coefficients share the labels λ_1, λ_2, that is, the coefficients after the summations can be written as $V_{\bar{\mu}_m\bar{\nu}_m}(\lambda_1;\lambda_2)\, V_{\bar{\mu}'_{m'}\bar{\nu}'_{m'}}(-\lambda_1;-\lambda_2;\lambda'_3;-\lambda'_3;\ldots)$. The Green's functions on the third line of Eq. (3.16) connect the vertices and are therefore represented by the semicircle shaped lines in diagram n) of Fig. 3.9. Few example calculations corresponding to the second and third-order diagrams are given in Appendix C.

As stated in Article IV, the perturbation expansion for arbitrary macroscopic parameters is similar in all such cases provided the coefficients have the same symmetry properties and the number of parameters is the same. For instance, if the parameters are electric field components, the expansion allows the calculation of the pyroelectric coefficient from the derivatives of free energy [79]. Furthermore, if the macroscopic parameters in the expansion [Eq. (2.55)] are the infinitesimal strain parameters and electric field components, one may obtain, for example, the components of the piezoelectric tensor from the mixed derivatives of free energy [79]. The lowest-order terms of expansions where the macroscopic parameters are infinitesimal strains and electric field components are considered in Refs. [15] and [41] and the latter work is based on the Green's function technique. With the preceding discussion in mind, all the diagrams shown in Figs. 3.8-3.10 are valid for arbitrary macroscopic parameters in Eq. (2.55) difference being in the coefficients $g_{\lambda_{1_1}\cdots\lambda_{k_m}}$ (superscripts omitted). This can be indicated by changing the symbols in the diagrams which refer to the parameters used.

The CTE can be calculated by using Eq. (2.135). Thus, the diagrams of Figs. 3.8-3.10 which contribute to the CTE are those having one or two strained vertices. For example, the first-order contributions needed to calculate the CTE can be written as (results of Article IV)

$$
\tilde{c}^{T(1)}_{\bar{\mu}_k\bar{\nu}_k} = \frac{1}{k!}\sum_{n=2m}\sum_{\bar{\lambda}_{n/2}} V_{\bar{\mu}_k\bar{\nu}_k}\left(\bar{\lambda}_{n/2};-\bar{\lambda}_{n/2}\right)\xi^{(1)}\left(\bar{\lambda}_{n/2}\right)+\frac{1}{k!}V_{\bar{\mu}_k\bar{\nu}_k}, \qquad (3.17)
$$

$$\sigma_{\mu\nu}^{A(1)} - \sigma_{\mu\nu}^{T(1)} = -\beta\hbar \sum_{n=2m} \sum_{\bar{\lambda}_{n/2}} V_{\mu\nu}\left(\bar{\lambda}_{n/2}; -\bar{\lambda}_{n/2}\right) \xi^{(2)}\left(\bar{\lambda}_{n/2}\right). \tag{3.18}$$

In Eqs. (3.17) and (3.18), $m = 1, 2, \ldots$ and the notation introduced in Appendix B is used for $\xi^{(1)}\left(\bar{\lambda}_{n/2}\right)$ and $\xi^{(2)}\left(\bar{\lambda}_{n/2}\right)$. From Eqs. (3.17) and (3.18) it follows that only the compliance tensor $\tilde{s}_{\bar{\mu}_k\bar{\nu}_k}^{T(1)}$ has the so-called static term $V_{\bar{\mu}_k\bar{\nu}_k}$, while in the expression for $\sigma_{\mu\nu}^{A(1)} - \sigma_{\mu\nu}^{T(1)}$ this term is absent. In order to calculate the lowest-order non-static contributions to $s_{\mu_1\nu_1\mu_2\nu_2}^{T(1)}$, the fourth-order IFCs are needed while the lowest-order contribution to $\sigma_{\mu\nu}^{A(1)} - \sigma_{\mu\nu}^{T(1)}$ requires third-order IFCs. Few second-order contributions to $\sigma_{\mu\nu}^{A(2)} - \sigma_{\mu\nu}^{T(2)}$, derived in Article IV, are shown in Appendix B. In the calculations of the present work (Article I), only the static contribution to the second-order elastic constants and the lowest-order term ($n = 2$) of Eq. (3.18) were taken into account.

Symmetry restrictions simplify the calculation of the CTE and for cubic crystals, for example, Eq. (2.135) can be written as

$$\alpha_{\mu\mu} = \frac{1}{T} \frac{\sigma_{\mu\mu}^{A} - \sigma_{\mu\mu}^{T}}{c_{1111}^{T} + 2c_{1122}^{T}}. \tag{3.19}$$

To obtain the elastic constants $c_{\bar{\mu}_k\bar{\nu}_k}^{T}$, defined in terms of finite strain parameters, from the elastic constants $\tilde{c}_{\bar{\mu}_k\bar{\nu}_k}$, which are defined in terms of infinitesimal strain parameters, transformation equations must be used. The aforementioned equations are considered in Refs. [15, 78] and the transformation equation for the second-order elastic constants was given in Article IV. Since for cubic crystals $c_{1111}^{T} + 2c_{1122}^{T} > 0$ [79], the NTE occurs in cubic crystals only if $\sigma_{\mu\mu}^{A} - \sigma_{\mu\mu}^{T} < 0$. Thus, only the non-static terms cause the NTE. As can be seen from Eqs. (3.17) and (3.18), to first-order, the magnitude of the CTE is proportional to $V_{\mu\nu}\left(\bar{\lambda}_{n/2}; -\bar{\lambda}_{n/2}\right) / V_{\bar{\mu}_2\bar{\nu}_2}\left(\bar{\lambda}_{n/2}; -\bar{\lambda}_{n/2}\right)$. That is, the magnitude of the CTE is proportional to the ratio of the IFCs of odd and even-order.

The explicit algebraic expressions derived in Article IV can be used to calculate the CTE such that the method goes beyond the QHA and more rigorous results can be obtained. By applying such methods, one may obtain some further understanding about the NTE phenomenon.

4 Conclusions

The thermal conductivity and thermal properties of silicon clathrates were studied. In Article I, the silicon clathrate framework VII was found to have NTE temperature range up to 255 K. The reason for this rather anomalous NTE behavior seems to be a relatively strong anharmonicity through the third-order IFCs. Since some of the reasons behind the NTE phenomena are unknown, further and more detailed study of the materials such as the silicon clathrate framework VII may give some useful information about the NTE in general. More detailed calculations of the CTE including higher-order perturbative terms, given for example in Article IV, may be used to test the validity of the present results.

The lattice thermal conductivity of two different silicon clathrate frameworks and two different semiconducting (or Zintl) clathrates was calculated by using an iterative solution of the linearized BTE and *ab initio* lattice dynamics. The validity of the method was tested by comparing computational results with the experimental ones in the case of *d*-Si. At 300 K, the obtained lattice thermal conductivities were 52 W/(m K), 43 W/(m K), 25 W/(m K) and 2 W/(m K) for the clathrates II, VIII (Si_{23}), $[Si_{19}P_4]Cl_4$ and $Na_4[Al_4Si_{19}]$, respectively. The one-order of magnitude lower lattice thermal conductivity of the clathrate $Na_4[Al_4Si_{19}]$ seems to be due to increased anharmonicity and smaller phonon group velocities which in turn appear to result mostly from rather different harmonic phonon spectrum. The results indicate that in some cases, the harmonic quantities can make relatively large differences in the anharmonicity of two similar crystal structures, even when the anharmonic IFCs appear to be rather similar. The possible shortcomings of the present method used to calculate the lattice thermal conductivity were discussed and further studies of these materials with more rigorous methods are needed to assess the validity of the present results. The results of the present work may give some insight on what properties are needed in the development of new crystalline materials with relatively low lattice thermal conductivity, which in turn is expected to increase the thermoelectric efficiency through the thermoelectric figure of merit ZT.

Derivation of the expressions for different elastic and thermal quantities was established by using the method of many-body Green's functions and many-body perturbation theory. A physical interpretation of the phonon eigenvectors from a quantum mechanical point of view was also discussed. The expressions obtained extend the existing results and allow the calculation of the adiabatic and isothermal kth-order elastic constants whenever the needed IFCs are available. The results can be also

used to calculate the anharmonic thermal properties of a crystal such as the internal energy, Helmholtz free energy, heat capacity at constant strain (volume), heat capacity at constant stress (pressure), entropy and CTE. In particular, the derived expressions may be used to give some further insights about the NTE phenomenon. Further, the derived expressions can be used for systems, which are not described appropriately by the QHA. However, when the anharmonicity is sufficiently strong, few lowest-order terms in the expansion, considered in this thesis, may not describe the system appropriately and more rigorous methods are needed.

The quest for more efficient thermoelectric materials is a relatively complicated one. In addition to the properties considered in this thesis, one has to describe the electronic transport problem in order to describe quantities such as the thermoelectric efficiency. The description of the electronic transport problem, in turn, is a rather challenging task since couplings like the electron-phonon interactions must usually be included. Further, all the quantities needed to calculate the thermoelectric efficiency are somehow dependent on each other. For instance, the electronic structure partly determines the values of the IFCs and thus the harmonic phonon spectrum and anharmonic IFCs. The harmonic and anharmonic IFCs, in turn, determine the CTE which shows how the crystal expands or contracts as a function of temperature. While the crystal expands or contracts, the electronic structure changes determining again the phonon spectrum, phonon-phonon interactions, electron-phonon interactions and so on, which leads to the chance in the values of lattice thermal conductivity, electronic part of thermal conductivity *et cetera*. At the present, to the author's knowledge, there is no such method, which takes all the aforementioned properties into account. Thus, there are many open questions related to the lattice thermal conductivity and thermoelectricity and it is thus probably useful to continue the development of theoretical, computational and experimental techniques to achieve deeper understanding, which may lead to the actual applications in a more extensive manner. While pursuing this understanding, some unpredictable findings may occur as the history of science has shown.

A Solutions for integrals

Some rather complicated integrals appear when the perturbation series of Article IV is evaluated (Sec. 2.4.3). By using the Fourier transforms of Green's functions, these integrals are transformed into infinite series. In this Appendix, a method, which can be used to simplify these series is described. The method is based on the residue theorem.

A.1 Generic method

The residue theorem states that [154]

$$\oint_C dz g(z) = 2\pi i \left(a_{-1} + b_{-1} + c_{-1} + \cdots\right). \tag{A.1}$$

where $g(z)$ is an analytic function within a simple closed curve C except at singularities $a, b, c, \ldots$, with residues $a_{-1} + b_{-1} + c_{-1}$. Let $g(z) = f(z)\, m(z)$, then, one may write the residue theorem as

$$\oint_C dz f(z)\, m(z) = 2\pi i \left[\text{sum of res. of } f(z)\, m(z) \text{ at the poles of } f(z) \text{ and } m(z)\right]. \tag{A.2}$$

The contour C and the function $m(z)$ is chosen in such that the integral in Eq. (A.2) vanishes and in this case one obtains

$$\sum_{n=-\infty}^{\infty} f(n) = -\left[\text{sum of res. of } f(z)\, m(z) \text{ at the poles of } f(z)\right]. \tag{A.3}$$

Let

$$m(z) = \pi \cot \pi z, \tag{A.4}$$

then, it can be shown that if [154]

$$|f(z)| \leq \frac{M}{|z|^k}, \quad k > 1 \wedge M \in \mathbb{R}, \tag{A.5}$$

then

$$\oint_C dz f(z)\, m(z) = 0, \tag{A.6}$$

as one considers a limit where the contour C encircles all the poles of the function $m(z)$ (the number of simple poles is infinite). Since $m(z)$ has simple poles at $z = n = 0, \pm 1, \pm 2, \ldots$, one obtains the following residues for these poles

$$\lim_{z \to n} (z - n)\, m(z)\, f(z) = \pi \lim_{z \to n} (z - n) \cot \pi z f(z) = f(n). \tag{A.7}$$

Since there is an infinite number of these poles, one may write Eq. (A.2) as [noting also Eq. (A.6)]

$$\sum_{n=-\infty}^{\infty} f(n) = -\sum_{n} Res\left[f(z)\, \pi \cot \pi z, p_n\right], \tag{A.8}$$

where the right hand side is the sum of residues of $f(z)\, m(z)$ at the poles $\{p_n\}$ of $f(z)$.

A.2 Example calculations

As an example, the following calculation is established. From Eq. (2.120)

$$G_0(\lambda|\omega_n) = \frac{1}{\beta\hbar} \frac{2\omega_\lambda}{\omega_\lambda^2 + \omega_n^2}, \quad \omega_n = \frac{2\pi n}{\beta\hbar}. \tag{A.9}$$

Let

$$f(n) = G_0(\lambda|\omega_n) = \frac{1}{\beta\hbar} \frac{2\omega_\lambda}{\omega_\lambda^2 + \omega_n^2} = \frac{1}{\beta\hbar} \frac{2\omega_\lambda}{\omega_\lambda^2 + \left(\frac{2\pi n}{\beta\hbar}\right)^2}, \tag{A.10}$$

$$f(z) = G_0(\lambda|\omega_n, n \to z) = \frac{1}{\beta\hbar} \frac{2\omega_\lambda}{\omega_\lambda^2 + \left(\frac{2\pi z}{\beta\hbar}\right)^2}. \tag{A.11}$$

The poles of $f(z)$ are at (poles are simple)

$$p_m = \pm i\omega_\lambda \frac{\beta\hbar}{2\pi}. \tag{A.12}$$

One may calculate the residues at these simple poles as follows

$$\pi \lim_{z \to +i\omega_\lambda \frac{\beta\hbar}{2\pi}} \left(z - i\omega_\lambda \frac{\beta\hbar}{2\pi}\right) \cot(\pi z) \frac{1}{\beta\hbar} \frac{2\omega_\lambda}{\omega_\lambda^2 + \left(\frac{2\pi z}{\beta\hbar}\right)^2} = -\frac{1}{2} \coth\left(\frac{\beta\hbar\omega_\lambda}{2}\right), \tag{A.13}$$

$$\pi \lim_{z \to -i\omega_\lambda \frac{\beta\hbar}{2\pi}} \left(z + i\omega_\lambda \frac{\beta\hbar}{2\pi}\right) \cot(\pi z) \frac{1}{\beta\hbar} \frac{2\omega_\lambda}{\omega_\lambda^2 + \left(\frac{2\pi z}{\beta\hbar}\right)^2} = -\frac{1}{2} \coth\left(\frac{\beta\hbar\omega_\lambda}{2}\right). \tag{A.14}$$

Thus, from Eqs. (A.8), (A.13) and (A.14), it follows that

$$\sum_{n=-\infty}^{\infty} f(n) = \coth\left(\frac{\beta\hbar\omega_\lambda}{2}\right). \tag{A.15}$$

One may write

$$\coth\left(\frac{\beta\hbar\omega_\lambda}{2}\right) = 2\bar{n}_\lambda + 1, \quad \bar{n}_\lambda = \frac{1}{e^{\beta\hbar\omega_\lambda} - 1}, \tag{A.16}$$

and thus

$$\sum_{n=-\infty}^{\infty} f(n) = \sum_{n=-\infty}^{\infty} G_0(\lambda|\omega_n) = \sum_{n=-\infty}^{\infty} \frac{1}{\beta\hbar} \frac{2\omega_\lambda}{\omega_\lambda^2 + \omega_n^2} = 2\bar{n}_\lambda + 1. \tag{A.17}$$

Another example to be considered is

$$\sum_{n,n''=-\infty}^{\infty} G_0(\lambda|\omega_n) G_0(\lambda'|\omega_{n''}) \delta_{-m+n+n''} = \sum_{n=-\infty}^{\infty} G_0(\lambda|\omega_n) G_0(\lambda'|\omega_n - \omega_m) \tag{A.18}$$

where

$$G_0(\lambda|\omega_n) G_0(\lambda'|\omega_n - \omega_m) = \frac{1}{\beta\hbar} \frac{2\omega_\lambda}{\omega_\lambda^2 + \omega_n^2} \frac{1}{\beta\hbar} \frac{2\omega_{\lambda'}}{\omega_{\lambda'}^2 + (\omega_n - \omega_m)^2}. \tag{A.19}$$

From Eq. (A.8)

$$\sum_{n=-\infty}^{\infty} f(n) = -\sum_m Res\left[f(z)\,\pi\cot\pi z, p_m\right], \tag{A.20}$$

where

$$f(n) = G_0(\lambda|\omega_n) G_0(\lambda'|\omega_n - \omega_m), \tag{A.21}$$

$$\begin{aligned} f(z) &= G_0(\lambda|\omega_n, n \to z) G_0(\lambda'|\omega_n - \omega_m, n \to z) \\ &= \frac{1}{\beta\hbar} \frac{2\omega_\lambda}{\omega_\lambda^2 + \left(\frac{2\pi z}{\beta\hbar}\right)^2} \frac{1}{\beta\hbar} \frac{2\omega_{\lambda'}}{\omega_{\lambda'}^2 + \left(\frac{2\pi z}{\beta\hbar} - \omega_m\right)^2}. \end{aligned} \tag{A.22}$$

The poles of $f(z)$ are at

$$p_m = \left\{ \pm i\omega_\lambda \frac{\beta\hbar}{2\pi}, +i\frac{\beta\hbar}{2\pi}(\omega_{\lambda'} - i\omega_m), -i\frac{\beta\hbar}{2\pi}(\omega_{\lambda'} + i\omega_m) \right\}. \tag{A.23}$$

The residues at these poles can be written as

$$Res\left[f(z)\,\pi\cot\pi z, +i\omega_\lambda\frac{\beta\hbar}{2\pi}\right] = -\frac{1}{\beta\hbar} \frac{\omega_{\lambda'} \coth\left(\frac{\beta\hbar\omega_\lambda}{2}\right)}{(-\omega_\lambda + \omega_{\lambda'} - i\omega_m)(\omega_\lambda + \omega_{\lambda'} + i\omega_m)}, \tag{A.24}$$

$$Res\left[f(z)\,\pi\cot\pi z, -i\omega_\lambda\frac{\beta\hbar}{2\pi}\right] = -\frac{1}{\beta\hbar} \frac{\omega_{\lambda'} \coth\left(\frac{\beta\hbar\omega_\lambda}{2}\right)}{(\omega_\lambda + \omega_{\lambda'} - i\omega_m)(-\omega_\lambda + \omega_{\lambda'} + i\omega_m)}, \tag{A.25}$$

$$Res\left[f(z)\,\pi\cot\pi z, +i\frac{\beta\hbar}{2\pi}(\omega_{\lambda'} - i\omega_m)\right] = -\frac{1}{\beta\hbar} \frac{\omega_\lambda \coth\left(\frac{\beta\hbar\omega_{\lambda'}}{2} - \frac{i\beta\hbar\omega_m}{2}\right)}{(\omega_\lambda + \omega_{\lambda'} - i\omega_m)(\omega_\lambda - \omega_{\lambda'} + i\omega_m)}, \tag{A.26}$$

$$Res\left[f\left(z\right)\pi\cot\pi z,-i\frac{\beta\hbar}{2\pi}\left(\omega_{\lambda'}+i\omega_m\right)\right]=-\frac{1}{\beta\hbar}\frac{\omega_\lambda\coth\left(\frac{\beta\hbar\omega_{\lambda'}}{2}+\frac{i\beta\hbar\omega_m}{2}\right)}{\left(\omega_\lambda-\omega_{\lambda'}-i\omega_m\right)\left(\omega_\lambda+\omega_{\lambda'}+i\omega_m\right)}. \tag{A.27}$$

In Eqs. (A.26) and (A.27)

$$\coth\left(\frac{\beta\hbar\omega_{\lambda'}}{2}\pm\frac{i\beta\hbar\omega_m}{2}\right)=\coth\left(\frac{\beta\hbar\omega_{\lambda'}}{2}\right). \tag{A.28}$$

By using Eq. (A.28) and decomposition to partial fractions, one may write Eqs. (A.24)-(A.27) as

$$\begin{aligned}\sum_{n=-\infty}^{\infty}f\left(n\right) &= -\frac{1}{2\beta\hbar}\left[-\frac{\coth\left(\frac{\beta\hbar\omega_{\lambda'}}{2}\right)+\coth\left(\frac{\beta\hbar\omega_\lambda}{2}\right)}{\omega_\lambda+\omega_{\lambda'}+i\omega_m}\right.\\ &+ \frac{\coth\left(\frac{\beta\hbar\omega_\lambda}{2}\right)-\coth\left(\frac{\beta\hbar\omega_{\lambda'}}{2}\right)}{\omega_\lambda-\omega_{\lambda'}+i\omega_m}+\frac{\coth\left(\frac{\beta\hbar\omega_\lambda}{2}\right)+\coth\left(\frac{\beta\hbar\omega_{\lambda'}}{2}\right)}{-\omega_\lambda-\omega_{\lambda'}+i\omega_m}\\ &+ \left.\frac{\coth\left(\frac{\beta\hbar\omega_{\lambda'}}{2}\right)-\coth\left(\frac{\beta\hbar\omega_\lambda}{2}\right)}{-\omega_\lambda+\omega_{\lambda'}+i\omega_m}\right].\end{aligned} \tag{A.29}$$

One may write

$$\coth\left(\frac{\beta\hbar\omega_\lambda}{2}\right)=2\bar{n}_\lambda+1,\quad \bar{n}_\lambda=\frac{1}{e^{\beta\hbar\omega_\lambda}-1}, \tag{A.30}$$

and thus

$$\begin{aligned}\sum_{n=-\infty}^{\infty}f\left(n\right) &= \sum_{n=-\infty}^{\infty}G_0\left(\lambda|\omega_n\right)G_0\left(\lambda'|\omega_n-\omega_m\right)\\ &= \frac{1}{\beta\hbar}\left[\frac{\bar{n}_{\lambda'}+\bar{n}_\lambda+1}{\omega_\lambda+\omega_{\lambda'}+i\omega_m}-\frac{\bar{n}_\lambda+\bar{n}_{\lambda'}+1}{-\omega_\lambda-\omega_{\lambda'}+i\omega_m}\right.\\ &+ \left.\frac{\bar{n}_\lambda-\bar{n}_{\lambda'}}{-\omega_\lambda+\omega_{\lambda'}+i\omega_m}-\frac{\bar{n}_\lambda-\bar{n}_{\lambda'}}{\omega_\lambda-\omega_{\lambda'}+i\omega_m}\right].\end{aligned} \tag{A.31}$$

Next summation to be considered is

$$\sum_{n=-\infty}^{\infty}f\left(n\right)=-\sum_m Res\left[f\left(z\right)\pi\cot\pi z,p_m\right], \tag{A.32}$$

where

$$f\left(n\right)=G_0\left(\lambda|\omega_n\right)G_0\left(\lambda'|\omega_n\right), \tag{A.33}$$

and thus

$$\begin{aligned}f\left(z\right) &= G_0\left(\lambda|\omega_n,n\to z\right)G_0\left(\lambda'|\omega_n,n\to z\right)\\ &= \frac{1}{\beta\hbar}\frac{2\omega_\lambda}{\omega_\lambda^2+\left(\frac{2\pi z}{\beta\hbar}\right)^2}\frac{1}{\beta\hbar}\frac{2\omega_{\lambda'}}{\omega_{\lambda'}^2+\left(\frac{2\pi z}{\beta\hbar}\right)^2}.\end{aligned} \tag{A.34}$$

The poles of $f(z)$ are at (poles are simple)

$$p_m = \left\{ \pm i\omega_\lambda \frac{\beta\hbar}{2\pi}, \pm i\omega_{\lambda'} \frac{\beta\hbar}{2\pi} \right\}. \tag{A.35}$$

The residues at these simple poles are

$$Res\left[f(z)\,\pi\cot\pi z, +i\omega_\lambda \frac{\beta\hbar}{2\pi} \right] = -\frac{1}{\beta\hbar} \frac{\omega_{\lambda'} \coth\left(\frac{\beta\hbar\omega_\lambda}{2}\right)}{-\omega_\lambda^2 + \omega_{\lambda'}^2}, \tag{A.36}$$

$$Res\left[f(z)\,\pi\cot\pi z, -i\omega_\lambda \frac{\beta\hbar}{2\pi} \right] = -\frac{1}{\beta\hbar} \frac{\omega_{\lambda'} \coth\left(\frac{\beta\hbar\omega_\lambda}{2}\right)}{-\omega_\lambda^2 + \omega_{\lambda'}^2}, \tag{A.37}$$

$$Res\left[f(z)\,\pi\cot\pi z, +i\omega_{\lambda'} \frac{\beta\hbar}{2\pi} \right] = -\frac{1}{\beta\hbar} \frac{\omega_\lambda \coth\left(\frac{\beta\hbar\omega_{\lambda'}}{2}\right)}{\omega_\lambda^2 - \omega_{\lambda'}^2}, \tag{A.38}$$

$$Res\left[f(z)\,\pi\cot\pi z, -i\omega_{\lambda'} \frac{\beta\hbar}{2\pi} \right] = -\frac{1}{\beta\hbar} \frac{\omega_\lambda \coth\left(\frac{\beta\hbar\omega_{\lambda'}}{2}\right)}{\omega_\lambda^2 - \omega_{\lambda'}^2}. \tag{A.39}$$

Thus, from Eq. (A.32) and from Eqs. (A.36)-(A.39) it follows that

$$\sum_{n=-\infty}^{\infty} f(n) = \frac{2}{\beta\hbar} \frac{\omega_\lambda \coth\left(\frac{\beta\hbar\omega_{\lambda'}}{2}\right) - \omega_{\lambda'} \coth\left(\frac{\beta\hbar\omega_\lambda}{2}\right)}{\omega_\lambda^2 - \omega_{\lambda'}^2}. \tag{A.40}$$

One may write

$$\coth\left(\frac{\beta\hbar\omega_\lambda}{2}\right) = 2\bar{n}_\lambda + 1, \tag{A.41}$$

and thus

$$\sum_{n=-\infty}^{\infty} f(n) = \frac{2}{\beta\hbar} \frac{\omega_\lambda (2\bar{n}_{\lambda'} + 1) - \omega_{\lambda'} (2\bar{n}_\lambda + 1)}{\omega_\lambda^2 - \omega_{\lambda'}^2}. \tag{A.42}$$

In the limit $\omega_\lambda \to \omega_{\lambda'}$

$$\begin{aligned} \lim_{\omega_\lambda \to \omega_{\lambda'}} \sum_{n=-\infty}^{\infty} G_0(\lambda|\omega_n)\, G_0(\lambda'|\omega_n) &= \frac{2}{\beta\hbar} \lim_{\omega_\lambda \to \omega_{\lambda'}} \frac{\omega_\lambda (2\bar{n}_{\lambda'} + 1) - \omega_{\lambda'} (2\bar{n}_\lambda + 1)}{\omega_\lambda^2 - \omega_{\lambda'}^2} \\ &= 2\left[\bar{n}_\lambda (\bar{n}_\lambda + 1) + \frac{\bar{n}_\lambda + \frac{1}{2}}{\beta\hbar\omega_\lambda} \right]. \end{aligned} \tag{A.43}$$

B Contributions to CTE

The following notations are sometimes used in this Appendix and in this thesis in general

$$\begin{aligned}
\xi^{(1)}\left(\bar{\lambda}_{n/2}\right) &\equiv \prod_{k=1\wedge k=\,odd}^{n-1} k\, 2^{n/2}\left(\bar{n}_{\lambda_1}+\frac{1}{2}\right)\left(\bar{n}_{\lambda_2}+\frac{1}{2}\right)\cdots\left(\bar{n}_{\lambda_{n/2}}+\frac{1}{2}\right), \\
\xi^{(2)}\left(\bar{\lambda}_{n/2}\right) &\equiv \prod_{k=1\wedge k=\,odd}^{n-1} k\, 2^{n/2}\sum_{i=1}^{n/2}\omega_{\lambda_i}\bar{n}_{\lambda_i}\left(\bar{n}_{\lambda_i}+1\right)\prod_{l=1\wedge l\neq i}^{n/2}\left(\bar{n}_{\lambda_l}+\frac{1}{2}\right),
\end{aligned} \tag{B.1}$$

$$\begin{aligned}
\xi^{(3)}\left(\bar{\lambda}_{n/2}\right) \equiv \prod_{k=1\wedge k=\,odd}^{n-1} k \Bigg[& 2^{n/2}\sum_{i=1}^{n/2}\omega_{\lambda_i}^2\bar{n}_{\lambda_i}\left(\bar{n}_{\lambda_i}+1\right)\left(\bar{n}_{\lambda_i}+1\right)\prod_{l=1\wedge l\neq i}^{n/2}\left(\bar{n}_{\lambda_l}+\frac{1}{2}\right) \\
& + 2\sum_{i=1}^{n/2}\omega_{\lambda_i}\bar{n}_{\lambda_i}\left(\bar{n}_{\lambda_i}+1\right)\prod_{l=1\wedge l\neq i}^{n/2}\omega_{\lambda_l}\bar{n}_{\lambda_l}\left(\bar{n}_{\lambda_l}+1\right)\Bigg],
\end{aligned} \tag{B.2}$$

$$\begin{aligned}
G^{(3)}\left(\lambda;\lambda';\lambda''\right) \equiv \Bigg[& 3\frac{\bar{n}_{\lambda}\left(\bar{n}_{\lambda'}+\bar{n}_{\lambda''}+1\right)-\bar{n}_{\lambda'}\bar{n}_{\lambda''}}{-\omega_{\lambda}+\omega_{\lambda'}+\omega_{\lambda''}} \\
& + \frac{\left(\bar{n}_{\lambda}+1\right)\left(\bar{n}_{\lambda'}+1\right)\left(\bar{n}_{\lambda''}+1\right)-\bar{n}_{\lambda}\bar{n}_{\lambda'}\bar{n}_{\lambda''}}{\omega_{\lambda}+\omega_{\lambda'}+\omega_{\lambda''}}\Bigg],
\end{aligned} \tag{B.3}$$

$$\begin{aligned}
G^{(3,\beta)}\left(\lambda;\lambda';\lambda''\right) \equiv \Bigg[& \frac{2\omega_{\lambda'}\bar{n}_{\lambda'}\left(\bar{n}_{\lambda'}+1\right)\left(\bar{n}_{\lambda''}-\bar{n}_{\lambda}\right)}{-\omega_{\lambda}+\omega_{\lambda'}+\omega_{\lambda''}} - \frac{\omega_{\lambda}\bar{n}_{\lambda}\left(\bar{n}_{\lambda}+1\right)\left(\bar{n}_{\lambda'}+\bar{n}_{\lambda''}+1\right)}{-\omega_{\lambda}+\omega_{\lambda'}+\omega_{\lambda''}} \\
& + \frac{\omega_{\lambda}\bar{n}_{\lambda}\left(\bar{n}_{\lambda}+1\right)\bar{n}_{\lambda'}\bar{n}_{\lambda''}}{\omega_{\lambda}+\omega_{\lambda'}+\omega_{\lambda''}} - \frac{\omega_{\lambda}\bar{n}_{\lambda}\left(\bar{n}_{\lambda}+1\right)\left(\bar{n}_{\lambda'}+1\right)\left(\bar{n}_{\lambda''}+1\right)}{\omega_{\lambda}+\omega_{\lambda'}+\omega_{\lambda''}}\Bigg].
\end{aligned} \tag{B.4}$$

The second-order contribution to the quantity can be approximated as

$$\begin{aligned}
\sigma_{\mu\nu}^{A(2)} - \sigma_{\mu\nu}^{T(2)} \approx & -12\beta \sum_{\lambda} \sum_{\lambda'} V_{\mu\nu}(\lambda)\, V(-\lambda;\lambda';-\lambda')\, \frac{\omega_{\lambda'} \bar{n}_{\lambda'} (\bar{n}_{\lambda'}+1)}{\omega_{\lambda}} \\
& -72\beta \sum_{\lambda} \sum_{\lambda'} \sum_{\lambda''} V_{\mu\nu}(\lambda;-\lambda;\lambda')\, \frac{V(-\lambda';\lambda'';-\lambda'')}{\omega_{\lambda'}} \\
& \times \left[\omega_{\lambda} \bar{n}_{\lambda} (\bar{n}_{\lambda}+1) \left(\bar{n}_{\lambda''} + \frac{1}{2} \right) + \omega_{\lambda''} \bar{n}_{\lambda''} (\bar{n}_{\lambda''}+1) \left(\bar{n}_{\lambda} + \frac{1}{2} \right) \right] \\
& +36\beta \sum_{\lambda} \sum_{\lambda'} \sum_{\lambda''} V_{\mu\nu}(\lambda;\lambda';\lambda'')\, V(-\lambda;-\lambda';-\lambda'')\, G^{(3,\beta)}(\lambda;\lambda';\lambda'') \\
& -192\beta \sum_{\lambda} \sum_{\lambda'} \sum_{\lambda''} V_{\mu\nu}(\lambda;\lambda')\, V(-\lambda;-\lambda',\lambda'';-\lambda'') \\
& \times \left[\frac{\omega_{\lambda} \omega_{\lambda''} \bar{n}_{\lambda''} (\bar{n}_{\lambda''}+1) \left(\bar{n}_{\lambda'} + \frac{1}{2} \right)}{\omega_{\lambda}^2 - \omega_{\lambda'}^2} + \frac{\omega_{\lambda'} \bar{n}_{\lambda'} (\bar{n}_{\lambda'}+1) \left(\bar{n}_{\lambda''} + \frac{1}{2} \right)}{\omega_{\lambda}^2 - \omega_{\lambda'}^2} \right].
\end{aligned} \tag{B.5}$$

The second-order terms contribute to the NTE if $\sigma_{\mu\nu}^{A(2)} - \sigma_{\mu\nu}^{T(2)} < 0$.

C Evaluation of perturbation expansion

In this Appendix, few evaluations of the perturbation expansion used in Article IV are shown.

C.1 Second-order examples

First example is taken to be [see Eq. (2.137)]

$$\begin{aligned}\left\langle \hat{S}\left(\beta\right)\right\rangle_{0,c,h=2,ss} &\equiv \frac{1}{2}\int_0^\beta d\tau_1 \int_0^\beta d\tau_2 \left\langle \mathcal{T}\left\{\hat{H}_s\left(\tau_1\right)\hat{H}_s\left(\tau_2\right)\right\}\right\rangle_{0,c} \\ &= \frac{1}{2}\sum_{n=0}\sum_{\bar{\lambda}_n}\sum_{m=1}\frac{1}{m!}\sum_{\bar{\mu}_m}\sum_{\bar{\nu}_m}\sum_{n'=0}\sum_{\bar{\lambda}'_{n'}}\sum_{m'=1}\frac{1}{m'!}\sum_{\bar{\mu}'_{m'}}\sum_{\bar{\nu}'_{m'}} \\ &\quad \times V_{\bar{\mu}_m\bar{\nu}_m}\left(\bar{\lambda}_n\right)V_{\bar{\mu}'_{m'}\bar{\nu}'_{m'}}\left(\bar{\lambda}'_{n'}\right)\bar{u}_{\mu_m\nu_m}\bar{u}_{\mu'_{m'}\nu'_{m'}} \\ &\quad \times \int_0^\beta d\tau_1 \int_0^\beta d\tau_2 \left\langle \mathcal{T}\left\{\hat{A}_{\bar{\lambda}_n}\left(\tau_1\right)\hat{A}_{\bar{\lambda}'_{n'}}\left(\tau_2\right)\right\}\right\rangle_{0,c}, \end{aligned} \tag{C.1}$$

where the notation given by Eq. (2.60) is used and furthermore

$$\hat{A}_{\bar{\lambda}_n}\left(\tau_1\right) \equiv \hat{A}_{\lambda_1}\left(\tau_1\right)\cdots\hat{A}_{\lambda_n}\left(\tau_1\right). \tag{C.2}$$

The special cases of Eq. (C.1) considered in this section are

$$\begin{aligned}\left\langle \hat{S}\left(\beta\right)\right\rangle_{h=2,1} &\equiv \left\langle \hat{S}\left(\beta\right)\right\rangle_{0,c,h=2,ss,n=1,n'=odd} = \left\langle \hat{S}\left(\beta\right)\right\rangle_{0,c,h=2,ss,n=odd,n'=1} \\ &= \frac{1}{2}\sum_{\lambda_1}\sum_{m=1}\frac{1}{m!}\sum_{\bar{\mu}_m}\sum_{\bar{\nu}_m}\sum_{n'=1}\sum_{\lambda'_1}\cdots\sum_{\lambda'_{2n'-1}}\sum_{m'=1}\frac{1}{m'!}\sum_{\bar{\mu}'_{m'}}\sum_{\bar{\nu}'_{m'}} \\ &\quad \times V_{\bar{\mu}_m\bar{\nu}_m}\left(\lambda_1\right)\bar{u}_{\mu_m\nu_m}V_{\bar{\mu}'_{m'}\bar{\nu}'_{m'}}\left(\bar{\lambda}'_{2n'-1}\right)\bar{u}_{\mu'_{m'}\nu'_{m'}} \\ &\quad \times \int_0^\beta d\tau_1 \int_0^\beta d\tau_2 \left\langle \mathcal{T}\left\{\hat{A}_{\lambda_1}\left(\tau_1\right)\hat{A}_{\bar{\lambda}'_{2n'-1}}\left(\tau_2\right)\right\}\right\rangle_{0,c}, \end{aligned} \tag{C.3}$$

and

$$\begin{aligned}
\left\langle \hat{S}\left(\beta\right)\right\rangle_{h=2,2} &\equiv \left\langle \hat{S}\left(\beta\right)\right\rangle_{0,c,h=2,ss,n=2,n'=even} = \left\langle \hat{S}\left(\beta\right)\right\rangle_{0,c,h=2,ss,n=even,n'=2} \\
&= \frac{1}{2}\sum_{\lambda_1}\sum_{\lambda_2}\sum_{m=1}\frac{1}{m!}\sum_{\bar{\mu}_m}\sum_{\bar{\nu}_m}\sum_{n'=1}\sum_{\lambda'_1}\cdots\sum_{\lambda'_{2n'}}\sum_{m'=1}\frac{1}{m'!}\sum_{\bar{\mu}'_{m'}}\sum_{\bar{\nu}'_{m'}} \\
&\quad \times V_{\bar{\mu}_m\bar{\nu}_m}\left(\lambda_1;\lambda_2\right)\bar{u}_{\mu_m\nu_m}V_{\bar{\mu}'_{m'}\bar{\nu}'_{m'}}\left(\lambda'_1;\ldots;\lambda'_{2n'}\right)\bar{u}_{\mu'_{m'}\nu'_{m'}} \\
&\quad \times \int_0^\beta d\tau_1\int_0^\beta d\tau_2\left\langle \mathcal{T}\left\{\hat{A}_{\lambda_1}\left(\tau_1\right)\hat{A}_{\lambda_2}\left(\tau_1\right)\hat{A}_{\bar{\lambda}'_{2n'}}\left(\tau_2\right)\right\}\right\rangle_{0,c}. \qquad \text{(C.4)}
\end{aligned}$$

By using Wick's Theorem [Eq. (2.108)], the ensemble averages in Eqs. (C.3) and (C.4) can be written as

$$\begin{aligned}
&\left\langle \mathcal{T}\left\{\hat{A}_{\lambda_1}\left(\tau_1\right)\hat{A}_{\bar{\lambda}'_{2n'-1}}\left(\tau_2\right)\right\}\right\rangle_{0,c} \\
&= \left(2n'-1\right)\left\langle \mathcal{T}\left\{\hat{A}_{\lambda_1}\left(\tau_1\right)\hat{A}_{\lambda'_1}\left(\tau_2\right)\right\}\right\rangle_0\left\langle \mathcal{T}\left\{\hat{A}_{\lambda'_2}\left(\tau_2\right)\cdots\hat{A}_{\lambda'_{2n'-1}}\left(\tau_2\right)\right\}\right\rangle_{0,c} \\
&= \prod_{k=1\wedge k=odd}^{2n'-1} k\left\langle \mathcal{T}\left\{\hat{A}_{\lambda_1}\left(\tau_1\right)\hat{A}_{\lambda'_1}\left(\tau_2\right)\right\}\right\rangle_0 \\
&\quad \times\left\langle \mathcal{T}\left\{\hat{A}_{\lambda'_2}\left(\tau_2\right)\hat{A}_{\lambda'_3}\left(\tau_2\right)\right\}\right\rangle_0\cdots\left\langle \mathcal{T}\left\{\hat{A}_{\lambda'_{2n'-2}}\left(\tau_2\right)\hat{A}_{\lambda'_{2n'-1}}\left(\tau_2\right)\right\}\right\rangle_0 \\
&= \delta_{\lambda_1\left(-\lambda'_1\right)}\delta_{\lambda'_2\left(-\lambda'_3\right)}\delta_{\lambda'_4\left(-\lambda'_5\right)}\cdots\delta_{\lambda'_{2n'-2}\left(-\lambda'_{2n'-1}\right)}\prod_{k=1\wedge k=odd}^{2n'-1} k \\
&\quad \times G_0\left(\lambda_1\tau_1|\lambda_1\tau_2\right)\left(2\bar{n}_{\lambda'_2}+1\right)\left(2\bar{n}_{\lambda'_4}+1\right)\cdots\left(2\bar{n}_{\lambda'_{2n''-2}}+1\right), \qquad \text{(C.5)}
\end{aligned}$$

and

$$\begin{aligned}
&\left\langle \mathcal{T}\left\{\hat{A}_{\bar{\lambda}_2}\left(\tau_1\right)\hat{A}_{\bar{\lambda}'_{2n'}}\left(\tau_2\right)\right\}\right\rangle_{0,c} \\
&= 2n'\left\langle \mathcal{T}\left\{\hat{A}_{\lambda_1}\left(\tau_1\right)\hat{A}_{\lambda'_1}\left(\tau_2\right)\right\}\right\rangle_0\left\langle \mathcal{T}\left\{\hat{A}_{\lambda_2}\left(\tau_1\right)\hat{A}_{\lambda'_2}\left(\tau_2\right)\cdots\hat{A}_{\lambda'_{2n'}}\left(\tau_2\right)\right\}\right\rangle_{0,c} \\
&= 2n'\prod_{k=1\wedge k=odd}^{2n'-3} k\left\langle \mathcal{T}\left\{\hat{A}_{\lambda_1}\left(\tau_1\right)\hat{A}_{\lambda'_1}\left(\tau_2\right)\right\}\right\rangle_0\left\langle \mathcal{T}\left\{\hat{A}_{\lambda_2}\left(\tau_1\right)\hat{A}_{\lambda'_2}\left(\tau_2\right)\right\}\right\rangle_0 \\
&\quad \times\left\langle \mathcal{T}\left\{\hat{A}_{\lambda'_3}\left(\tau_2\right)\hat{A}_{\lambda'_4}\left(\tau_2\right)\right\}\right\rangle_0\cdots\left\langle \mathcal{T}\left\{\hat{A}_{\lambda'_{2n'-1}}\left(\tau_2\right)\hat{A}_{\lambda'_{2n'}}\left(\tau_2\right)\right\}\right\rangle_0 \\
&= 2n'\delta_{\lambda_1\left(-\lambda'_1\right)}\delta_{\lambda_2\left(-\lambda'_2\right)}\delta_{\lambda'_3\left(-\lambda'_4\right)}\delta_{\lambda'_5\left(-\lambda'_6\right)}\cdots\delta_{\lambda'_{2n'-1}\left(-\lambda'_{2n'}\right)}\prod_{k=1\wedge k=odd}^{2n'-3} k \\
&\quad \times G_0\left(\lambda_1\tau_1|\lambda_1\tau_2\right)G_0\left(\lambda_2\tau_1|\lambda_2\tau_2\right)\left(2\bar{n}_{\lambda'_3}+1\right)\left(2\bar{n}_{\lambda'_5}+1\right)\cdots\left(2\bar{n}_{\lambda'_{2n'-1}}+1\right). \qquad \text{(C.6)}
\end{aligned}$$

In Eqs. (C.5) and (C.6) $n' = 1, 2, \ldots$. By using the results given by Eqs. (C.5) and (C.6), Eqs. (C.3) and (C.4) can be written as

$$\begin{aligned}
\left\langle \hat{S}(\beta) \right\rangle_{h=2,1} &= \frac{1}{2} \sum_{\lambda_1} \sum_{m=1} \frac{1}{m!} \sum_{\bar{\mu}_m} \sum_{\bar{\nu}_m} \sum_{n'=1} \sum_{\lambda'_1} \cdots \sum_{\lambda'_{2n'-1}} \sum_{m'=1} \frac{1}{m'!} \sum_{\bar{\mu}'_{m'}} \sum_{\bar{\nu}'_{m'}} \\
&\times V_{\bar{\mu}_m \bar{\nu}_m}(\lambda_1) V_{\bar{\mu}'_{m'} \bar{\nu}'_{m'}}\left(\lambda'_1; \ldots; \lambda'_{2n'-1}\right) \bar{u}_{\mu_m \nu_m} \bar{u}_{\mu'_{m'} \nu'_{m'}} \prod_{k=1 \wedge k=odd}^{2n'-1} k \\
&\times \int_0^\beta d\tau_1 \int_0^\beta d\tau_2 \delta_{\lambda_1(-\lambda'_1)} \delta_{\lambda'_2(-\lambda'_3)} \delta_{\lambda'_4(-\lambda'_5)} \cdots \delta_{\lambda'_{2n'-2}\left(-\lambda'_{2n'-1}\right)} \\
&\times G_0(\lambda_1 \tau_1 | \lambda_1 \tau_2) \left(2\bar{n}_{\lambda'_2} + 1\right) \left(2\bar{n}_{\lambda'_4} + 1\right) \cdots \left(2\bar{n}_{\lambda'_{2n''-2}} + 1\right) \\
&= \frac{1}{2} \sum_{\lambda_1} \sum_{m=1} \frac{1}{m!} \sum_{\bar{\mu}_m} \sum_{\bar{\nu}_m} \sum_{n'=1} \sum_{\bar{\lambda}'_{n'-1}} \sum_{m'=1} \frac{1}{m'!} \sum_{\bar{\mu}'_{m'}} \sum_{\bar{\nu}'_{m'}} \\
&\times V_{\bar{\mu}_m \bar{\nu}_m}(\lambda_1) V_{\bar{\mu}'_{m'} \bar{\nu}'_{m'}}\left(-\lambda_1; \lambda'_1; -\lambda'_1 \ldots; \lambda'_{n'-1}; -\lambda'_{n'-1}\right) \bar{u}_{\mu_m \nu_m} \bar{u}_{\mu'_{m'} \nu'_{m'}} \\
&\times \prod_{k=1 \wedge k=odd}^{2n'-1} k \int_0^\beta d\tau_1 \int_0^\beta d\tau_2 G_0(\lambda_1 \tau_1 | \lambda_1 \tau_2) \\
&\times \left(2\bar{n}_{\lambda'_1} + 1\right) \left(2\bar{n}_{\lambda'_2} + 1\right) \cdots \left(2\bar{n}_{\lambda'_{n'-1}} + 1\right), \qquad \text{(C.7)}
\end{aligned}$$

and

$$\begin{aligned}
\left\langle \hat{S}(\beta) \right\rangle_{h=2,2} &= \frac{1}{2} \sum_{\lambda_1} \sum_{\lambda_2} \sum_{m=1} \frac{1}{m!} \sum_{\bar{\mu}_m} \sum_{\bar{\nu}_m} \sum_{n'=1} \sum_{\bar{\lambda}'_{2n'}} \sum_{m'=1} \frac{1}{m'!} \sum_{\bar{\mu}'_{m'}} \sum_{\bar{\nu}'_{m'}} \\
&\times V_{\bar{\mu}_m \bar{\nu}_m}(\lambda_1; \lambda_2) V_{\bar{\mu}'_{m'} \bar{\nu}'_{m'}}\left(\bar{\lambda}'_{2n'}\right) \bar{u}_{\mu_m \nu_m} \bar{u}_{\mu'_{m'} \nu'_{m'}} \prod_{k=1 \wedge k=odd}^{2n'-3} k \\
&\times \int_0^\beta d\tau_1 \int_0^\beta d\tau_2 2n' \delta_{\lambda_1(-\lambda'_1)} \delta_{\lambda_2(-\lambda'_2)} \delta_{\lambda'_3(-\lambda'_4)} \delta_{\lambda'_5(-\lambda'_6)} \cdots \delta_{\lambda'_{2n'-1}(-\lambda'_{2n'})} \\
&\times G_0(\lambda_1 \tau_1 | \lambda_1 \tau_2) G_0(\lambda_2 \tau_1 | \lambda_2 \tau_2) \\
&\times \left(2\bar{n}_{\lambda'_3} + 1\right) \left(2\bar{n}_{\lambda'_5} + 1\right) \cdots \left(2\bar{n}_{\lambda'_{2n''-1}} + 1\right) \\
&= \frac{1}{2} \sum_{\lambda_1} \sum_{\lambda_2} \sum_{m=1} \frac{1}{m!} \sum_{\bar{\mu}_m} \sum_{\bar{\nu}_m} \sum_{n'=1} \sum_{\lambda'_3} \sum_{\lambda'_5} \cdots \sum_{\lambda'_{2n'-1}} \sum_{m'=1} \frac{1}{m'!} \sum_{\bar{\mu}'_{m'}} \sum_{\bar{\nu}'_{m'}} \\
&\times V_{\bar{\mu}_m \bar{\nu}_m}(\lambda_1; \lambda_2) V_{\bar{\mu}'_{m'} \bar{\nu}'_{m'}}\left(-\lambda_1; -\lambda_2; \lambda'_3; -\lambda'_3; \ldots; \lambda'_{2n'-1}; -\lambda'_{2n'-1}\right) \\
&\times \bar{u}_{\mu_m \nu_m} \bar{u}_{\mu'_{m'} \nu'_{m'}} \int_0^\beta d\tau_1 \int_0^\beta d\tau_2 2n' G_0(\lambda_1 \tau_1 | \lambda_1 \tau_2) G_0(\lambda_2 \tau_1 | \lambda_2 \tau_2) \\
&\times \prod_{k=1 \wedge k=odd}^{2n'-3} k \left(2\bar{n}_{\lambda'_3} + 1\right) \left(2\bar{n}_{\lambda'_5} + 1\right) \cdots \left(2\bar{n}_{\lambda'_{2n'-1}} + 1\right). \qquad \text{(C.8)}
\end{aligned}$$

The integral in Eq. (C.7) is of the form

$$\int_0^\beta d\tau \int_0^\beta d\tau' G_0(\lambda \tau | \lambda \tau'). \qquad \text{(C.9)}$$

One may write Eq. (C.9) in terms of the Fourier transform of the Green's function (Sec. 2.4)

$$\begin{aligned}&\int_0^\beta d\tau \int_0^\beta d\tau' \sum_{n_1=-\infty}^{\infty} G_0\left(\lambda|\omega_{n_1}\right) e^{i\omega_{n_1}(\tau-\tau')} \\ &= \int_0^\beta d\tau e^{i\omega_{n_1}\tau} \int_0^\beta d\tau' e^{-i\omega_{n_1}\tau'} \sum_{n_1=-\infty}^{\infty} G_0\left(\lambda|\omega_{n_1}\right),\end{aligned} \tag{C.10}$$

and then by using Eq. (2.113), Eq. (C.10) becomes

$$\int_0^\beta d\tau \int_0^\beta d\tau' \sum_{n_1=-\infty}^{\infty} G_0\left(\lambda|\omega_{n_1}\right) e^{i\omega_{n_1}(\tau-\tau')} = \beta^2 G_0\left(\lambda|0\right). \tag{C.11}$$

Since $G_0\left(\lambda|0\right) = 2/\left(\beta\hbar\omega_\lambda\right)$, Eq. (C.11) can be written as

$$\int_0^\beta d\tau \int_0^\beta d\tau' G_0\left(\lambda\tau|\lambda\tau'\right) = \frac{2\beta}{\hbar\omega_\lambda}. \tag{C.12}$$

The integral in Eq. (C.8) is more complicated, one may write

$$\int_0^\beta d\tau \int_0^\beta d\tau' G_0\left(\lambda\tau|\lambda\tau'\right) G_0\left(\lambda'\tau|\lambda'\tau'\right). \tag{C.13}$$

One may write Eq. (C.13) in terms of the Fourier transforms

$$\begin{aligned}&\int_0^\beta d\tau \int_0^\beta d\tau' \sum_{n_1,n_2=-\infty}^{\infty} G_0\left(\lambda|\omega_{n_1}\right) G_0\left(\lambda'|\omega_{n_2}\right) e^{i\omega_{n_1}(\tau-\tau')} e^{i\omega_{n_2}(\tau-\tau')} \\ &= \sum_{n_1,n_2=-\infty}^{\infty} G_0\left(\lambda|\omega_{n_1}\right) G_0\left(\lambda'|\omega_{n_2}\right) \int_0^\beta d\tau e^{i\left(\omega_{n_1}+\omega_{n_2}\right)\tau} \int_0^\beta d\tau' e^{-i\left(\omega_{n_1}+\omega_{n_2}\right)\tau'},\end{aligned} \tag{C.14}$$

and then, by using Eq. (2.113) and the result given by Eq. (A.42) for the summation, Eq. (C.14) may be written as

$$\sum_{n=-\infty}^{\infty} G_0\left(\lambda|\omega_n\right) G_0\left(\lambda'|\omega_n\right) = \frac{2}{\beta\hbar} \frac{\omega_\lambda\left(2\bar{n}_{\lambda'}+1\right) - \omega_{\lambda'}\left(2\bar{n}_\lambda+1\right)}{\omega_\lambda^2 - \omega_{\lambda'}^2}. \tag{C.15}$$

Thus, Eq. (C.15) and hence the integral in Eq. (C.13) can be written as

$$\int_0^\beta d\tau \int_0^\beta d\tau' G_0\left(\lambda\tau|\lambda\tau'\right) G_0\left(\lambda'\tau|\lambda'\tau'\right) = \frac{2\beta}{\hbar} \frac{\omega_\lambda\left(2\bar{n}_{\lambda'}+1\right) - \omega_{\lambda'}\left(2\bar{n}_\lambda+1\right)}{\omega_\lambda^2 - \omega_{\lambda'}^2}. \tag{C.16}$$

By using these results for the integrals, Eqs. (C.7) and (C.8) can be written as

$$\begin{aligned}\left\langle \hat{S}\left(\beta\right)\right\rangle_{h=2,1} &= \frac{\beta}{\hbar}\sum_{\lambda_1}\sum_{m=1}\frac{1}{m!}\sum_{\bar{\mu}_m}\sum_{\bar{\nu}_m}\sum_{n'=1}\sum_{\bar{\lambda}'_{n'-1}}\sum_{m'=1}\frac{1}{m'!}\sum_{\bar{\mu}'_{m'}}\sum_{\bar{\nu}'_{m'}} \\ &\times V_{\bar{\mu}_m\bar{\nu}_m}\left(\lambda_1\right)\frac{V_{\bar{\mu}'_{m'}\bar{\nu}'_{m'}}\left(-\lambda_1;\lambda'_1;-\lambda'_1\ldots;\lambda'_{n'-1};-\lambda'_{n'-1}\right)}{\omega_{\lambda_1}}\bar{u}_{\mu_m\nu_m}\bar{u}_{\mu'_{m'}\nu'_{m'}} \\ &\times\left(\prod_{k=1\wedge k=odd}^{2n'-1}k\right)2^{n'-1}\left(\bar{n}_{\lambda'_1}+\frac{1}{2}\right)\left(\bar{n}_{\lambda'_2}+\frac{1}{2}\right)\cdots\left(\bar{n}_{\lambda'_{n'-1}}+\frac{1}{2}\right),\end{aligned} \tag{C.17}$$

and

$$\begin{aligned}\left\langle \hat{S}\left(\beta\right)\right\rangle_{h=2,2} &= \frac{2\beta}{\hbar}\sum_{\lambda_1}\sum_{\lambda_2}\sum_{m=1}\frac{1}{m!}\sum_{\bar{\mu}_m}\sum_{\bar{\nu}_m}\sum_{n'=2}\sum_{\bar{\lambda}'_{n'-1}}\sum_{m'=1}\frac{1}{m'!}\sum_{\bar{\mu}'_{m'}}\sum_{\bar{\nu}'_{m'}} \\ &\times V_{\bar{\mu}_m\bar{\nu}_m}\left(\lambda_1;\lambda_2\right)V_{\bar{\mu}'_{m'}\bar{\nu}'_{m'}}\left(-\lambda_1;-\lambda_2;\lambda'_1;-\lambda'_1;\ldots;\lambda'_{n'-1};-\lambda'_{n'-1}\right) \\ &\times\bar{u}_{\mu_m\nu_m}\bar{u}_{\mu'_{m'}\nu'_{m'}}\frac{\omega_{\lambda_1}\left(\bar{n}_{\lambda_2}+\frac{1}{2}\right)-\omega_{\lambda_2}\left(\bar{n}_{\lambda_1}+\frac{1}{2}\right)}{\omega_{\lambda_1}^2-\omega_{\lambda_2}^2}\prod_{k=1\wedge k=odd}^{2n'-3}k \\ &\times\left(n'2^{n'}\right)\left(\bar{n}_{\lambda'_1}+\frac{1}{2}\right)\left(\bar{n}_{\lambda'_2}+\frac{1}{2}\right)\cdots\left(\bar{n}_{\lambda'_{n'-1}}+\frac{1}{2}\right).\end{aligned} \tag{C.18}$$

These terms are represented by diagrams l) and n) of Fig. 3.9. The contribution to elastic constants, for example, can be obtained by using Eq. (2.134). Eight additional second-order terms were represented in Article IV. All these terms were obtained by similar calculations that were shown here.

C.2 Third-order examples

In this section, some special cases of the following contribution are considered [see Eq. (2.138)]

$$\left\langle \hat{S}\left(\beta\right)\right\rangle_{0,c,ssa}=-\frac{1}{2}\int_0^\beta d\tau_1\int_0^\beta d\tau_2\int_0^\beta d\tau_3\left\langle \mathcal{T}\left\{\hat{H}_s\left(\tau_1\right)\hat{H}_s\left(\tau_2\right)\hat{H}_a\left(\tau_3\right)\right\}\right\rangle_{0,c}. \tag{C.19}$$

The first special case of Eq. (C.19) is taken to be

$$\begin{aligned}\left\langle \hat{S}\left(\beta\right)\right\rangle_{ssa,1} &\equiv \left\langle \hat{S}\left(\beta\right)\right\rangle_{0,c,ssA,n=2,n'=1,n''=3} + \left\langle \hat{S}\left(\beta\right)\right\rangle_{0,c,ssA,n=1,n'=2,n''=3} \\ &= -\sum_{\bar{\lambda}_2}\sum_{m=1}\frac{1}{m!}\sum_{\bar{\mu}_m}\sum_{\bar{\nu}_m}\sum_{\lambda_1'}\sum_{m'=1}\frac{1}{m'!}\sum_{\bar{\mu}'_{m'}}\sum_{\bar{\nu}'_{m'}}\sum_{\bar{\lambda}_3''} \\ &\quad\times V_{\bar{\mu}_m\bar{\nu}_m}\left(\bar{\lambda}_2\right)V_{\bar{\mu}'_{m'}\bar{\nu}'_{m'}}\left(\lambda_1'\right)V\left(\bar{\lambda}_3''\right)\bar{u}_{\mu_m\nu_m}\bar{u}_{\mu'_{m'}\nu'_{m'}} \\ &\quad\times\int_0^\beta d\tau_1\int_0^\beta d\tau_2\int_0^\beta d\tau_3\left\langle\mathcal{T}\left\{\hat{A}_{\bar{\lambda}_2}\left(\tau_1\right)\hat{A}_{\lambda_1'}\left(\tau_2\right)\hat{A}_{\bar{\lambda}_3''}\left(\tau_3\right)\right\}\right\rangle_{0,c}.\end{aligned} \tag{C.20}$$

By using Wick's Theorem [Eq. (2.108)], Eq. (C.20) can be written as

$$\begin{aligned}\left\langle \hat{S}\left(\beta\right)\right\rangle_{ssa,1} &= -6\sum_{\bar{\lambda}_2}\sum_{m=1}\frac{1}{m!}\sum_{\bar{\mu}_m}\sum_{\bar{\nu}_m}\sum_{\lambda_1'}\sum_{m'=1}\frac{1}{m'!}\sum_{\bar{\mu}'_{m'}}\sum_{\bar{\nu}'_{m'}}\sum_{\bar{\lambda}_3''} \\ &\quad\times V_{\bar{\mu}_m\bar{\nu}_m}\left(\bar{\lambda}_2\right)V_{\bar{\mu}'_{m'}\bar{\nu}'_{m'}}\left(\lambda_1'\right)V\left(\bar{\lambda}_3''\right)\bar{u}_{\mu_m\nu_m}\bar{u}_{\mu'_{m'}\nu'_{m'}} \\ &\quad\times\int_0^\beta d\tau_1\int_0^\beta d\tau_2\int_0^\beta d\tau_3\left[\left\langle\mathcal{T}\left\{\hat{A}_{\lambda_1}\left(\tau_1\right)\hat{A}_{\lambda_1'}\left(\tau_2\right)\right\}\right\rangle_0\right. \\ &\quad\times\left\langle\mathcal{T}\left\{\hat{A}_{\lambda_2}\left(\tau_1\right)\hat{A}_{\lambda_1''}\left(\tau_3\right)\right\}\right\rangle_0\left\langle\mathcal{T}\left\{\hat{A}_{\lambda_2''}\left(\tau_3\right)\hat{A}_{\lambda_3''}\left(\tau_3\right)\right\}\right\rangle_0 \\ &\quad+\left\langle\mathcal{T}\left\{\hat{A}_{\lambda_1}\left(\tau_1\right)\hat{A}_{\lambda_1''}\left(\tau_3\right)\right\}\right\rangle_0\left\langle\mathcal{T}\left\{\hat{A}_{\lambda_2}\left(\tau_1\right)\hat{A}_{\lambda_2''}\left(\tau_3\right)\right\}\right\rangle_0 \\ &\quad\times\left.\left\langle\mathcal{T}\left\{\hat{A}_{\lambda_1'}\left(\tau_2\right)\hat{A}_{\lambda_3''}\left(\tau_3\right)\right\}\right\rangle_0\right].\end{aligned} \tag{C.21}$$

Furthermore

$$\begin{aligned}\left\langle \hat{S}\left(\beta\right)\right\rangle_{ssa,1} &= -6\sum_{\lambda_1}\sum_{\lambda_2}\sum_{m=1}\frac{1}{m!}\sum_{\bar{\mu}_m}\sum_{\bar{\nu}_m}\sum_{m'=1}\frac{1}{m'!}\sum_{\bar{\mu}'_{m'}}\sum_{\bar{\nu}'_{m'}}\sum_{\lambda_2''}\sum_{\bar{\lambda}_3''} \\ &\quad\times V_{\bar{\mu}_m\bar{\nu}_m}\left(\lambda_1;\lambda_2\right)V_{\bar{\mu}'_{m'}\bar{\nu}'_{m'}}\left(-\lambda_1\right)V\left(-\lambda_2;\lambda_2'';-\lambda_2''\right)\bar{u}_{\mu_m\nu_m}\bar{u}_{\mu'_{m'}\nu'_{m'}} \\ &\quad\times\left(2\bar{n}_{\lambda_2''}+1\right)\int_0^\beta d\tau_1\int_0^\beta d\tau_2\int_0^\beta d\tau_3 G_0\left(\lambda_1\tau_1|\lambda_1\tau_2\right)G_0\left(\lambda_2\tau_1|\lambda_2\tau_3\right) \\ &\quad-6\sum_{\lambda_1}\sum_{\lambda_2}\sum_{m=1}\frac{1}{m!}\sum_{\bar{\mu}_m}\sum_{\bar{\nu}_m}\sum_{\lambda_1'}\sum_{m'=1}\frac{1}{m'!}\sum_{\bar{\mu}'_{m'}}\sum_{\bar{\nu}'_{m'}} \\ &\quad\times V_{\bar{\mu}_m\bar{\nu}_m}\left(\lambda_1;\lambda_2\right)V_{\bar{\mu}'_{m'}\bar{\nu}'_{m'}}\left(\lambda_1'\right)V\left(-\lambda_1;-\lambda_2;-\lambda_1'\right)\bar{u}_{\mu_m\nu_m}\bar{u}_{\mu'_{m'}\nu'_{m'}} \\ &\quad\times\int_0^\beta d\tau_1\int_0^\beta d\tau_2\int_0^\beta d\tau_3 G_0\left(\lambda_1\tau_1|\lambda_1\tau_3\right)G_0\left(\lambda_2\tau_1|\lambda_2\tau_3\right)G_0\left(\lambda_1'\tau_2|\lambda_1'\tau_3\right).\end{aligned} \tag{C.22}$$

The second integral in Eq. (C.22) is of the form

$$\int_0^\beta d\tau_1\int_0^\beta d\tau_2\int_0^\beta d\tau_3 G_0\left(\lambda_1\tau_1|\lambda_1\tau_3\right)G_0\left(\lambda_2\tau_2|\lambda_2\tau_3\right)G_0\left(\lambda_3\tau_2|\lambda_3\tau_3\right), \tag{C.23}$$

and in terms of the Fourier transforms (Sec. 2.4)

$$\int_0^\beta d\tau_1 \int_0^\beta d\tau_2 \int_0^\beta d\tau_3 \sum_{n_1,n_2,n_3=-\infty}^{\infty} G_0\left(\lambda_1|\omega_{n_1}\right) \times G_0\left(\lambda_2|\omega_{n_2}\right) G_0\left(\lambda_3|\omega_{n_3}\right) e^{i\omega_{n_1}(\tau_1-\tau_3)} e^{i\omega_{n_2}(\tau_2-\tau_3)} e^{i\omega_{n_3}(\tau_2-\tau_3)}, \tag{C.24}$$

By using Eq. (2.113), Eq. (C.24) becomes

$$\beta^3 G_0\left(\lambda_1|0\right) \sum_{n_1=-\infty}^{\infty} G_0\left(\lambda_2|\omega_{n_1}\right) G_0\left(\lambda_3|\omega_{n_1}\right). \tag{C.25}$$

Here $G_0\left(\lambda|0\right) = 2/\left(\omega_\lambda \beta\hbar\right)$. The result for the summation in Eq. (C.25) is given by Eq. (A.42), thus, Eq. (C.23) can be written as

$$\beta^3 G_0\left(\lambda_1|0\right) \sum_{n_1=-\infty}^{\infty} G_0\left(\lambda_2|\omega_{n_1}\right) G_0\left(\lambda_3|\omega_{n_1}\right) = \frac{8\beta}{\hbar^2\omega_{\lambda_1}} \frac{\omega_{\lambda_2}\left(\bar{n}_{\lambda_3}+\frac{1}{2}\right) - \omega_{\lambda_3}\left(\bar{n}_{\lambda_2}+\frac{1}{2}\right)}{\omega_{\lambda_2}^2 - \omega_{\lambda_3}^2}. \tag{C.26}$$

After the simplification of the first integral and by using Eq. (C.26) for the second integral, Eq. (C.22) can be written as

$$\begin{aligned}
\left\langle \hat{S}\left(\beta\right)\right\rangle_{ssa,1} &= -\frac{48\beta}{\hbar^2} \sum_{\lambda_1}\sum_{\lambda_2}\sum_{m=1} \frac{1}{m!} \sum_{\bar{\mu}_m}\sum_{\bar{\nu}_m}\sum_{m'=1} \frac{1}{m'!} \sum_{\bar{\mu}'_{m'}}\sum_{\bar{\nu}'_{m'}}\sum_{\lambda''_2}\sum_{\lambda''_3} \frac{\bar{n}_{\lambda''_2}+\frac{1}{2}}{\omega_{\lambda_1}\omega_{\lambda_2}} \\
&\times V_{\bar{\mu}_m\bar{\nu}_m}\left(\lambda_1;\lambda_2\right) V_{\bar{\mu}'_{m'}\bar{\nu}'_{m'}}\left(-\lambda_1\right) \bar{u}_{\mu_m\nu_m} \bar{u}_{\mu'_{m'}\nu'_{m'}} V\left(-\lambda_2;\lambda''_2;-\lambda''_2\right) \\
&- \frac{48\beta}{\hbar^2} \sum_{\lambda_1}\sum_{\lambda_2}\sum_{m=1} \frac{1}{m!} \sum_{\bar{\mu}_m}\sum_{\bar{\nu}_m}\sum_{\lambda'_1}\sum_{m'=1} \frac{1}{m'!} \sum_{\bar{\mu}'_{m'}}\sum_{\bar{\nu}'_{m'}} \\
&\times V_{\bar{\mu}_m\bar{\nu}_m}\left(\lambda_1;\lambda_2\right) V_{\bar{\mu}'_{m'}\bar{\nu}'_{m'}}\left(\lambda'_1\right) \bar{u}_{\mu_m\nu_m} \bar{u}_{\mu'_{m'}\nu'_{m'}} \\
&\times \frac{V\left(-\lambda_1;-\lambda_2;-\lambda'_1\right)}{\omega_{\lambda'_1}} \frac{\omega_{\lambda_2}\left(\bar{n}_{\lambda_1}+\frac{1}{2}\right) - \omega_{\lambda_1}\left(\bar{n}_{\lambda_2}+\frac{1}{2}\right)}{\omega_{\lambda_2}^2 - \omega_{\lambda_1}^2}.
\end{aligned} \tag{C.27}$$

Terms included in Eq. (C.27) are special cases of diagrams d) and e) of Fig. 3.10. In Article IV, general form for the algebraic expressions corresponding to these diagrams was given.

The last term to be considered is the algebraic expression for diagram m) of Fig. 3.10, namely

$$\begin{aligned}
\left\langle \hat{S}\left(\beta\right)\right\rangle_{ssa,2} &\equiv \left\langle \hat{S}\left(\beta\right)\right\rangle_{0,c,ssA,n=n'=2,2n''\geq 4} \\
&= -\sum_{\lambda_1}\sum_{\lambda_2}\sum_{m=1} \frac{1}{m!} \sum_{\bar{\mu}_m}\sum_{\bar{\nu}_m}\sum_{\lambda'_1}\sum_{\lambda'_2}\sum_{m'=1} \frac{1}{m'!} \sum_{\bar{\mu}'_{m'}}\sum_{\bar{\nu}'_{m'}}\sum_{\bar{\lambda}''_{2n''}} \\
&\times V_{\bar{\mu}_m\bar{\nu}_m}\left(\lambda_1;\lambda_2\right) V_{\bar{\mu}'_{m'}\bar{\nu}'_{m'}}\left(\lambda'_1;\lambda'_2\right) V\left(\bar{\lambda}''_{2n''}\right) \bar{u}_{\mu_m\nu_m} \bar{u}_{\mu'_{m'}\nu'_{m'}} \\
&\times \frac{1}{2}\int_0^\beta d\tau_1 \int_0^\beta d\tau_2 \int_0^\beta d\tau_3 \left\langle \mathcal{T}\left\{\hat{A}_{\bar{\lambda}_2}\left(\tau_1\right) \hat{A}_{\bar{\lambda}'_2}\left(\tau_2\right) \hat{A}_{\bar{\lambda}''_{2n''}}\left(\tau_3\right)\right\}\right\rangle_{0,c}, \\
&n'' = 2,3,\ldots.
\end{aligned} \tag{C.28}$$

By using Wick's Theorem

$$
\begin{aligned}
&\left\langle \mathcal{T}\left\{ \hat{A}_{\bar{\lambda}_2}\left(\tau_1\right) \hat{A}_{\bar{\lambda}'_2}\left(\tau_2\right) \hat{A}_{\bar{\lambda}''_{2n''}}\left(\tau_3\right)\right\}\right\rangle_{0,c} \\
= \;& 8n''\left(\prod_{k=1\wedge k=odd}^{2n''-1} k\right) \delta_{\lambda_1}\left(-\lambda'_1\right)\delta_{\lambda_2}\left(-\lambda''_1\right)\delta_{\lambda'_2}\left(-\lambda''_2\right)\delta_{\lambda''_3}\left(-\lambda''_4\right)\delta_{\lambda''_5}\left(-\lambda''_6\right)\cdots\delta_{\lambda''_{2n''-1}}\left(-\lambda''_{2n''}\right) \\
&\times G_0\left(\lambda_1\tau_1|\lambda_1\tau_2\right) G_0\left(\lambda_2\tau_1|\lambda_2\tau_3\right) G_0\left(\lambda'_2\tau_2|\lambda'_2\tau_3\right) \\
&\times\left(2\bar{n}_{\lambda''_3}+1\right)\left(2\bar{n}_{\lambda''_5}+1\right)\cdots\left(2\bar{n}_{\lambda''_{2n''-1}}+1\right) \\
&+2n''\left(2n''-2\right)\left(\prod_{k=1\wedge k=odd}^{2n''-1} k\right)\delta_{\lambda_1}\left(-\lambda''_1\right)\delta_{\lambda_2}\left(-\lambda''_2\right)\delta_{\lambda'_1}\left(-\lambda''_3\right)\delta_{\lambda'_2}\left(-\lambda''_4\right) \\
&\times\delta_{\lambda''_5}\left(-\lambda''_6\right)\delta_{\lambda''_7}\left(-\lambda''_8\right)\cdots\delta_{\lambda''_{2n''-1}}\left(-\lambda''_{2n''}\right) \\
&\times G_0\left(\lambda_1\tau_1|\lambda_1\tau_3\right) G_0\left(\lambda_2\tau_1|\lambda_2\tau_3\right) G_0\left(\lambda'_1\tau_2|\lambda'_1\tau_3\right) G_0\left(\lambda'_2\tau_2|\lambda'_2\tau_3\right) \\
&\times\left(2\bar{n}_{\lambda''_5}+1\right)\left(2\bar{n}_{\lambda''_5}+1\right)\cdots\left(2\bar{n}_{\lambda''_{2n''-1}}+1\right). \qquad \text{(C.29)}
\end{aligned}
$$

By using the result given in Eq. (C.29), Eq. (C.28) can be written as

$$
\begin{aligned}
\left\langle \hat{S}\left(\beta\right)\right\rangle_{ssa,2} \;=\; & -\frac{1}{2}\sum_{\lambda_1}\sum_{\lambda_2}\sum_{m=1}\frac{1}{m!}\sum_{\bar{\mu}_m}\sum_{\bar{\nu}_m}\sum_{\lambda'_1}\sum_{\lambda'_2}\sum_{m'=1}\frac{1}{m'!}\sum_{\bar{\mu}'_{m'}}\sum_{\bar{\nu}'_{m'}}\sum_{\bar{\lambda}''_{2n''}} \\
&\times V_{\bar{\mu}_m\bar{\nu}_m}\left(\lambda_1;\lambda_2\right) V_{\bar{\mu}'_{m'}\bar{\nu}'_{m'}}\left(\lambda'_1;\lambda'_2\right) V\left(\bar{\lambda}''_{2n''}\right) \\
&\times\bar{u}_{\mu_m\nu_m}\bar{u}_{\mu'_{m'}\nu'_{m'}} 8n''\left(\prod_{k=1\wedge k=odd}^{2n''-1} k\right) \\
&\times\delta_{\lambda_1}\left(-\lambda'_1\right)\delta_{\lambda_2}\left(-\lambda''_1\right)\delta_{\lambda'_2}\left(-\lambda''_2\right)\delta_{\lambda''_3}\left(-\lambda''_4\right)\delta_{\lambda''_5}\left(-\lambda''_6\right)\cdots\delta_{\lambda''_{2n''-1}}\left(-\lambda''_{2n''}\right) \\
&\times\int_0^\beta d\tau_1\int_0^\beta d\tau_2\int_0^\beta d\tau_3 G_0\left(\lambda_1\tau_1|\lambda_1\tau_2\right) G_0\left(\lambda_2\tau_1|\lambda_2\tau_3\right) \\
&\times G_0\left(\lambda'_2\tau_2|\lambda'_2\tau_3\right)\left(2\bar{n}_{\lambda''_3}+1\right)\left(2\bar{n}_{\lambda''_5}+1\right)\cdots\left(2\bar{n}_{\lambda''_{2n''-1}}+1\right) \\
&-\frac{1}{2}\sum_{\lambda_1}\sum_{\lambda_2}\sum_{m=1}\frac{1}{m!}\sum_{\bar{\mu}_m}\sum_{\bar{\nu}_m}\sum_{\lambda'_1}\sum_{\lambda'_2}\sum_{m'=1}\frac{1}{m'!}\sum_{\bar{\mu}'_{m'}}\sum_{\bar{\nu}'_{m'}} \\
&\times V_{\bar{\mu}_m\bar{\nu}_m}\left(\lambda_1;\lambda_2\right) V_{\bar{\mu}'_{m'}\bar{\nu}'_{m'}}\left(\lambda'_1;\lambda'_2\right)\bar{u}_{\mu_m\nu_m}\bar{u}_{\mu'_{m'}\nu'_{m'}} \\
&\times\sum_{\lambda''_1}\cdots\sum_{\lambda''_{2n''}} V\left(\lambda''_1;\ldots;\lambda''_{2n''}\right) 2n''\left(2n''-2\right)\prod_{k=1\wedge k=odd}^{2n''-1} k \\
&\times\delta_{\lambda_1}\left(-\lambda''_1\right)\delta_{\lambda_2}\left(-\lambda''_2\right)\delta_{\lambda'_1}\left(-\lambda''_3\right)\delta_{\lambda'_2}\left(-\lambda''_4\right)\delta_{\lambda''_5}\left(-\lambda''_6\right)\delta_{\lambda''_7}\left(-\lambda''_8\right)\cdots\delta_{\lambda''_{2n''-1}}\left(-\lambda''_{2n''}\right) \\
&\times\left(2\bar{n}_{\lambda''_5}+1\right)\left(2\bar{n}_{\lambda''_7}+1\right)\cdots\left(2\bar{n}_{\lambda''_{2n''-1}}+1\right) \\
&\times\int_0^\beta d\tau_1\int_0^\beta d\tau_2\int_0^\beta d\tau_3 G_0\left(\lambda_1\tau_1|\lambda_1\tau_3\right) G_0\left(\lambda_2\tau_1|\lambda_2\tau_3\right) \\
&\times G_0\left(\lambda'_1\tau_2|\lambda'_1\tau_3\right) G_0\left(\lambda'_2\tau_2|\lambda'_2\tau_3\right), \quad n''=2,3,\ldots, \qquad \text{(C.30)}
\end{aligned}
$$

and furthermore

$$
\begin{aligned}
\left\langle \hat{S}\left(\beta\right)\right\rangle_{ssa,2} &= -4\sum_{\bar{\lambda}_2}\sum_{m=1}\frac{1}{m!}\sum_{\bar{\mu}_m}\sum_{\bar{\nu}_m}\sum_{\lambda_2'}\sum_{m'=1}\frac{1}{m'!}\sum_{\bar{\mu}'_{m'}}\sum_{\bar{\nu}'_{m'}}\sum_{\lambda_3''}\sum_{\lambda_5''}\cdots\sum_{\lambda''_{2n''-1}} \\
&\times V_{\bar{\mu}_m\bar{\nu}_m}\left(\lambda_1;\lambda_2\right)V_{\bar{\mu}'_{m'}\bar{\nu}'_{m'}}\left(-\lambda_1;\lambda_2'\right)\bar{u}_{\mu_m\nu_m}\bar{u}_{\mu'_{m'}\nu'_{m'}} \\
&\times V\left(-\lambda_2;-\lambda_2';\lambda_3'';-\lambda_3'';\ldots;\lambda''_{2n''-1};-\lambda''_{2n''-1}\right) \\
&\times n''\prod_{k=1\wedge k=odd}^{2n''-1}k\left(2\bar{n}_{\lambda_3''}+1\right)\left(2\bar{n}_{\lambda_5''}+1\right)\cdots\left(2\bar{n}_{\lambda''_{2n''-1}}+1\right) \\
&\times\int_0^\beta d\tau_1\int_0^\beta d\tau_2\int_0^\beta d\tau_3 G_0\left(\lambda_1\tau_1|\lambda_1\tau_2\right)G_0\left(\lambda_2\tau_1|\lambda_2\tau_3\right)G_0\left(\lambda_2'\tau_2|\lambda_2'\tau_3\right) \\
&-2\sum_{\lambda_1}\sum_{\lambda_2}\sum_{m=1}\frac{1}{m!}\sum_{\bar{\mu}_m}\sum_{\bar{\nu}_m}\sum_{\bar{\lambda}_2'}\sum_{m'=1}\frac{1}{m'!}\sum_{\bar{\mu}'_{m'}}\sum_{\bar{\nu}'_{m'}}\sum_{\lambda_5''}\sum_{\lambda_7''}\cdots\sum_{\lambda''_{2n''-1}} \\
&\times V_{\bar{\mu}_m\bar{\nu}_m}\left(\lambda_1;\lambda_2\right)V_{\bar{\mu}'_{m'}\bar{\nu}'_{m'}}\left(\lambda_1';\lambda_2'\right)\bar{u}_{\mu_m\nu_m}\bar{u}_{\mu'_{m'}\nu'_{m'}} \\
&\times V\left(-\lambda_1;-\lambda_2;-\lambda_1';-\lambda_2';\lambda_5'';-\lambda_5'';\ldots;\lambda''_{2n''-1};-\lambda''_{2n''-1}\right) \\
&\times n''\left(n''-1\right)\prod_{k=1\wedge k=odd}^{2n''-1}k\left(2\bar{n}_{\lambda_5''}+1\right)\left(2\bar{n}_{\lambda_7''}+1\right)\cdots\left(2\bar{n}_{\lambda''_{2n''-1}}+1\right) \\
&\times\int_0^\beta d\tau_1\int_0^\beta d\tau_2\int_0^\beta d\tau_3 G_0\left(\lambda_1\tau_1|\lambda_1\tau_3\right)G_0\left(\lambda_2\tau_1|\lambda_2\tau_3\right) \\
&\times G_0\left(\lambda_1'\tau_2|\lambda_1'\tau_3\right)G_0\left(\lambda_2'\tau_2|\lambda_2'\tau_3\right),\quad n''=2,3,\ldots,
\end{aligned}
\tag{C.31}
$$

The integrals in Eq. (C.31) are rather complicated, but can be simplified with the same method as before. Let

$$
\begin{aligned}
X_{\lambda_1\lambda_2\lambda_2'} \equiv &\left[\frac{\omega_{\lambda_1}\left(\bar{n}_{\lambda_2}-\bar{n}_{\lambda_2'}\right)}{\left(\omega_{\lambda_1}-\omega_{\lambda_2}\right)\left(\omega_{\lambda_1}+\omega_{\lambda_2}\right)\left(\omega_{\lambda_2'}-\omega_{\lambda_2}\right)}\right. \\
&+\frac{\omega_{\lambda_1}\left(\bar{n}_{\lambda_2}+\bar{n}_{\lambda_2'}+1\right)}{\left(\omega_{\lambda_1}-\omega_{\lambda_2}\right)\left(\omega_{\lambda_1}+\omega_{\lambda_2}\right)\left(\omega_{\lambda_2}+\omega_{\lambda_2'}\right)} \\
&+\frac{\omega_{\lambda_2}\left(\bar{n}_{\lambda_1}-\bar{n}_{\lambda_2'}\right)}{\left(\omega_{\lambda_2}-\omega_{\lambda_1}\right)\left(\omega_{\lambda_1}+\omega_{\lambda_2}\right)\left(\omega_{\lambda_2'}-\omega_{\lambda_1}\right)} \\
&\left.+\frac{\omega_{\lambda_2}\left(\bar{n}_{\lambda_1}+\bar{n}_{\lambda_2'}+1\right)}{\left(\omega_{\lambda_2}-\omega_{\lambda_1}\right)\left(\omega_{\lambda_1}+\omega_{\lambda_2}\right)\left(\omega_{\lambda_1}+\omega_{\lambda_2'}\right)}\right],
\end{aligned}
\tag{C.32}
$$

then, after the calculation, Eq. (C.31) becomes

$$\begin{aligned}
\left\langle \hat{S}\left(\beta\right)\right\rangle_{ssa,2} \;=\; & -\frac{16\beta}{\hbar^2}\sum_{\bar{\lambda}_2}\sum_{m=1}\frac{1}{m!}\sum_{\bar{\mu}_m}\sum_{\bar{\nu}_m}\sum_{\lambda'_2}\sum_{m'=1}\frac{1}{m'!}\sum_{\bar{\mu}'_{m'}}\sum_{\bar{\nu}'_{m'}}\sum_{n''=2}\sum_{\bar{\lambda}''_{n''-1}} \\
& \times V_{\bar{\mu}_m\bar{\nu}_m}\left(\bar{\lambda}_2\right)V_{\bar{\mu}'_{m'}\bar{\nu}'_{m'}}\left(-\lambda_1;\lambda'_2\right)\bar{u}_{\mu_m\nu_m}\bar{u}_{\mu'_{m'}\nu'_{m'}} \\
& \times V\left(-\lambda_2;-\lambda'_2;\lambda''_1;-\lambda''_1;\ldots;\lambda''_{n''-1};-\lambda''_{n''-1}\right) \\
& \times n''\prod_{k=1\wedge k=odd}^{2n''-1}k\left(2\bar{n}_{\lambda''_1}+1\right)\left(2\bar{n}_{\lambda''_2}+1\right)\cdots\left(2\bar{n}_{\lambda''_{n''-1}}+1\right)X_{\lambda_1\lambda_2\lambda'_2} \\
& -\frac{32\beta}{\hbar^2}\sum_{\bar{\lambda}_2}\sum_{m=1}\frac{1}{m!}\sum_{\bar{\mu}_m}\sum_{\bar{\nu}_m}\sum_{\bar{\lambda}'_2}\sum_{m'=1}\frac{1}{m'!}\sum_{\bar{\mu}'_{m'}}\sum_{\bar{\nu}'_{m'}}\sum_{n''=2}\sum_{\bar{\lambda}''_{n''-2}} \\
& \times V_{\bar{\mu}_m\bar{\nu}_m}\left(\bar{\lambda}_2\right)V_{\bar{\mu}'_{m'}\bar{\nu}'_{m'}}\left(\bar{\lambda}'_2\right)\bar{u}_{\mu_m\nu_m}\bar{u}_{\mu'_{m'}\nu'_{m'}} \\
& \times V\left(-\lambda_1;-\lambda_2;-\lambda'_1;-\lambda'_2;\lambda''_1;-\lambda''_1;\ldots;\lambda''_{n''-2};-\lambda''_{n''-2}\right) \\
& \times n''\left(n''-1\right)\prod_{k=1\wedge k=odd}^{2n''-1}k\left(2\bar{n}_{\lambda''_1}+1\right)\left(2\bar{n}_{\lambda''_2}+1\right)\cdots\left(2\bar{n}_{\lambda''_{n''-2}}+1\right) \\
& \times\frac{\omega_{\lambda_1}\left(\bar{n}_{\lambda_2}+\frac{1}{2}\right)-\omega_{\lambda_2}\left(\bar{n}_{\lambda_1}+\frac{1}{2}\right)}{\omega^2_{\lambda_1}-\omega^2_{\lambda_2}}\frac{\omega_{\lambda'_1}\left(\bar{n}_{\lambda'_2}+\frac{1}{2}\right)-\omega_{\lambda'_2}\left(\bar{n}_{\lambda'_1}+\frac{1}{2}\right)}{\omega^2_{\lambda'_1}-\omega^2_{\lambda'_2}}.
\end{aligned} \tag{C.33}$$

As before, the contribution to elastic constants, for example, can be obtained by using Eq. (2.134).

References

[1] T. Takabatake, K. Suekuni, T. Nakayama and E. Kaneshita. *Phonon-glass electron-crystal thermoelectric clathrates: Experiments and theory.* Rev. Mod. Phys. **86**, 669 (2014).

[2] J. S. Kasper, P. Hagenmuller, M. Pouchard and C. Cros. *Clathrate structure of silicon Na_8Si_{46} and Na_xSi_{136} ($x < 11$).* Science **150**, 1713 (1965).

[3] G. S. Nolas, J. L. Cohn, G. A. Slack and S. B. Schujman. *Semiconducting Ge clathrates: Promising candidates for thermoelectric applications.* Appl. Phys. Lett. **73**, 178 (1998).

[4] K. A. Kovnir and A. V. Shevelkov. *Semiconducting clathrates: synthesis, structure and properties.* Russ. Chem. Rev. **73**, 923 (2004).

[5] A. J. Karttunen, T. F. Fässler, M. Linnolahti and T. A. Pakkanen. *Structural principles of semiconducting Group 14 clathrate frameworks.* Inorg. Chem. **50**, 1733 (2010).

[6] A. Shevelkov and K. Kovnir. *Zintl Clathrates.* Struct. Bond. **139**, 97 (2011).

[7] P. Norouzzadeh, C. W. Myles and D. Vashaee. *Prediction of giant thermoelectric power factor in type-VIII clathrate Si_{46}.* Sci. Rep. **4**, 7028 (2014).

[8] J. Gryko, P. F. McMillan, R. F. Marzke, G. K. Ramachandran, D. Patton, S. K. Deb and O. F. Sankey. *Low-density framework form of crystalline silicon with a wide optical band gap.* Phys. Rev. B **62**, R7707 (2000).

[9] A. Ammar, C. Cros, M. Pouchard, N. Jaussaud, J. Bassat, G. Villeneuve, M. Duttine, M. Menetrier and E. Reny. *On the clathrate form of elemental silicon, Si_{136}: preparation and characterisation of Na_xSi_{136} ($x \to 0$).* Solid State Sci. **6**, 393 (2004).

[10] A. F. Ioffe. *Semiconductor Thermoelements and Thermoelectric Cooling.* Infosearch Limited London (1957).

[11] G. D. Mahan and J. O. Sofo. *The best thermoelectric.* Proc. Nat. Acad. Sci. **93**, 7436 (1996).

[12] E. K. U. Gross, E. Runge and O. Heinonen. *Many-particle theory.* IOP Publishing (1991).

[13] G. D. Mahan. *Many-Particle Physics*. Plenum Press (1990).

[14] G. Stefanucci and R. van Leeuwen. *Nonequilibrium Many-Body Theory of Quantum Systems*. Cambridge University Press (2013).

[15] K. Huang and M. Born. *Dynamical Theory of Crystal Lattices*. Clarendon Press Oxford (1954).

[16] P. Giannozzi, S. de Gironcoli, P. Pavone and S. Baroni. *Ab initio calculation of phonon dispersions in semiconductors*. Phys. Rev. B **43**, 7231 (1991).

[17] S. Baroni, S. de Gironcoli, A. Dal Corso and P. Giannozzi. *Phonons and related crystal properties from density-functional perturbation theory*. Rev. Mod. Phys. **73**, 515 (2001).

[18] P. Giannozzi, S. Baroni, N. Bonini, M. Calandra, R. Car, C. Cavazzoni, D. Ceresoli, G. L. Chiarotti, M. Cococcioni, I. Dabo, A. Dal Corso, S. de Gironcoli, S. Fabris, G. Fratesi, R. Gebauer, U. Gerstmann, C. Gougoussis, A. Kokalj, M. Lazzeri, L. Martin-Samos, N. Marzari, F. Mauri, R. Mazzarello, S. Paolini, A. Pasquarello, L. Paulatto, C. Sbraccia, S. Scandolo, G. Sclauzero, A. P. Seitsonen, A. Smogunov, P. Umari and R. M. Wentzcovitch. *QUANTUM ESPRESSO: a modular and open-source software project for quantum simulations of materials*. J. Phys.: Condens. Matter **21**, 395502 (2009).

[19] L. Paulatto, I. Errea, M. Calandra and F. Mauri. *First-principles calculations of phonon frequencies, lifetimes, and spectral functions from weak to strong anharmonicity: The example of palladium hydrides*. Phys. Rev. B **91**, 054304 (2015).

[20] W. Li, N. Mingo, L. Lindsay, D. A. Broido, D. A. Stewart and N. A. Katcho. *Thermal conductivity of diamond nanowires from first principles*. Phys. Rev. B **85**, 195436 (2012).

[21] W. Li, L. Lindsay, D. A. Broido, D. A. Stewart and N. Mingo. *Thermal conductivity of bulk and nanowire $Mg_2Si_xSn_{1-x}$ alloys from first principles*. Phys. Rev. B **86**, 174307 (2012).

[22] W. Li, J. Carrete, N. A. Katcho and N. Mingo. *ShengBTE: A solver of the Boltzmann transport equation for phonons*. Comput. Phys. Commun. **185**, 1747 (2014).

[23] J. Casas-Vázquez and D. Jou. *Temperature in non-equilibrium states: a review of open problems and current proposals*. Rep. Prog. Phys. **66**, 1937 (2003).

[24] S. R. De Groot and P. Mazur. *Non-Equilibrium Thermodynamics*. Dover Publications (1962).

[25] J. M. Ziman. *Electrons and Phonons: The Theory of Transport Phenomena in Solids*. Oxford University Press (1960).

[26] G. D. Barrera, J. A. O. Bruno, T. H. K. Barron and N. L. Allan. *Negative thermal expansion*. J. Phys.: Condens. Matter **17**, R217 (2005).

[27] M. T. Dove and H. Fang. *Negative thermal expansion and associated anomalous physical properties: review of the lattice dynamics theoretical foundation*. Rep. Prog. Phys. **79**, 066503 (2016).

[28] C. A. Kennedy and M. A. White. *Unusual thermal conductivity of the negative thermal expansion material, ZrW_2O_8*. Solid State Commun. **134**, 271 (2005). ISSN 0038-1098.

[29] C. A. Kennedy, M. A. White, A. P. Wilkinson and T. Varga. *Low thermal conductivity of the negative thermal expansion material, $HfMo_2O_8$*. Appl. Phys. Lett. **90**, 151906 (2007).

[30] N. W. Ashcroft and D. N. Mermin. *Solid State Physics*. Harcourt (1976).

[31] A. H. Romero, E. K. U. Gross, M. J. Verstraete and O. Hellman. *Thermal conductivity in PbTe from first principles*. Phys. Rev. B **91**, 214310 (2015).

[32] C. H. Xu, C. Z. Wang, C. T. Chan and K. M. Ho. *Theory of the thermal expansion of Si and diamond*. Phys. Rev. B **43**, 5024 (1991).

[33] P. Pavone, K. Karch, O. Schütt, D. Strauch, W. Windl, P. Giannozzi and S. Baroni. *Ab initio lattice dynamics of diamond*. Phys. Rev. B **48**, 3156 (1993).

[34] Siqing Wei, Changlin Li and M. Y. Chou. *Ab initio calculation of thermodynamic properties of silicon*. Phys. Rev. B **50**, 14587 (1994).

[35] K. Karch, P. Pavone, W. Windl, O. Schütt and D. Strauch. *Ab initio calculation of structural and lattice-dynamical properties of silicon carbide*. Phys. Rev. B **50**, 17054 (1994). doi:10.1103/PhysRevB.50.17054.

[36] J. Xie, S. P. Chen, J. S. Tse, S. Gironcoli and S. Baroni. *High-pressure thermal expansion, bulk modulus, and phonon structure of diamond*. Phys. Rev. B **60**, 9444 (1999).

[37] H. Zhao, Z. Tang, G. Li and N. R. Aluru. *Quasiharmonic models for the calculation of thermodynamic properties of crystalline silicon under strain*. J. Appl. Phys. **99**, 064314 (2006).

[38] K. V. Zakharchenko, M. I. Katsnelson and A. Fasolino. *Finite Temperature Lattice Properties of Graphene beyond the Quasiharmonic Approximation*. Phys. Rev. Lett. **102**, 046808 (2009).

[39] P. Norouzzadeh and C. W. Myles. *A first-principles lattice dynamical study of type-I, type-II, and type-VIII silicon clathrates*. J. Mater. Sci. **51**, 4538 (2016).

[40] T. Matsubara. *A new approach to quantum-statistical mechanics*. Prog. Theor. Phys. **14**, 351 (1955).

[41] R. A. Cowley. *The lattice dynamics of an anharmonic crystal*. Adv. Phys. **12**, 421 (1963).

[42] A. A. Maradudin and G. K. Horton. *Elements of The Theory of Lattice Dynamics*, volume 1. North-Holland (1974).

[43] P. Rogl. *Thermoelectrics Handbook: Macro to Nano*. CRC Press (2006).

[44] K. Momma and F. Izumi. *VESTA 3 for three-dimensional visualization of crystal, volumetric and morphology data*. J. Appl. Crystallogr. **44**, 1272 (2011).

[45] G. Leibfried, W. Ludwig, F. Seitz and D. Turnbull. *Theory of anharmonic effects in crystals*. Solid State Phys. **12**, 275 (1961).

[46] A. A. Maradudin, E. W. Montroll, G. H. Weiss and I. P. Ipatova. *Theory of The Lattice Dynamics in The Harmonic Approximation*, volume Supplement 3. Academic Press (1971).

[47] R. P. Feynman. *Forces in molecules*. Phys. Rev. **56**, 340 (1939).

[48] M. Born and R. Oppenheimer. *Zur quantentheorie der molekeln*. Ann. Phys. **389**, 457 (1927).

[49] O. H. Nielsen and R. M. Martin. *First-principles calculation of stress*. Phys. Rev. Lett. **50**, 697 (1983).

[50] P. A. M. Dirac. *The quantum theory of the emission and absorption of radiation*. Proc. R. Soc. Lond. A **114**, 243 (1927).

[51] P. A. M. Dirac. *The Principles of Quantum Mechanics*. Oxford University Press (1958).

[52] R. B. Griffiths. *Consistent Quantum Theory*. Cambridge University Press (2003).

[53] M. Reed and B. Simon. *Methods of Modern Mathematical Physics. Functional Analysis*, volume 1. Academic Press (1972).

[54] T. H. K. Barron, M. L. Klein, G. K. Horton and A. A. Maradudin. *Perturbation Theory of Anharmonic Crystals*, volume 1. North-Holland (1974).

[55] W. Greiner and J. Reinhardt. *Field Quantization*. Springer Science & Business Media (1996).

[56] R. J. Hardy. *Energy-flux operator for a lattice*. Phys. Rev. **132**, 168 (1963).

[57] G. P. Srivastava. *The Physics of Phonons*. CRC Press (1990).

[58] M. Omini and A. Sparavigna. *Beyond the isotropic-model approximation in the theory of thermal conductivity*. Phys. Rev. B **53**, 9064 (1996).

[59] M. Omini and A. Sparavigna. *An iterative approach to the phonon Boltzmann equation in the theory of thermal conductivity*. Physica B **212**, 101 (1995).

[60] A. Ward, D. A. Broido, Derek A. Stewart and G. Deinzer. *Ab initio theory of the lattice thermal conductivity in diamond*. Phys. Rev. B **80**, 125203 (2009).

[61] P. Carruthers. *Theory of thermal conductivity of solids at low temperatures*. Rev. Mod. Phys. **33**, 92 (1961).

[62] A. A. Maradudin and A. E. Fein. *Scattering of neutrons by an anharmonic crystal*. Phys. Rev. **128**, 2589 (1962).

[63] P. G. Klemens, F. Seitz and D. Turnbull. *Thermal Conductivity and Lattice Vibrational Modes*. Solid State Phys. **7**, 1 (1958).

[64] J. Callaway. *Model for Lattice Thermal Conductivity at Low Temperatures*. Phys. Rev. **113**, 1046 (1959).

[65] S. Simons. *Formulation and use of a model for the phonon Umklapp collision operator*. J. Phys. C **8**, 1147 (1975).

[66] G. P. Srivastava. *Calculation of lattice thermal conductivity of Ge from 4 to 900 K*. Philos. Mag. **34**, 795 (1976).

[67] G. P. Srivastava. *Phonon conductivity of insulators and semiconductors*. J. Phys. Chem. Solids **41**, 357 (1980).

[68] D. N. Zubarev. *Double-time Green functions in statistical physics*. Sov. Phys. Usp. **3**, 320 (1960).

[69] L. P. Kadanoff and G. Baym. *Quantum Statistical Mechanics*. W.A. Benjamin, Inc. (1962).

[70] A. L. Fetter and J. D. Walecka. *Quantum Theory of Many-Particle Systems*. McGraw-Hill (1971).

[71] W. Götze, K. H. Michel, G. K. Horton and A. A. Maradudin. *Self-consistent Phonons*, volume 1. North-Holland (1974).

[72] S. Doniach and E. H. Sondheimer. *Green's Functions for Solid State Physicists*. Benjamin (1974).

[73] G. Rickayzen. *Green's Functions and Condensed Matter, Acad*. Academic Press (1980).

[74] J. Rammer. *Quantum Field Theory of Non-Equilibrium States*. Cambridge University Press (2007).

[75] R. P. Feynman. *Space-time approach to quantum electrodynamics*. Phys. Rev. **76**, 769 (1949).

[76] M. E. Peskin and D. V. Schroeder. *An Introduction to Quantum Field Theory*. Westview (1995).

[77] C. Itzykson and J. Zuber. *Quantum field theory*. Dover Publications (2005).

[78] D. C. Wallace. *Thermodynamics of Crystals*. John Wiley & Sons (1972).

[79] J. F. Nye. *Physical properties of crystals: their representation by tensors and matrices*. Oxford University Press (1985).

[80] K. Brugger. *Thermodynamic definition of higher order elastic coefficients*. Phys. Rev. **133**, A1611 (1964).

[81] E. Grüneisen. *Theorie des festen Zustandes einatomiger Elemente*. Ann. Phys. **344**, 257 (1912).

[82] P. Choquard. *The Anharmonic Crystal*. W.A. Benjamin (1967).

[83] L. Amico, R. Fazio, A. Osterloh and V. Vedral. *Entanglement in many-body systems*. Rev. Mod. Phys. **80**, 517 (2008).

[84] L. J. Sham, G. K. Horton and A. A. Maradudin. *Theory of Lattice Dynamics of Covalent Crystals*, volume 1. North-Holland (1974).

[85] R. G. Parr and W. Yang. *Density Functional Theory of Atoms and Molecules*. Oxford University Press (1989).

[86] R. M. Dreizler and E. K. U. Gross. *Density Functional Theory: An Approach to the Quantum Many-Body Problem*. Springer-Verlag (1990).

[87] H. Eschrig. *The Fundamentals of Density Functional Theory*. Teubner (1996).

[88] R. van Leeuwen. *Density functional approach to the many-body problem: key concepts and exact functionals*. Adv. Quantum Chem. **43**, 25 (2003).

[89] P. Hohenberg and W. Kohn. *Inhomogeneous electron gas*. Phys. Rev. **136**, B864 (1964).

[90] W. Kohn and L. J. Sham. *Self-consistent equations including exchange and correlation effects.* Phys. Rev. **140**, A1133 (1965).

[91] P. A. M. Dirac. *Note on exchange phenomena in the Thomas atom.* Proc. Cambridge Philos. Soc. **26**, 376 (1930).

[92] J. C. Slater. *A simplification of the Hartree-Fock method.* Phys. Rev. **81**, 385 (1951).

[93] D. C. Langreth and M. J. Mehl. *Beyond the local-density approximation in calculations of ground-state electronic properties.* Phys. Rev. B **28**, 1809 (1983).

[94] A. D. Becke. *Density-functional exchange-energy approximation with correct asymptotic behavior.* Phys. Rev. A **38**, 3098 (1988).

[95] J. P. Perdew, J. A. Chevary, S. H. Vosko, K. A. Jackson, M. R. Pederson, D. J. Singh and C. Fiolhais. *Atoms, molecules, solids, and surfaces: Applications of the generalized gradient approximation for exchange and correlation.* Phys. Rev. B **46**, 6671 (1992).

[96] J. P. Perdew, K. Burke and M. Ernzerhof. *Generalized gradient approximation made simple.* Phys. Rev. Lett. **77**, 3865 (1996).

[97] J. C. Phillips and L. Kleinman. *New method for calculating wave functions in crystals and molecules.* Phys. Rev. **116**, 287 (1959).

[98] L. Kleinman and J. C. Phillips. *Crystal potential and energy bands of semiconductors. III. Self-consistent calculations for silicon.* Phys. Rev. **118**, 1153 (1960).

[99] M. H. Cohen and V. Heine. *Cancellation of kinetic and potential energy in atoms, molecules, and solids.* Phys. Rev. **122**, 1821 (1961).

[100] B. J. Austin, V. Heine and L. J. Sham. *General theory of pseudopotentials.* Phys. Rev. **127**, 276 (1962).

[101] S. Baroni, P. Giannozzi and A. Testa. *Green's-function approach to linear response in solids.* Phys. Rev. Lett. **58**, 1861 (1987).

[102] X. Gonze and J.-P. Vigneron. *Density-functional approach to nonlinear-response coefficients of solids.* Phys. Rev. B **39**, 13120 (1989).

[103] X. Gonze. *Adiabatic density-functional perturbation theory.* Phys. Rev. A **52**, 1096 (1995).

[104] X. Gonze and C. Lee. *Dynamical matrices, Born effective charges, dielectric permittivity tensors, and interatomic force constants from density-functional perturbation theory.* Phys. Rev. B **55**, 10355 (1997).

[105] C. D. Meyer. *Matrix Analysis and Applied Linear Algebra*. Siam (2000).

[106] R. J. Bell, P. Dean and D. C. Hibbins-Butler. *Localization of normal modes in vitreous silica, germania and beryllium fluoride*. J. Phys. C **3**, 2111 (1970).

[107] J. Hafner and M. Krajci. *Propagating and confined vibrational excitations in quasicrystals*. J. Phys.: Condens. Matter **5**, 2489 (1993).

[108] S. Pailhès, H. Euchner, V. M. Giordano, R. Debord, A. Assy, S. Gomès, A. Bosak, D. Machon, S. Paschen and M. de Boissieu. *Localization of propagative phonons in a perfectly crystalline solid*. Phys. Rev. Lett. **113**, 025506 (2014).

[109] T. Tadano, Y. Gohda and S. Tsuneyuki. *Impact of rattlers on thermal conductivity of a thermoelectric clathrate: A first-principles study*. Phys. Rev. Lett. **114**, 095501 (2015).

[110] A. A. Maradudin and G. F. Nardelli. *Elementary Excitations in Solids: The Cortina Lectures*. Plenum Press (1969).

[111] R. R. Reeber and K. Wang. *Thermal expansion and lattice parameters of group IV semiconductors*. Mater. Chem. Phys. **46**, 259 (1996).

[112] H. J. McSkimin. *Measurement of elastic constants at low temperatures by means of ultrasonic waves–data for silicon and germanium single crystals, and for fused silica*. J. Appl. Phys. **24**, 988 (1953).

[113] J. J. Hall. *Electronic effects in the elastic constants of n-type silicon*. Phys. Rev. **161**, 756 (1967).

[114] A. V. Inyushkin. *Thermal conductivity of isotopically modified silicon: current status of research*. Inorg. mater. **38**, 427 (2002).

[115] K. Esfarjani, G. Chen and H. T. Stokes. *Heat transport in silicon from first-principles calculations*. Phys. Rev. B **84**, 085204 (2011).

[116] G. S. Nolas, M. Beekman, J. Gryko, G. A. Lamberton Jr, T. M. Tritt and P. F. McMillan. *Thermal conductivity of elemental crystalline silicon clathrate* Si_{136}. Appl. Phys. Lett. **82**, 910 (2003).

[117] J. L. Cohn, G. S. Nolas, V. Fessatidis, T. H. Metcalf and G. A. Slack. *Glasslike heat conduction in high-mobility crystalline semiconductors*. Phys. Rev. Lett. **82**, 779 (1999).

[118] J. S. Tse, K. Uehara, R. Rousseau, A. Ker, C. I. Ratcliffe, M. A. White and G. MacKay. *Structural principles and amorphouslike thermal conductivity of Na-doped Si clathrates*. Phys. Rev. Lett. **85**, 114 (2000).

[119] J. Dong, O. F. Sankey and C. W. Myles. *Theoretical study of the lattice thermal conductivity in Ge framework semiconductors.* Phys. Rev. Lett. **86**, 2361 (2001).

[120] A. Bentien, M. Christensen, J. D. Bryan, A. Sanchez, S. Paschen, F. Steglich, G. D. Stucky and B. B. Iversen. *Thermal conductivity of thermoelectric clathrates.* Phys. Rev. B **69**, 045107 (2004).

[121] M. A. Avila, K. Suekuni, K. Umeo, H. Fukuoka, S. Yamanaka and T. Takabatake. *Glasslike versus crystalline thermal conductivity in carrier-tuned* $Ba_8Ga_{16}X_{30}$ *clathrates* ($X = \mathrm{Ge}, \mathrm{Sn}$). Phys. Rev. B **74**, 125109 (2006).

[122] K. Suekuni, M. A. Avila, K. Umeo and T. Takabatake. *Cage-size control of guest vibration and thermal conductivity in* $Sr_8Ga_{16}Si_{30-x}Ge_x$. Phys. Rev. B **75**, 195210 (2007).

[123] Y. Takasu, T. Hasegawa, N. Ogita, M. Udagawa, M. A. Avila, K. Suekuni and T. Takabatake. *Off-Center Rattling and Anisotropic Expansion of Type-I Clathrates Studied by Raman Scattering.* Phys. Rev. Lett. **100**, 165503 (2008).

[124] M. Christensen, A. B. Abrahamsen, N. B. Christensen, F. Juranyi, N. H. Andersen, K. Lefmann, J. Andreasson, C. R. H. Bahl and B. B. Iversen. *Avoided crossing of rattler modes in thermoelectric materials.* Nature Mater. **7**, 811 (2008).

[125] M. A. Avila, K. Suekuni, K. Umeo, H. Fukuoka, S. Yamanaka and T. Takabatake. *$Ba_8Ga_{16}Sn_{30}$ with type-I clathrate structure: Drastic suppression of heat conduction.* Appl. Phys. Lett. **92**, 041901 (2008).

[126] M. Christensen, S. Johnsen, F. Juranyi and B. B. Iversen. *Clathrate guest atoms under pressure.* J. Appl. Phys. **105**, 073508 (2009).

[127] M. Christensen, S. Johnsen and B. B. Iversen. *Thermoelectric clathrates of type I.* Dalton Trans. **39**, 978 (2010).

[128] C. Candolfi, U. Aydemir, A. Ormeci, W. Carrillo-Cabrera, U. Burkhardt, M. Baitinger, N. Oeschler, F. Steglich and Y. Grin. *Transport properties of the clathrate $BaGe_5$.* J. Appl. Phys. **110**, 043715 (2011).

[129] H. Euchner, S. Pailhès, L. T. K. Nguyen, W. Assmus, F. Ritter, A. Haghighirad, Y. Grin, S. Paschen and M. de Boissieu. *Phononic filter effect of rattling phonons in the thermoelectric clathrate $Ba_8Ge_{40+x}Ni_{6-x}$.* Phys. Rev. B **86**, 224303 (2012).

[130] J. Fulmer, O. I. Lebedev, V. V. Roddatis, D. C. Kaseman, S. Sen, J. Dolyniuk, K. Lee, A. V. Olenev and K. Kovnir. *Clathrate $Ba_8Au_{16}P_{30}$: The gold standard for lattice thermal conductivity.* J. Am. Chem. Soc. **135**, 12313 (2013).

[131] Y. He and G. Galli. *Nanostructured Clathrate Phonon Glasses: Beyond the Rattling Concept.* Nano Lett. **14**, 2920 (2014).

[132] R. Castillo, W. Schnelle, M. Bobnar, U. Burkhardt, B. Böhme, M. Baitinger, U. Schwarz and Y. Grin. *The Clathrate Ba_{8-x}-Si_{46} Revisited: Preparation routes, electrical and thermal transport properties.* Z. Anorg. Allg. Chem. **641**, 206 (2015).

[133] K. Kishimoto, S. Koda, K. Akai and T. Koyanagi. *Thermoelectric properties of sintered type-II clathrates (K, Ba)$_{24}$ (Ga, Sn)$_{136}$ with various carrier concentrations.* J. Appl. Phys. **118**, 125103 (2015).

[134] G. K. H. Madsen, A. Katre and C. Bera. *Calculating the thermal conductivity of the silicon clathrates using the quasi-harmonic approximation.* Phys. Status Solidi A **213**, 802 (2016).

[135] W. Li and N. Mingo. *Thermal conductivity of fully filled skutterudites: Role of the filler.* Phys. Rev. B **89**, 184304 (2014).

[136] W. Li and N. Mingo. *Ultralow lattice thermal conductivity of the fully filled skutterudite $YbFe_4Sb_{12}$ due to the flat avoided-crossing filler modes.* Phys. Rev. B **91**, 144304 (2015).

[137] P. B. Allen and J. L. Feldman. *Thermal conductivity of disordered harmonic solids.* Phys. Rev. B **48**, 12581 (1993).

[138] P. B. Allen, J. L. Feldman, J. Fabian and F. Wooten. *Diffusons, locons and propagons: Character of atomie vibrations in amorphous Si.* Philos. Mag. B **79**, 1715 (1999).

[139] T. Sun and P. B. Allen. *Lattice thermal conductivity: Computations and theory of the high-temperature breakdown of the phonon-gas model.* Phys. Rev. B **82**, 224305 (2010).

[140] A. A. Maradudin, P. A. Flinn and R. A. Coldwell-Horsfall. *Anharmonic contributions to vibrational thermodynamic properties of solids: Part I. General formulation and application to the linear chain.* Ann. Phys. **15**, 337 (1961).

[141] A. A. Maradudin. *Thermal expansion and phonon frequency shifts.* Phys. Status Solidi B **2**, 1493 (1962).

[142] R. A. Cowley. *Anharmonic crystals.* Rep. Prog. Phys. **31**, 123 (1968).

[143] R. C. Shukla and E. B. Muller. *Helmholtz free energy of an anharmonic crystal: A Green function approach.* Phys. Status Solidi B **43**, 413 (1971).

[144] R. C. Shukla and E. R. Cowley. *Helmholtz free energy of an anharmonic crystal to $O(\lambda^4)$.* Phys. Rev. B **3**, 4055 (1971).

[145] R. C. Shukla and L. Wilk. *Helmholtz free energy of an anharmonic crystal to $O(\lambda^4)$. II.* Phys. Rev. B **10**, 3660 (1974).

[146] W. P. Mason and R. N. Thurston. *Physical Acoustics*, volume 8. Academic Press (1971).

[147] R. A. Graham. *Solids Under High Pressure Shock Compression: Mechanics.* Springer Verlag (1993).

[148] H. Wang and M. Li. *Ab initio calculations of second-, third-, and fourth-order elastic constants for single crystals.* Phys. Rev. B **79**, 224102 (2009).

[149] M. Łopuszyński and J. A. Majewski. *Ab initio calculations of third-order elastic constants and related properties for selected semiconductors.* Phys. Rev. B **76**, 045202 (2007).

[150] R. Golesorkhtabar, P. Pavone, J. Spitaler, P. Puschnig and C. Draxl. *ElaStic: A tool for calculating second-order elastic constants from first principles.* Comput. Phys. Commun. **184**, 1861 (2013).

[151] T. R. Koehler. *Theory of the Self-Consistent Harmonic Approximation with Application to Solid Neon.* Phys. Rev. Lett. **17**, 89 (1966).

[152] W. Götze and K. H. Michel. *Transport theory for quantum crystals.* Z. Phys. **223**, 199 (1969).

[153] N. R. Werthamer. *Self-Consistent Phonon Formulation of Anharmonic Lattice Dynamics.* Phys. Rev. B **1**, 572 (1970).

[154] M. R. Spiegel. *Complex Variables.* McGraw-Hill Book Co. (1981).